Selective Crystallisation Facilitated by Nanonucleants for Downstream Bioseparation of a Protein Mixture

by

Xiaoyu Li

A dissertation submitted to Imperial College London for the degree of Doctor of Philosophy

Supervisor: Professor Jerry Y.Y. Heng

Department of Chemical Engineering, Imperial College London,

South Kensington, London, SW7 2AZ

2021

Copyright Declaration

Declaration

The work in this thesis is the original work of the author, except where acknowledged. No part of this thesis has been submitted for a degree at any other university.

The contents in Chapter 4 were published in Xiaoyu Li, Wenqian Chen, Huaiyu Yang, Zhongqiang Yang and Jerry Y. Y. Heng, Protein crystal occurrence domains in selective protein crystallisation for bio-separation, *CrystEngComm*, 2020, Volume 22, Pages 4566-4572.

The contents in Chapter 5 were published in Xiaoyu Li, Jerry Y.Y. Heng, The critical role of agitation in moving from preliminary screening results to reproducible batch protein crystallisation, *Chemical Engineering Research and Design*, Volume 173, 2021, Pages 81-88.

The contents in Chapter 6 were published in Xiaoyu Li, Jerry Y.Y. Heng, Protein crystallisation facilitated by silica particles to compensate the adverse impact from protein impurity, *CrystEngComm*, 2021, Volume 23, Pages 8386-8391.

For any reuse or redistribution, researchers must make clear to others the licence terms of these works and please seek permission from the copyright holder.

Acknowledgement

Pursuing a PhD in the Department of Chemical Engineering at Imperial College London has been such a great adventure in my life. It was a privilege to work with all the passionate and talented people throughout this journey. First of all, I would like to thank my supervisor, Professor Jerry Heng. This work wouldn't have been possible without his guidance and constant support. I'm grateful to be part of this generous and inclusive research group he developed. This work was supported by Seeding and Continuous Biopharmaceutical Crystallisation (SCoBiC) Project (EP/N015916/1) funded by EPSRC. It's my honour to contribute to this project. I would also like to thank everyone in the Heng Group, especially Dr Huaiyu Yang and Dr Wenqian Chen for their advice, ideas, and supports for the experiments. This is an inspirational group with motivation and passion and caring for each other.

I also want to say thank you to all my friends who see me through the good times and bum times, especially those who in other time zones for tolerating my messages waking you up in the midnight. Thanks for bearing with my complaints ranging from the unexpected experimental results to the gloomy weather in London.

Most importantly, I would like to thank my parents for all their supports and encouragements. Thank you for all the efforts and sacrifices you made to give me the freedom to make the choices of the road I took in my life.

I may have kept hundreds of thousands quotes in my diary for the acknowledgement section but none of them can express my gratefulness to all the support and encouragement I have received.

Abstract

Bioseparation is a major bottleneck in the manufacture of biopharmaceuticals such as proteins. Crystallisation is a cost-effective, rapid, and robust alternative technology to conventional chromatography steps in downstream separation processes. This thesis aims to investigate protein crystallisation as a feasible approach to separate proteins from a mixture for bioseparation. In this work, lysozyme- thaumatin mixture is used as the model binary protein mixture. Both µL-scale hanging-drop vapour-diffusion (HDVD) and mL-scale batch crystallisation methods were employed. We report an experimental evidence of direct selective protein crystallisation from a binary protein mixture solution where both proteins are supersaturated and crystallisable under an identical crystallisation condition. Results from both methods showed that protein impurity, even at low concentration level, would delay target protein crystallisation with an extended induction time. When silica particles were introduced as nanonucleants to facilitate crystallisation, target protein crystallisation was significantly improved with much shorter induction time. It was also indicated that the effectiveness of silica on crystallisation depended on the type of silica particle, silica loading amount, and impurity concentration. This study also revealed the critical role of agitation in obtaining consistent and reproducible results when moving from preliminary qualitative screenings using HDVD method to quantitative batch crystallisation experiments. Apart from improving reproducibility of crystallisation experiments, agitation also had impacts on both crystallisation rate, yield, and crystal size. In conclusion, this work demonstrates that protein crystallisation is a feasible and scalable methodology to separate a target protein from a complex mixture environment.

Publications

1. Xiaoyu Li, Wenqian Chen, Huaiyu Yang, Zhongqiang Yang and Jerry Y. Y. Heng, Protein crystal occurrence domains in selective protein crystallisation for bio-separation, *CrystEngComm*, 2020, Volume 22, Pages 4566-4572.

2. Xiaoyu Li, Jerry Y.Y. Heng, The critical role of agitation in moving from preliminary screening results to reproducible batch protein crystallisation, *Chemical Engineering Research and Design*, Volume 173, 2021, Pages 81-88.

3. Xiaoyu Li, Jerry Y.Y. Heng, Protein crystallisation facilitated by silica particles to compensate the adverse impact from protein impurity, *CrystEngComm*, 2021, Volume 23, Pages 8386-8391

4. Huaiyu Yang, Peter Peczulis, Pavan Inguva, Xiaoyu Li, Jerry Y.Y. Heng, Continuous protein crystallisation platform and process: Case of lysozyme, Chemical Engineering Research and Design, 2018, Volume 136, Pages 529-535.

5. Yang, Huaiyu, Benny D. Belviso, Xiaoyu Li, Wenqian Chen, Teresa F. Mastropietro, Gianluca Di Profio, Rocco Caliandro, and Jerry Y.Y. Heng, Optimization of vapor diffusion conditions for anti-cd20 crystallization and scale-up to meso batch, *Crystals*, 2019, Volume 9(5), 230.

6. Wenqian Chen, Sung Joon Park, Fanlu Kong, Xiaoyu Li, Huaiyu Yang, and Jerry Y. Y. Heng, High protein-loading silica template for heterogeneous protein crystallization, *Crystal Growth & Design*, 2020, Volume 20 (2), Pages 866-873.

7. Wenqian Chen, Thomas N.H. Cheng, Liang Fa Khaw, Xiaoyu Li, Huaiyu Yang, Jinbo Ouyang, Jerry Y.Y. Heng, Protein purification with nanoparticle-enhanced crystallisation, *Separation and Purification Technology*, 2021, Volume 255, 117384.

8. Wenqian Chen, Xiaoyu Li, Mingxia Guo, Frederik J. Link, Siti S. Ramli, Jinbo Ouyang, Ian Rosbottom, Jerry Y.Y. Heng, Biopurification of monoclonal antibody (mAb) through crystallisation, *Separation and Purification Technology*, 2021, Volume 263, 118358.

Conferences

1. Xiaoyu Li, Huaiyu Yang, Wenqian Chen, Mingxia Guo and Jerry Y. Y. Heng, Bioseperation from protein mixtures, Asian Crystallization Technology Symposium (ACTS), Singapore, 2018 (Oral Presentation)

2. Xiaoyu Li, Huaiyu Yang, Wenqian Chen, Mingxia Guo and Jerry Y. Y. Heng, Continuous crystallisation oscillatory flow platform for protein purification and bio-separation, 3rd International Symposium on Continuous Manufacturing of Pharmaceuticals (ISCMP), London, United Kingdom, 2018 (Poster)

3. Xiaoyu Li, Jerry Y.Y. Heng, Bio-separation via protein crystallisation: a case study of crystallisation from lysozyme-thaumatin model binary protein mixture, 50th annual conference of the British Association of Crystal Growth (BACG), London, United Kingdom, 2019 (Poster)

4. Xiaoyu Li, Huaiyu Yang, Wenqian Chen and Jerry Y. Y. Heng, Continuous crystallisation oscillatory flow platform for protein purification and bio-separation, 2019 Annual Meeting of American Institute of Chemical Engineers (AIChE), Orlando, United States, 2019 (Oral Presentation)

Xiaoyu Li, Wenqian Chen, and Jerry Y. Y. Heng, Bio-separation via selective protein crystallisation facilitated by porous silica templates: a case study using mesoporous nanoparticles in lysozyme-thaumatin model binary protein mixture, 2019 Annual Meeting of American Institute of Chemical Engineers (AIChE), Orlando, United States, 2019 (Oral Presentation)

Table of Contents

List of Tables

List of Figures

List of Symbols

A	Arrhenius reaction coefficient
k	Boltzmann constant
c*	concentration at saturation at the given temperature
Δc	concentration difference
c	concentration of solute in the solution
r_c	critical size
ΔG	free energy change of nucleation
g	gram
kDa	kilodalton
L	litre
ΔG_{crit}	maximum free energy
µL	microlitre
mg	milligram
mL	millilitre
v	molecular volume
nL	nanolitre
r	radius of the nucleus
σ	relative supersaturation
rpm	Revolutions per minute
S	supersaturation ratio
γ	surface free energy
ΔG_v	surface free energy change of nuleation
J	the rate of nucleation
ΔG_s	volume free energy change of nucleation

List of Abbreviations

AFM	atomic force microscopy
ALC	airlift crystalliser
API	active pharmaceutical ingredients
BET	Brunauer−Emmett−Teller
BJH	Barrett−Joyner−Halenda
BSA	bovine serum albumin
CNT	classical nucleation theory
CSFC	continuous slug flow crystalliser
DLS	dynamic light scattering
DNA	deoxyribonucleic acid
FID	free interface diffusion
HDVD	hanging-drop vapour-diffusion
HEWL	hen egg white lysozyme
Lyso.	lysozyme
mAb	monoclonal antibody
MOF	metal organic frameworks
MSMPR	mixed suspension mixed product removal
NaAc	sodium acetate
NaCl	sodium chloride
OBC	oscillatory baffled crystalliser
PEG	polyethylene glycol
pH	potential hydrogen
pI	isoelectric point
PIPES	1,4-piperazinediethanesulfonic acid
SBA-15	Santa Barbara amorphous-15
SDCD	sitting-drop vapour-diffusion
SEM	scanning electron microscopy
SFC	segmented slug flow crystalliser
SMART-EM	single-molecule atomic-resolution real-time electron microscopy
STC	stirred-tank crystalliser
TEWL	turkey egg white lysozyme
Thau.	thaumatin

1. Introduction

1.1. Background

Progress of advanced biotechnology has enhanced the recent development of biopharmaceutical products. These biopharmaceuticals mainly involve proteins and other biopolymer macromolecules manufactured from live organisms.[15] Compared to conventional small molecule pharmaceuticals, the biopharmaceuticals have the ability to treat a wide range of disease with high specificity, high bioactivity, and reduced side effects, and therefore biopharmaceuticals such as monoclonal antibody (mAb) have appealed major interests in the market.[16-18] Since introduced to the market in the 1980s, 374 individual biopharmaceutical products involving 285 distinct biopharmaceutical ingredients have been proved in EU/US by 2018 and the ten top-selling biopharmaceuticals had reached the sale value of $80.2 billion alone in 2017.[19, 20] Albeit biopharmaceuticals have the high efficacy mentioned above, they are still not easily accessible to the patients worldwide partly due to their unaffordable high prices. The development of biosimilars which contain previously registered biological active pharmaceutical ingredients (API), was driven by the high sale price and increasing market demand of the generic biopharmaceuticals and the registration of biosimilars started in 2006 in EU.[18, 21] A new wave of biosimilar approval is inevitable. In the 20 top-selling biopharmaceutical products in 2017, 14 products have patent expiry date before 2022 and 9 products have various biosimilars registered. Therefore, a more cost-effective manufacturing is required for biopharmaceutical companies in the future to produce more affordable products to patients while maintaining its economy benefits.

Bioseparation is the major bottleneck in the manufacture of biopharmaceuticals such as proteins. Up to 80% of the manufacturing cost comes from the downstream separation and purification processes, especially the multi-step protein A chromatography technology. Furthermore, improvements in upstream processes have led to a high titre of proteins secreted, beyond 5 g/L, which can be challenging to be handled effectively by the current chromatography technology.[22, 23] Both academia and industry are seeking alternatives to replace or partially replace the conventional chromatography steps.[24, 25] A wide range of separation approaches were investigated, involving crystallisation[26, 27], precipitation[28, 29], extraction[30, 31], and various membrane-based methods[32, 33]. Crystallisation often serves as common separation and isolation steps of both inorganic and organic small molecule products in numerous conventional chemical industries. Additionally, protein in crystalline form has higher purity and stability, which is beneficial to formulation, drug delivery, downstream handling, and storage.[34-36] Researchers have demonstrated the feasibility of using protein crystallisation as a scalable and robust approach of bioseparation.[37-39]

A great proportion of protein crystallisation studies focus on application of protein X-ray crystallography. In these applications, researchers usually aimed for large single crystals with minimum of defects and the experiments usually involve high-purity protein solution, long period of experimental time spam, and at only μL-scale. For industrial crystallisation for bioseparation, the requirements would be different from crystallography applications. It requires rapid, robust, and controllable crystallisation from a complex broth containing the target protein and other impurities at a L-scale. Systematic knowledge of the difference in crystallisation from a high-purity protein solution and from a mixture is still absent. Additionally, small-scale protein crystallisation for crystallography studies often has a low success rate, i.e., low

reproducibility. Works need to be done to improve the reproducibility to maintain the consistency of product quality in a larger scale for bioseparation applications.

1.2. Research Objectives

This project aims to investigate the role of protein impurity in selective crystallisation of the target protein and to demonstrate the efficiency of silica nanonucleants on facilitating protein crystallisation.

In this work, lysozyme-thaumatin mixture was used as the model binary protein mixture. Both μL-scale hanging-drop vapour-diffusion (HDVD) and mL-scale batch crystallisation methods were employed. The role of agitation in moving from HDVD experiments to batch experiments was investigated. Engineered silica particles with different porosities and particle sizes were used as nanonucleants, including SBA-15, mesoporous and non-porous. The efficiency of these nanonucleants at different loading amount were reviewed in protein mixtures at varied impurity levels.

The specific objectives of this research are:

1) To investigate the effect of protein impurity on target protein crystallisation over a wide range of mixture compositions in -μL HDVD experiments for qualitative preliminary results.
2) To study the effect of protein impurity on target protein crystallisation in -mL batch crystallisation experiments to obtain quantitative results. In this study, agitation may play a critical role in obtaining consistent conclusions.

3) To demonstrate that the employment of silica nanonucleants can improve protein crystallisation in both pure protein solution and protein mixture. And to validate that the effectiveness of silica on crystallisation depended on the type of silica particle, silica loading amount, and impurity concentration.

2. Literature Review

2.1. Background

Protein crystallisation is considered as a promising alternative bioseparation technique to conquer the major bottleneck in the manufacture of biopharmaceuticals. Crystallisation is a commonly employed purification step of both inorganic and organic small molecule products in various conventional chemical industries as it is a process of forming solid in crystalline form from liquid phase. Sublimation which is the process of crystallisation from supersaturated vapour is not discussed in this thesis since this type of crystallisation process is rarely applicable in protein crystallisation. Compared to solid in amorphous state, crystalline-state solid is considered highly pure and ordered where the constituent molecules, atoms or ions of the substance are fixed into characteristic rigid lattice.[9, 40] Due to the highly regular internal structure of crystalline solid, crystals usually possess characteristic shapes with defined external crystal faces.[40] Moreover, proteins in crystalline form have higher purity and stability, which is beneficial to formulation, drug delivery, downstream handling, and storage.[34-36]

The first report of protein crystallisation was in 1840, in which haemoglobin was crystallised via controlled evaporation from a concentrated solution.[41-43] In the studies of the 19th century, protein crystallisation was considered as a purification for enzyme and the process was considered to be similar to small molecule crystallisation, with demonstrated feasibility to grow crystals from crude samples with relatively low purity.[42] In 1934, the first X-ray photograph of a protein crystal, crystalline pepsin, was published.[44, 45] Later in 1950s, Max Perutz and John Kendrew solved the structure of two related proteins, myoglobin and haemoglobin via X-Ray crystallography, and since then, more works of protein crystallisation began to focus on protein crystallography.[43,

[45-47] Currently, a great proportion of the protein crystallisation works still focused on X-Ray crystallography where studies use protein crystallisation to obtain single crystals for biological molecule structural studies. New drug discovery has generally been benefited from protein crystallography so far, albeit advances in new protein characterisation technologies such as cryo-electron microscopy[48] and computational protein structure prediction method such as AlphaFold[49] may mean that crystallisation is less essential in the future of protein structure studies. Nevertheless, protein crystallisation started to be studied as a purification technique again and hopefully to be a cost-effective method for downstream bioseparation.

2.2. Fundamentals of Protein Crystallisation

2.2.1. Complexity of Protein Crystallisation

Though protein crystallisation has been studied for over 180 years, it is still regarded as a state of art rather than a science by many researchers.[10, 50] Most of the proteins are difficult to be crystallised. There are several model proteins, such as lysozyme, canavalin, concanavalin A, thaumatin, catalase, and insulin reported Protein Data Bank which are relatively well studied and reported comparatively easier to be crystallised. The study of mechanisms of the protein crystallisation is still in progress mainly using these model proteins since their properties and behaviours in crystallisation systems are better acknowledged. Even for model proteins, high number of parameters in protein crystallisation process must be considered cautiously and manipulated accordingly in the experiments. The major problem challenging protein crystallisation is the lack of knowledge of mechanisms of physico-chemical

interactions between protein-protein, protein-solvent and protein-nucleant in protein crystallisation.[10, 26] Comparing to small molecule crystallisation, which was more thoroughly investigated, the lack of knowledge in the fundamentals of nucleation and crystal growth in protein crystallisation resulted in the empirical approach based on trial-and-error methods. Though Wiencek emphasised that the basic principles of protein crystallisation were not different from small molecule crystallisation, research showed that protein crystallisation was still more challenging and inherently different from small molecule crystallisation.[10, 15, 51]

First, small molecules contain fewer atoms compared to proteins and thus are with simpler structures which are two or three orders of magnitude less complex than the structure of protein molecules.[15] Proteins possess three-dimensional conformation containing intra- and inter-chains in the size of kDa. Second, small molecule products are often manufactured from a highly consistent chemical process while protein manufacturing involves various impurities such as amino acids, nucleotides, cells, denatured target proteins, other proteins, and biopolymers.[15] Third, there is no universal way to handle the proteins for crystallisation purpose and hence numerous experimental works are required to do individual design for various proteins. Additionally, even for the same protein, different strategies may be required for crystallisation from its pure solution and crystallisation from the impure mixture like the bioreactor broth. This makes the practical application of protein crystallisation even more difficult compared to the currently problematic experimental work in trials. Furthermore, the crystallisation requires a supersaturation solution which may involve the solvation of proteins which is also a complicated process due to various sophisticated interactions. As shown in Table 2.1, there are many variables having influences on protein crystallisation, including pH, temperature, protein quality,

concentration of protein, types and concentration of crystallisation reagents, etc.[26] All the variables listed can be used to control the degree of supersaturation of the protein solution directly or indirectly and hence are able to manipulate the rates of nucleation and crystal growth processes.[52]

Table 2.1 Parameters affecting protein crystallisation process [7, 52]

Physical factors	Chemical factors	Biochemical factors
Temperature	Precipitant type	Sample impurities
Pressure	Precipitant concentration	Sample homogeneity
Gravity	pH	Sequence modifications
Magnetic fields	Buffer type	Posttranslational modifications
Electric fields	Ionic strength	Chemical modifications
Dielectric properties	Sample concentration	Aggregation
Viscosity	Metal ions	Proteolysis
Vibrations and sound	Polymers	Sample pI
Time	Detergents	Ligands
Equilibration rate	Heavy metals	Co-factors
Nucleants	Small molecule impurities	Inhibitors
Methodology	Crosslinkers	
Surface of crystallization Device	Reagent source	
Sample handling	Reagent formulation	

2.2.2. Solubility and Supersaturation

A liquid solution is a homogeneous mixture of more than one substance, involving solvents and solutes.[53] Solubility is the maximum amount of a solute able to be dissolved in a fixed amount of solvent at a particular temperature. Solubility is a

thermodynamical property of the given solute-solvent system as saturation is the result of phase equilibrium between the liquid phase and the solid phase.[54] Various factors have influences on protein crystallisation as listed in Table 2.1.

In crystallisation, supersaturation is the driving force of the process. When a solution is supersaturated, it contains more solute than that in saturated solution at a given temperature and thus the solution is thermodynamically unstable. There are different expressions of supersaturation, including the concentration difference (Δc), the supersaturation ratio (S), and relative supersaturation (σ).[53]

$$\Delta c = c - c^* \quad (1)$$

$$S = \frac{c}{c^*} \quad (2)$$

$$\sigma = \frac{\Delta c}{c^*} = S - 1 \quad (3)$$

Where c is the concentration of solute in the solution and c* is the concentration at saturation at the given temperature.

Solubility can be determined by crystallisation method using a supersaturated solution and dissolution method via dissolving of crystals in an unsaturated solution.[2, 12, 55] Theoretically, as shown in Figure 2.1, the protein concentrations from crystallisation method and dissolution method should converge to the value of equilibrium protein concentration, c*, at the given condition. The challenges in dissolution method is to obtain sufficient amount of protein crystals prior to the solubility experiments.[2] Nevertheless, it is harder to reach an equilibrium using crystallisation method due to the potential of cessation of crystal growth caused by surface poisoning by the impurities or constituent protein molecules with unmatching orientations.[2, 56, 57] In this case of growth termination, the apparent value would be higher than the true

equilibrium concentration. Moreover, the typical process of protein solubility determination could take days to weeks, and it is important to make sure that protein molecules are stable under the tested conditions. In general, if time and quantity of materials allow, it is recommended to measure from both paths as well as to start the measurement from different starting concentrations for more accurate data.[12, 58] The experiments can be conducted in conventional batch crystallisation method in a non-specialist vessel. Additionally, various alternative methods have been developed to measure the solubility in a less time-consuming, material-consuming, more robust, more automated, or higher-throughput manner.[12, 57-63]

2.2.3. Phase Diagram

The phase diagram is one of the most useful tool in the design of protein crystallisation experiments.[10, 64] A phase diagram is a map denoting the stable state of the substance under the given conditions, usually as a function of adjustable crystallisation parameters.[2, 10] The phase diagram is able to deliver the information of the influences of different parameters quantitatively depending on temperature, pH, precipitant, additive, and protein itself.

As illustrated in Figure 2.2, there are four main regions in a typical protein crystallisation phase diagram, unsaturated zone, metastable zone, nucleation zone and precipitation zone. Solubility curve denotes the maximum amount of a solute able to be dissolved in a fixed amount of solvent at a particular temperature.[54] Supersolubility curve implies the minimum supersaturation level where spontaneous nucleation can occur.[65] As supersaturation is the driving force in crystallisation, these zones represent different levels of supersaturation and thus whether the material is crystallisable under the given condition. Precipitation zone has a high degree of

supersaturation, usually occurs when protein concentration or the adjustable parameter is relatively high. In this region, protein will precipitate out from the solution as amorphous solid. Nucleation zone is where spontaneous nucleation may occur and the supersaturation in this region should be at a moderate level. Metastable zone is the region below the supersolubility curve and above the solubility curve where crystals may grow but spontaneous nucleation will not take place. It is commonly recognised as the suitable region for seeding to obtain more controllable crystal products.[10] Under the solubility line is the unsaturated zone where crystals are unstable and will dissolve. In more complex systems, liquid-liquid phase separation may also occur prior to crystallisation, especially for mAb proteins with PEG as additives.[66]

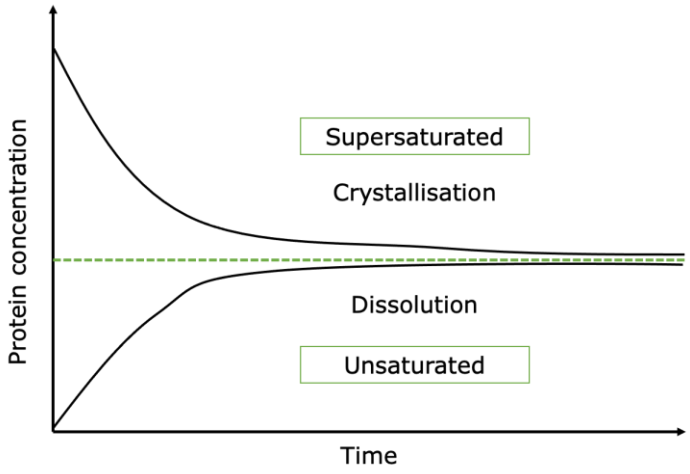

Figure 2.1 Schematic illustration of solubility measurements.[12]

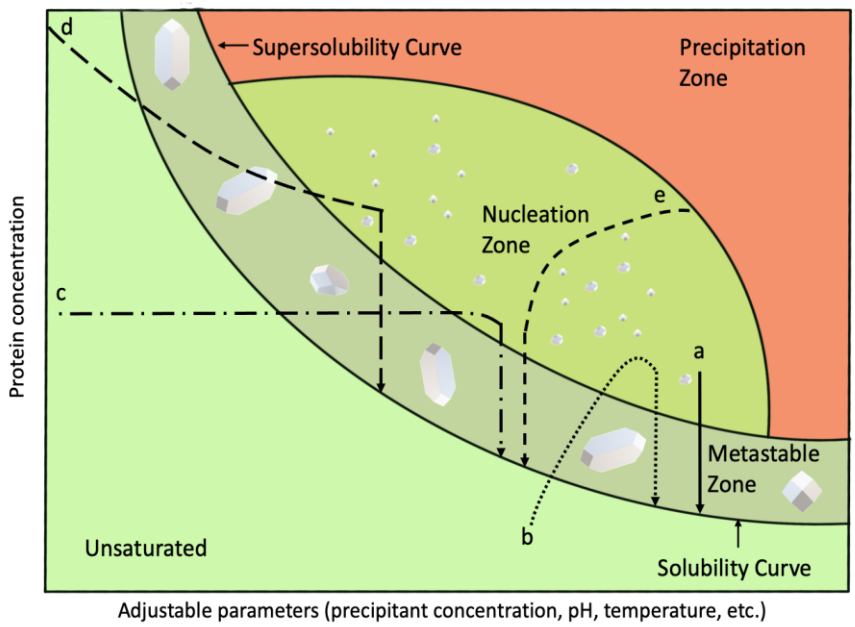

Figure 2.2 Graphic illustration of a representative phase diagram for protein crystallisation.
The lines represent the paths of five main crystallisation methods providing precipitant concentration is the adjustable parameter. (a) Batch; (b) Vapour-diffusion; (c) Dialysis; (d) Free-interface diffusion; (e) Counterdiffusion.[9, 10]

To obtain a phase diagram is not the easiest job. It needs to be determined specifically for individual protein and combination of crystallisation conditions. One of the problems is that the construction of the phase diagram for individual proteins under certain condition requires large amount of experimental work due to the high-dependency and high-sensitivity to the change of the conditions.[10] For example, when the crystallisation is scaled-up using different containers and mixing technique, the supersolubility curve, which is not a thermodynamic characteristic but a kinetic related property, would shift and hence metastable zone would change.[67] This process could be time-consuming and also costly. Additionally, it could not be used universally if one of the fixed parameters changed. Hence, though phase diagram could be a powerful

tool to facilitate the design of protein crystallisation, it is not feasible to be determined for different proteins in every case.

2.2.3. Protein Crystallisation Methods

Crystallisation is achieved by firstly reaching a supersaturated solution state leading to a phase transition where molecules come out of the solution phase to form crystal nuclei and this process is called nucleation. As the nuclei formation process continues, the solute concentration in the solution would drop and the solution is driven into the metastable zone. Crystallisation process will cease when the solution reaches saturated state where dynamic equilibrium between solid phase and liquid phase is achieved. Nevertheless, as mentioned above in solubility determination via crystallisation, crystal growth might halt before reaching solubility line due to surface poisoning.[2] As shown in Figure 2.2 , all crystallisation methods intend to create supersaturation. Supersaturation could be achieved in various ways as listed in Table 2.2.

Table 2.2 Methods to create supersaturation.[7]

Alter temperature
Alter ionic strength by addition or removal of salts
Alter pH
Alter solubility of protein by addition of ligands
Alter solubility of protein by removal of chaotropic agents
Alter dielectric of the medium by addition of organic solvents
Alter protein concentration by removal of solvent using membrane
Alter concentrations by evaporation
Introduce volume exclusion effects by addition of polymers
Promote lattice interactions by addition of cross-bridging agents

There are more than 20 techniques developed for protein crystallisation.[64, 68] In Figure 2.3, the most popular protein crystallisation techniques are illustrated schematically. Crystallisation methods can be basically classified into three types: vapour-diffusion, liquid-diffusion, and batch methods.

Batch method is set up by mixing precipitant solution and protein solution to immediately create a certain degree of supersaturation at the start of the experiments. Batch crystallisation is straightforward to set up and to characterise. Figure 2.3 (ai) shows the microbatch crystallisation under oil. This method is designed for protein crystallographers with the aid of automated liquid-handling systems.[69] This method uses oil to cover very small, a few μL, pre-mixed protein-precipitant droplets. The oil is added to reduce the evaporation, contamination, and other disturbances from the ambient. Batch crystallisation method is the most popular one for industrial crystallisation it and able to offer more quantitative data if using a -mL or -L scale. As shown in Figure 2.3 (aii), batch crystallisation could be set in a container by mixing the protein and precipitant solutions at the start of the experiments. Both mass and heat homogeneity in the system can be critical to the final results as well as the reproducibility between batches. For protein crystallisation, there are less studies focusing on bulk crystallisation in batch mode mainly due to the limited amount of proteins. Large-scale protein crystallisation in batch mode will be discussed in Section 2.6.

Vapour-diffusion method is to reach the supersaturation state by vapour-liquid phase equilibration between the under saturated solution and a dehydrating solution. Vapour-diffusion crystallisation method is the most popular method for X-ray diffraction crystallography.[68] Figure 2.3 (bi) and (bii) show the representations of hanging-drop

vapour-diffusion (HDVD) method and sitting-drop vapour-diffusion (SDVD) method, respectively. HDVD is usually in the scale of less than 10 μL while SDVD ranges from a few hundred nL to tens of μL, depending on the crystallisation plate used. Due to the availability of using automated liquid-handling systems, SDVD method, providing a higher throughput, could be more popular in the initial screening of crystallisation conditions.[68]

Liquid-diffusion method is to use direct contact between protein solution and the crystallisation cocktail. Figure 2.3 (c), (d) and (e) demonstrate dialysis method, free interface diffusion (FID) method and counterdiffusion method. In liquid-diffusion method, the rate of diffusion depends on the size of the solute and proteins as macromolecules usually diffuses slowly. The slow diffusion allows liquid-diffusion experiments to test a wider range of precipitant solutions in one run based on the concentration gradient formed.[7]

In general, vapour-diffusion and liquid-diffusion methods have advantage in screening and optimisation of crystallisation conditions for protein as they require smaller amount of raw protein materials to cover a wider range of potential conditions. However, due to its small scale (μL) and dynamic change of liquid composition, the reproducibility was relatively poor, and it is inherently difficulty of further evaluate the crystallisation process quantitively in respect of performances such as the protein concentration profile, yield, and crystal size distribution, which are important to industrial crystallisation compared biological structural study. And it is not feasible to evaluate the kinetics of the crystallisation process while the solubility changes with the crystallising agent concentration. Hence, batch crystallisation is preferable for protein crystallisation for bioseparation.

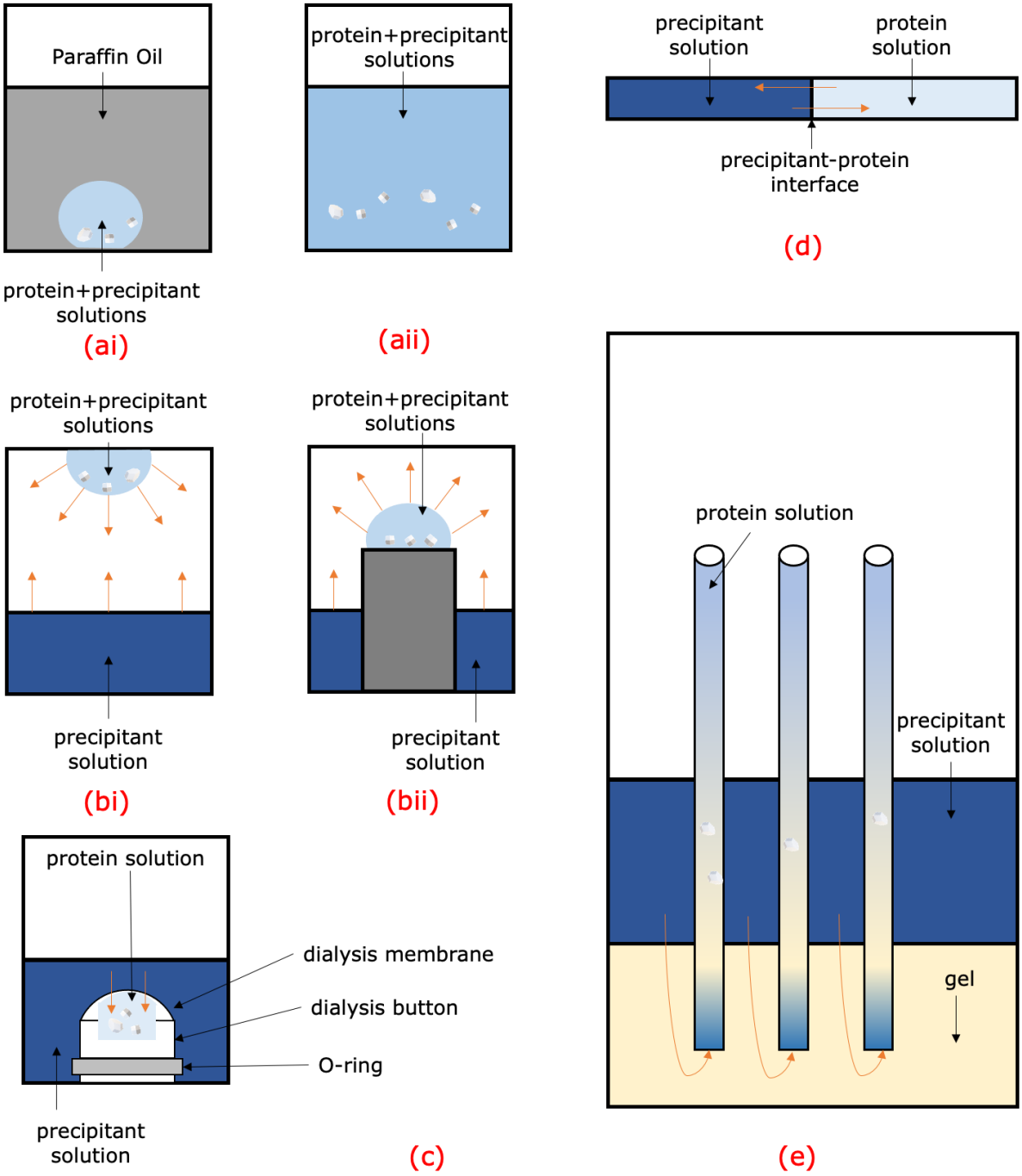

Figure 2.3 Schematic illustrations of the main crystallisation methods.

(ai) Batch (microbatch); (aii)Batch; (bi) Vapour-diffusion (hanging-drop); (bii) Vapour-diffusion (sitting-drop); (c) Dialysis; (d) Free-interface diffusion; (e) Counterdiffusion.[7-9]

2.3. Nucleation

Nucleation is the very first step in crystallisation referred as the birth of new crystals.[1] It is a critical step in crystallisation as it would influence the later crystal habit formation, crystal sizes, and crystal size distribution.[70] Hence, it is essential to understand the mechanisms of nucleation to get better control of the crystallisation process. The exact process of formation of the stable nuclei remains uncertain and the researches on atomic level are incredibly challenging due to the stochastic nature of nucleation.[1]

2.3.1. Nucleation Classification

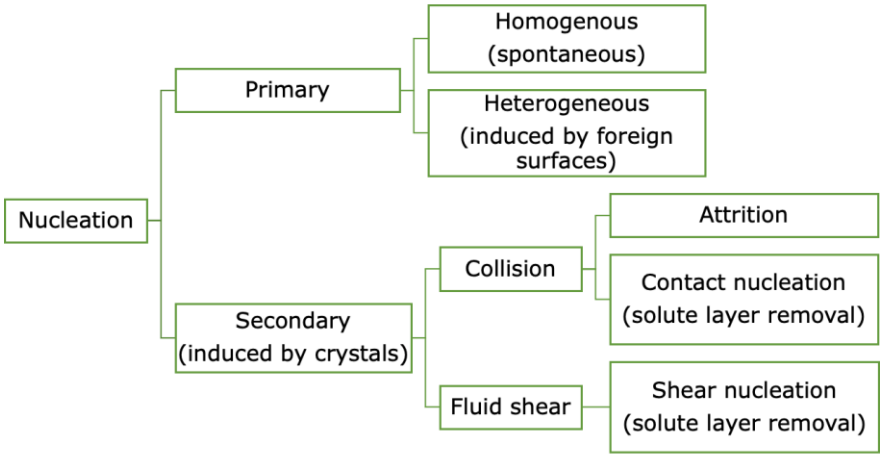

Figure 2.4 Classifications of nucleation[1-3]

Figure 2.4 shows the classifications of nucleation. Primary nucleation is referred as formation of nuclei in absence of crystals in the system. And primary nucleation can be further divided into two categories, homogeneous and heterogeneous nucleation. The difference between homogenous nucleation and heterogenous nucleation is that nucleus formation in homogenous involves no surface and critical nucleus arises from

homogeneous bulk.[1, 71] Homogenous nucleation engages critical nucleus formation from random events where adequate amount of molecules assemble in the same region and at the same time in a supersaturated solution.[72] Heterogenous nucleation usually involves surfaces of insoluble particles or impurities such as dust which attract molecules via electrostatic, hydrophobic or other interactions and thus a reduced nucleation barrier due to the lower surface energy.[71, 72]

Secondary nucleation is referred as formation of nuclei in the presence of previously existing crystals in the supersaturated system. Secondary nucleation is often a result of contact between crystal and crystal or crystal and impeller/vessel.[73] Mechanisms include crystal attrition or breakage, surface breeding, and embryo coagulation.[74] In industrial crystallisation for small molecule crystallisation, secondary nucleation is the principal nucleation mechanism since seeding is usually employed to obtain controllable crystal products. Albeit seeding is widely used in most conventional crystallisation industries, it is less common in protein crystallisation due to lack of previously crystals grown as the seeds and the difficulty of protein crystal handling.

2.3.2. Nucleation Theories

Though crystallisation has been used as a purification and isolation step for centuries, the accurate mechanism of nucleation is still not clear. And thus the crystallisation process is mainly based on empirical methods.[10, 13] The size of the critical nucleus is normally in the range of 10-1000 molecules and the time scale of critical nucleus formation is typically in the range of second to days, which makes both experimental and computational analysis of nucleation mechanisms tremendously difficult.[70] Only recently, sodium chloride nucleation process inside vibrating conical carbon nanotubes was captured via real-time electron microscopy (SMART-EM).[75] Classical

nucleation theory (CNT) was developed based on condensation of vapour to liquid and extended to apply in crystallisation from solution and melt, and the theory was based on the works of Becker and Döring (1935) [76] Volmer (1939)[77], Gibbs (1948)[78] and others.[1] It is commonly used to predict nucleation rates in primary nucleation. Researchers found CNT may not describe the experimental results accurately and modern theories of nucleation is developed. Two-step nucleation theory is one of the most popular modern theories of nucleation. Figure 2.5 shows a schematic representation of the different routes of nucleation described by CNT and two-step

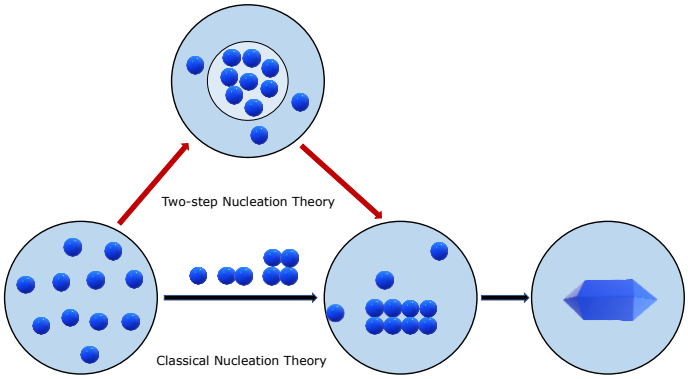

Figure 2.5 Schematic illustration of nucleation of crystals from solution[13]

nucleation theory.

Classical Nucleation Theory

Classical nucleation theory (CNT) is one of the widely applied mechanism proposed to describe homogeneous nucleation process. As mentioned above, it originates from the theory for condensation of vapour into liquid. CNT is based on the assumptions that small nuclei of a second phase is caused by the fluctuations of the solution directly. It assumes that the energy level is not the same in the system, albeit the energy of the system is constant at the given temperature and pressure. CNT only accounts for spherical and isotropic particles.

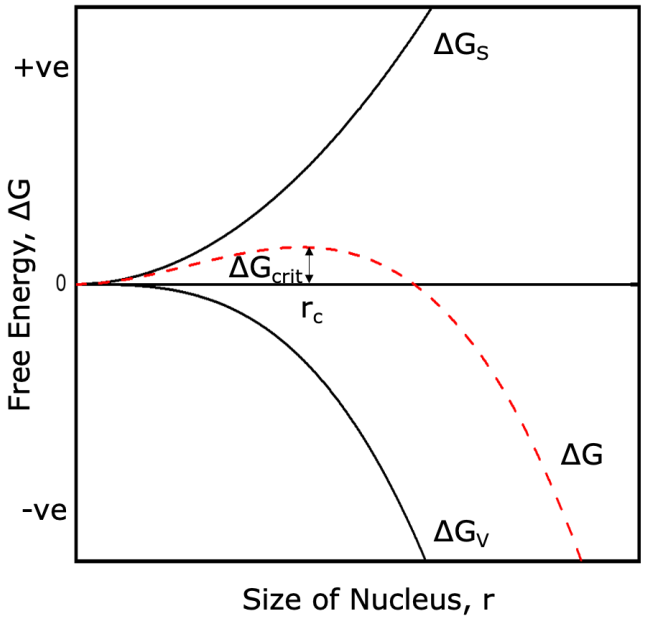

Figure 2.6 Schematic illustration of nucleation of crystals from solution [1]

The CNT is described in Figure 2.6. The thermodynamic explanation of the CNT is described using the equation below:

$$\Delta G = \Delta G_v + \Delta G_s \quad (4)$$

$$\Delta G = -\frac{4}{3}\pi r^3 \Delta G_v + 4\pi r^2 \gamma \quad (5)$$

ΔG is the free energy for a spherical nucleus and is the sum of the negative volume term and the positive surface term. ΔG_s is the excess free energy between the surface of the particle and the bulk of the particle. ΔG_s is a positive quantity which is proportional to r^2. ΔG_v is the bulk free energy difference per unit volume between the first phase and the second phase, i.e. the excess free energy between a very large particle and the solute in solution. ΔG_v is a negative quantity which is proportional to r^3. r is the radius of the nucleus. γ is the surface free energy. The positive surface free

energy term governs at small radii causing the increase in the total free energy and the negative volume free energy term dominates as the cluster increases reaching a maximum free energy (ΔG_{crit}) at a critical size (r_c) and then the total free energy decreases with increasing nucleus size. r_c is reached when $d\Delta G/dr=0$. And thus

$$r_c = \frac{-2\gamma}{\Delta G_v} \quad (6)$$

$$\Delta G_{crit} = \frac{4\pi\gamma r_c^2}{3} \quad (7)$$

r_c is the minimum size of a crystal nucleus stable in the system. If a crystalline particle is smaller than r_c, it will continue to grow. Otherwise, it will redissolve.

The rate of nucleation is described in the following equation:

$$J = A\exp\left(-\frac{\Delta G^*}{kT}\right) \quad (8)$$

J is the rate of nucleation, i.e. the number of nuclei formed per unit time per unit volume. A is the Arrhenius reaction coefficient. k is the Boltzmann constant. Based on Gibbs-Thomson relationship the equation can be written as

$$\ln S = \frac{2\gamma v}{kTr} \quad (9)$$

S is defined in previous section as the degree of supersaturation. v is the molecular volume.

$$\Delta G_{crit} = \frac{16\pi\gamma^3 v^2}{3(kT\ln S)^2} \quad (10)$$

$$J = A\exp\left[-\frac{16\pi\gamma^3 v^2}{3k^3T^3(\ln S)^2}\right] \quad (11)$$

This equation implies that the rate of nucleation is dominated by degree of supersaturation, temperature, and interfacial tension.

Though CNT has been widely used in nucleation and is a practical simplified theory for single-component nucleation, this theory is oversimplified and has limitations to more complex systems.[13] Firstly, CNT assumes clusters are spherical. Secondly, the composition in the system is assumed to be uniform. Thirdly, CNT only proposes a single energy barrier to overcome for the formation of crystalline phase. Furthermore, CNT is not able to give any information on the arrangement of the aggregates and structure transformation from solution phase to solid phase. This theory is not able to distinguish between the old phase and the new ordered phase assuming the change of density is discontinuous. In general, due to the oversimplication of the classical nucleation theory, it may fail to provide understanding, explain, or predict the nucleation behaviour of a binary or more complex system.

Two-Step Nucleation Theory

The two-step nucleation model is a non-classical nucleation mechanism which proposes that the cluster of solute with sufficient size was formed first and followed by a second step where the cluster organized into an ordered structure rather than formation of ordered clusters directly as assumed in CNT.[4-6] This model was motivated by the numerical simulation work of globular protein nucleation which showed the presence of a metastable critical point in the formation of nuclei.[79] As shown in Figure 2.7, the two-step nucleation therefore suggests that there are two energy barriers to be overcome in the formation of crystal nuclei. Dense liquid cluster formation is shown and crystal nuclei may form inside the clusters. There are two possible pathways for nucleation from solution according to the two-step model. In the upper line, when

dense liquid is unstable, $\Delta G^0_{L\text{-}L}>0$, where $\Delta G^0_{L\text{-}L}$ is the standard free energy of formation of dense liquid phase, the dense liquid exists as mesoscopic clusters and thus $\Delta G^0_{L\text{-}L}$ translates to ΔG^0_c. In the lower line, dense liquid is stable, $\Delta G^0_{L\text{-}L} <0$. ΔG_1^* is the energy barrier for the formation of dense liquid clusters and ΔG_2^* is the energy barrier for the formation of a structure fluctuation leading to ordered clusters. [4-6] This alternative nucleation theory takes the existence of spinodal for the phase transition from a solution to crystalline phase into consideration. [4-6] According to this theory, crystalline nuclei will appear inside the metastable dense cluster precursors. This theory was initially proposed for protein crystallisation and was found applicable to small molecule, colloid, and biomineral crystallisation.[5]

2.3.3. Application of Nucleants in Protein Crystallisation

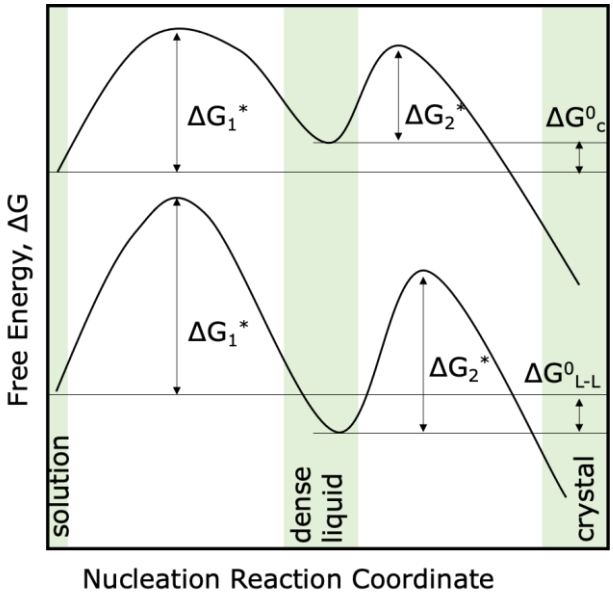

Figure 2.7 Schematic illustration of free energy pathways in two-step nucleation theory [4-6]

Nucleation is believed as the governing step for crystallisation control. Protein crystallisation remains challenging since spontaneous nucleation is a rare event. In

practice, most of the nucleation is initiated by heterogeneous nucleation. The ability to control protein nucleation and henceforward its crystallisation process is a major bottleneck. To address this concern, recent studies showed heterogeneous nucleants were able to provide a better control of the nucleation process and thus had the potential to facilitate rational design of selective protein crystallisation for isolation and purification steps.[80, 81] Many studies focused on systematic introduction of heterogeneous nucleants in screening to identify and optimize the crystallisation conditions. Heterogeneous nucleation agents developed include porous silicon, amorphous mesoporous bioactive bioglass, natural substance, porous hydrophobic membranes, porous zeolite, mica sheets and nanotemplates.[80] Novel heterogeneous nucleating agents developed include the modification of the properties of the materials to promote nucleation at low solution concentration, lower degree of supersaturation, higher success rate, controlled polymorphic form and other related concerns. A wide range of such nucleants with designed chemical and physical properties have been developed, for instance, porous silicon[82], nanowrinkle substrates[83, 84], mesoporous MOFs[85], magnetic particles[86], DNA origami[87], amino acids[88], etc. However, some limited cases of selective crystallisation were also described. [83, 89-92] Nonetheless, systematic knowledge of crystallisation behaviour of target protein from the mixture is still absent. The reported selective crystallisation cases only focused on specific scenarios either with ultralow protein concentration, with a very limited range of protein composition of the mixture, or at relatively small scale and long-time span which are not suitable for industrial application.

Engineered silica particles, both non-porous and mesoporous silica nanoparticles, are promising nanonucleants for protein cyrstallisation. Silica nanoparticles have the advantages of biocompatibility, possible siliane chemistry for surface functionalisation,

good chemical and thermal stability, and potential for low cost large-scale synthesis.[93, 94] Additionally, by tuning the composition and concentration of reagents during the synthesis process, non-porous silica can have well-controlled size and shape and mesoporous silica can have well-controlled pore size and structure.[93] Non-porous silica particles have been studied in drug delivery and molecular imaging.[93] Mesoporous silica materials are widely investigated in protein immobilization, encapsulation, biocatalysts, biosensing, purifications, and gas capture due to its high specific surface area, well-organised pore structure and tuneable pore size distribution.[95] The amount, orientation and distribution of proteins adsorbed on silica surface is related to the surface properties of the silica particles including chemistry, micro/nanostructure, morphology and texture.[95]

2.4. Crystal Growth

Nucleation is followed by crystal growth after the formation of stable nuclei in a supersaturated system. As shown in Figure 2.8, crystal growth involves the mass transport process of solute molecules onto the crystal/liquid interface and then incorporation of the adsorbed molecules into the crystal lattice. In terms of energy landscape, as shown in Figure 2.9 crystallisation is a phase transition process in which matter is transformed from a state of high free energy in a solvated state to a state of low free energy in crystalline state.[14] There are many crystal growth mechanisms proposed, including Surface energy theories, adsorption layer theories, kinematic theories, diffusion-reaction theories, and birth and spread models. The original idea of surface energy theory is an analogy to a liquid droplet. The surface energy theories are based on hypothesis that the growth of a crystal is to reach a minimum total free

energy in equilibrium with its surroundings at a given temperature and pressure for a given volume.[11] The theory was further developed to state that the equilibrium shape of a crystal is related to the free energies of the faces and thus the growth rate of a crystal surface is proportional the surface energy. Volmer (1939) first suggested the concept of adsorption layer theories that the crystal growth was based on an adsorbed layer of solute molecules on a crystal face.[77] Subsequent development of the adsorption layer theories mainly focused on the role of crystal imperfections in the growth process. As shown in Figure 2.10, illustrations of two-dimensional nucleation without dislocation, Kossel's model of crystal growth and spiral growth from dislocation were shown. The development of scanning electron microscopy (SEM) and atomic force microscopy (AFM) techniques has aided the understanding of crystal growth mechanisms mainly by examining the crystallisation of model proteins.[7]

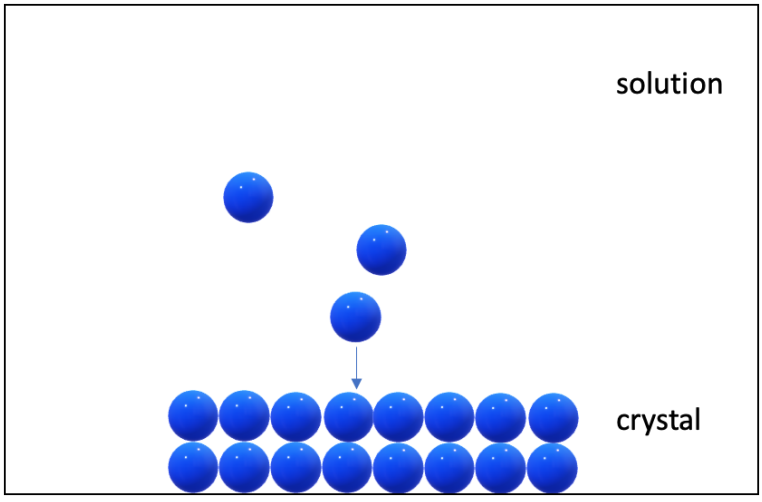

Figure 2.8 Schematic illustration of physical landscape of crystal growth [14]

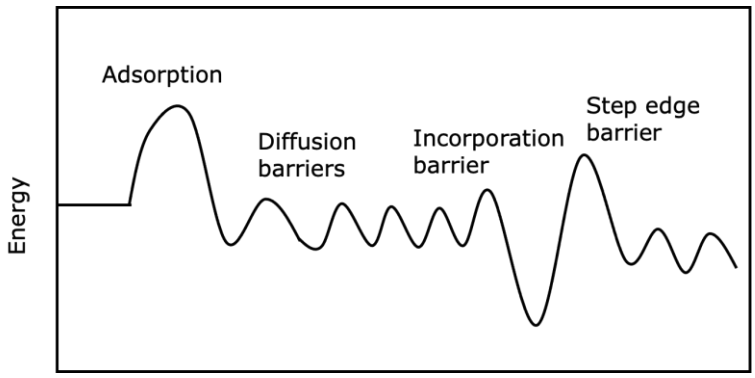

Figure 2.9 Schematic illustration of energy landscape of crystal growth [14]

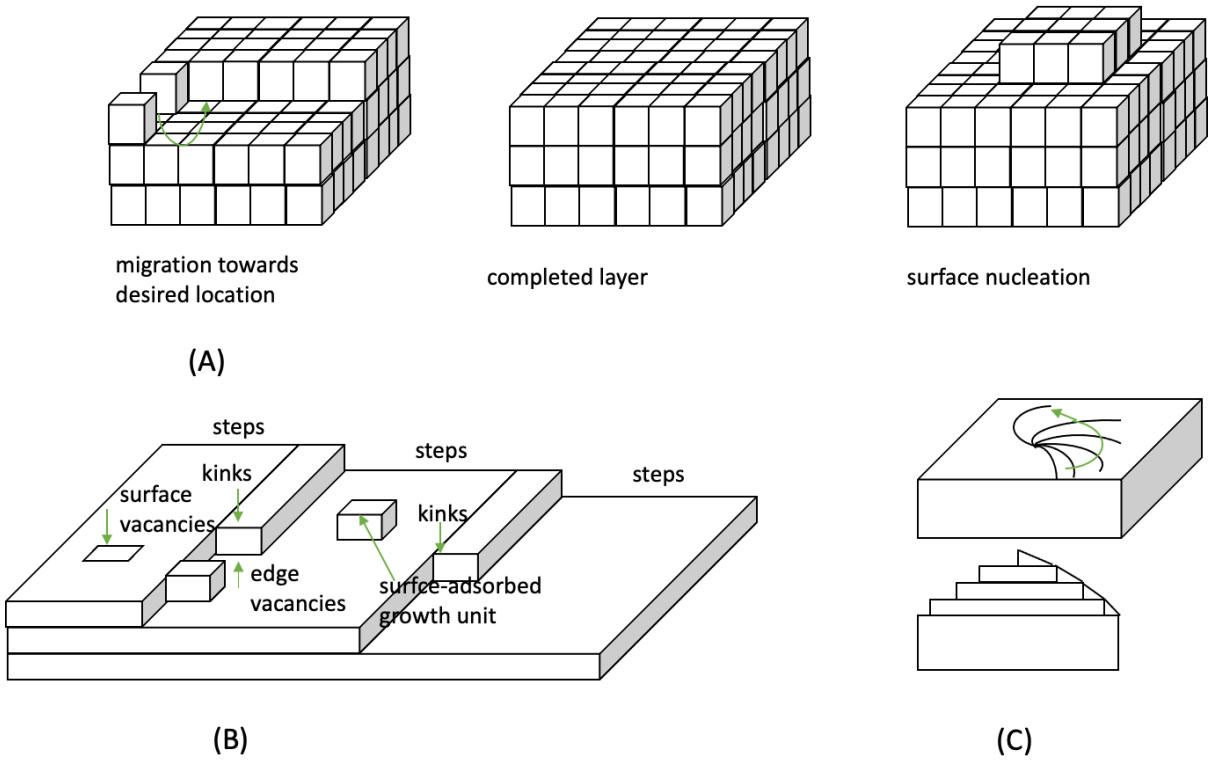

Figure 2.10 Schematic illustrations of adsorption layer theories.
(A) A model of crystal growth without dislocations; (B) Kossel's model of crystal growth; (C) Spiral growth from a screw dislocation.[11]

2.5. Protein Crystallisation in the presence of impurities

2.5.1. Impurities in Protein Crystallisation

Purity is one of the main parameters influencing crystallisation process and is also one of causes of low success rate and poor reproducibility of protein crystallisation.[96] Impurities in protein crystallisation include contaminating molecules in the starting material such as salts, lipid contents, solvents, host cell proteins of other species, and proteins without sequence integrity and conformational homogeneity.[96-100] Ewing et al. suggested three categories of the impurities in the commercial protein samples in their study: small molecules able to be removed by dialysis, macromolecules able to be removed by chromatography methods, and proteins in heterogeneous forms which are able to be removed by cation exchange chromatography.[101] Additionally, crystallisation agents such as salt, solvent, and polymers can also be regarded as impurities. Despite the impurities mentioned above, other foreign materials such as dust and nucleants mentioned in the previous section can also be regarded as impurities. Apart from bulk crystallisation, researchers in crystallography are also interested in the effects of impurities on crystallisation. Impurities, precipitant or other proteins, may influence the crystal quality and thus reduce the resolution of X-Ray diffraction.[102] Additionally, if the crystal quality is tolerant of impurities, the requirement for the purity level of the starting material would be reduce and the purification of proteins can be difficult and expensive.[99]

2.5.2. Effects of Impurities on Solubility

There are limited studies investigating the effect of protein impurities on solubility. No conclusion was drawn on whether impurity had any impact on protein solubility. Several studies have shown that structurally different protein impurities did not have

any significant effect on target protein solubility. Judge et al. (1995) stated that even high percentage of conalbumin and lysozyme impurities did not exhibit significant effect on ovalbumin solubility.[37] Skouri et al. (1995) also found no significant effect of trace amount of protein impurities on HEWL solubility.[103] Judge et al. (1998) also demonstrated structurally different protein impurities, avidin, conalbumin and ovalubumin up to 50%, had no significant effect on lysozyme solubility.[98] A structurally different impurity, thaumatin, also did not exist significant effect on HEWL solubility.[104] Lorber et al. (1993) suggested protein impurities reduced the solubility of lysozyme.[105] Bhamidi et al. (1999) reported slight increase of HEWL solubility with increasing amount of TEWL but the difference was not statistically significant.[106] Chen et al. (2021) reported BSA, a structurally different protein impurity, increased the HEWL solubility through protein-protein interactions.[107] Different from protein impurities, silica nanoparticles had no effects on HEWL solubility.[107]

2.5.3. Effects of Impurities on Nucleation and Crystal Growth

There was no universal conclusion drawn on whether impurity had negative impact on protein nucleation process. Due to the difficulty in direct observation and characterisation of nucleation process, there are few studies on the effects of impurities on nucleation in protein crystallisation. Whether nucleation is accelerated or decelerated in the presence of impurities remains unclear. Studies focused more on the impacts of impurities on crystal growth. Impurities may influence the quality of crystals as impurities often induce dislocation, lattice strain and stress. Most studies were focused on two main areas, whether the crystallisation process was influenced by the presence of impurities kinetically and whether the purity of the final crystal product was influenced, i.e. corporation of impurities in the crystals.

In terms of crystal growth rate, Judge et al. (1995) reported success bulk crystallisation of ovalbumin in the presence of conalbumin and lysozyme in a stirred 1-L batch crystalliser and protein impurities had no significant effect on the crystal growth rate.[37] In their later study of lysozyme crystallisation, impurity might have effect on specific face growth rate and could cause growth cessation at low supersaturation.[98] Thomas et al. (1996) showed a faster crystal growth and better structure homogeneity of highly purified HEWL compared to commercial HEWL without further purification.[97] In terms of morphology, Lorber et al. (1993) suggested that the presence of protein impurity, ovalbumin or BSA, would increase the number of twinned lysozyme crystals and reduce the reproducibility of crystallisation.[105] Hirschler et al. (1996) reported the effect of a structurally similar impurity, hen egg white lysozyme (HEWL) on the morphology of turkey egg white lysozyme (TEWL) crystals over a wide range of contamination level of 4 to 70% (w/w) while addition of a structurally similar impurity, ribonuclease A did not affect crystal morphology of TEWL.[108] Bhamidi et al. (1999) also tested the effects of TEWL on HEWL crystallisation and found a morphology change beacasue that TEWL inhibited the growth of HEWL in the [1 1 0] direction.[106] Ovalbumin and conalbumin, added to HEWL as structurally different protein impurities, introduced aggregates which might lead to heterogeneous nucleation of ill-shaped lysozyme crystals.[103] Hekmat et al. (2015) reported no host cell proteins were incorporated in the protein crystal lattices within detection limit of 1%, using lysozyme, lipase and enhanced green fluorescent protein as target proteins.[100] Vekilov et al. (1996) suggested that NaCl and protein impurity were nonuniformly incorporated in the crystal, mainly in a 40 μm core where the crystal growth rate was also slower.[102]

Crystal quality related to how well-ordered the crystalline material is can be evaluated from various aspects, such as qualitative visual quality, diffraction data resolution,

terminal size of the crystals, electron density and water structure, crystalline mosaic structure, etc.[109] The quality of protein crystals is believed to be strongly related to the impurities. Kurihara et al. (1999) measured local concentration of ovalbumin incorporated in HEWL crystal by fluorescence method and proposed that ovalbumin impurity was adsorbed at specific sites on the crystal during lysozyme crystal growth and the electrostatic interaction between protein molecules played a critical role in such impurity incorporation process.[110] Microgravity improved protein crystal quality and one of the reasons was that impurity incorporation was reduced via impurity depleted zone formation around the crystal under microgravity.[109, 111, 112] However, researchers also showed that microgravity crystals were more sensitive to impurity compared to crystals grown on earth.[113] The difference might be caused by the different crystallisation methods and experimental set-up. Otálora et al. (2009) suggested counterdiffusion crystallisation method was a suitable approach to minimise the effect of impurities.[114] Van Driessche et al. (2008) discussed the role of agarose gel in lysozyme crystallisation and showed that though the gel itself was an impurity, it could reduce the concentration of other impurities around the crystal surface and thus a net increase in crystal growth was observed.[115] Vekilov and Rosenberger (1998) showed that protein impurities up to 1% could lead to reduced growth rate and eventually growth cessation of lysozyme crystals.[116] Additionally, their studies emphasised the important role of convection which could increase supply of impurities to the crystal surface.[116, 117]

2.6. Protein Crystallisation for Bioseparation

2.6.1. Scaling-Up Protein Crystallisation

As described in Section 2.1, protein crystallisation is considered as a promising alternative bioseparation technique for therapeutic proteins. Crystalline proteins have higher purity and better stability, which is advantageous to formulation, downstream handling, and storage.[34-36] Albeit the benefits mentioned, protein crystallisation for bioseparation remains challenging and there are limited successful cases of scaled-up crystallisation of protein reported due to the lack of scale-up knowledge of protein crystallisation.[66, 118, 119] For crystallisation in a stirred tank, there are several criteria to be considered, including minimum agitation rate to keep crystals suspended, impeller tip speed, mean power input and the maximum local energy dissipation.[119] No general conclusion has been drawn on which parameter is the suitable scale-up criteria. Yang et al. (2019) proposed a scaling-up strategy of protein crystallisation from μL- to L-scale : 1) screening of crystallisation conditions using μl-scale vapour diffusion crystallisation method; 2) optimise the crystallisation conditions in mL-scale batch experiments on the shaker; 3) crystallisation in mL- to L-scale in stirred batch crystallisation or continuous mode crystallisation.[120]

2.6.2. Batch and Continuous Crystallisation Platform

Batch production remains the mainstream method in biopharmaceutical manufacture, especially for downstream separation, though continuous manufacture has the advantages of reduced footprint, lower cost, greater flexibility, better product quality and higher productivity.[121-125] Nevertheless, to integrate with the potential continuous upstream manufacturing of biopharmaceuticals, researchers have started to investigate different downstream separation and purification unit operations in continuous fashion, including chromatography[126-128], extraction[129-131], precipitation[63, 132, 133], crystallisation[120, 134, 135], etc. A limited number of newly developed novel

crystallisers have demonstrated the feasibility of protein crystallisation in a continuous platform as shown in Table 2.4. Challenges remain for continuous crystallisation in respect of process control and optimisation, real-time online analysis of solutions and crystals, as well as the current regulations in pharmaceutical manufacture.[118]

Table 2.3 A summary of recent bulk batch protein crystallisation studies

Protein	**Crystalliser**	**Scale**	**Mixing**	**Ref**
aprotinin variant	STC	<2000 mL	At 300 rpm	[136]
mAb01	STC	≤1000 mL	three-bladed segment impeller at 150-250 rpm	[137]
FabC225	STC	≤100 mL	Pitched-blade impeller at 100-300 rpm	[39]
Canakinumab Fab-fragment/lysozyme	STC	≤1000 mL	Three-bladed segment impeller at 50-300 rpm	[119]
single chain antibody	STC	≤220 mL	200 rpm	[138]
Lysozyme/lipase/eGFP	STC	5 mL	Three-bladed segment impeller at 100-170 rpm	[100]
lysozyme	ALC/ STC	≤500 mL	pneumatically agitated column (ALC)/pitched-blade turbine (STC) at 300 rpm	[139]
lipase	glass vessel (non-specific)	≤500 mL	none	[140]

Table 2.4 A summary of continuous protein crystallisation studies

Protein	Crystalliser	Scale	Mixing	Ref.
lysozyme	Forced Flow through Glass Capillaries	<8.5 mL	flow	[141]
lysozyme	segmented slug flow tubular crystallizer (SFC) with temperature variation	<41 mL	flow	[134]
lysozyme/ mAb01	stirred tank crystalliser (STC) with a cooled tubular reactor in bypass	180 mL	three-bladed segment impeller	[142]
lysozyme	oscillatory flow crystallizer	<20 mL	flow	[120, 143]
lysozyme	microfluidic device with coplanar electrodes	≤1mL	flow	[144]
lysozyme	oscillatory baffled crystallizer (OBC)	300/1250 mL	flow	[145]
insulin	segmented slug flow tubular crystallizer (SFC)	<135 mL	flow	[146]
lysozyme	MSMPR, airlift crystallizer (ALC), stirred tank crystalliser (STC)	≤400 mL	pneumatically agitated column (ALC), pitched-blade turbine (STC) at 300 rpm	[135]
lysozyme	segmented slug flow tubular crystallizer (SFC)	<40 mL	flow	[147]
lysozyme	continuous slug flow crystallizer (CSFC)	≤150 mL	flow	[148]

2.7. Model Proteins Used in the Study

2.7.1. Lysozyme

Lysozyme, first discovered by Sir Alexander Fleming in 1922, is the first enzyme completed an X-ray crystallographic analysis and is also one of the most extensively studied protein in crystallisation research.[149-151] Lysozymes are defined as bacterial

peptidoglycan 1,4-fl-N-acetylmuramidases that catalyses hydrolysis of the bond between the C-1 of N-acetylmuramic acid and the C-4 of N-acetylglucosamine.[152] Lysozymes are abundant in nature and hen egg white lysozyme (HEWL) is one of the most intensively studied lysozymes.[151] Lysozyme is also reported with anti-bacterial properties and thus is used in food preservation and in pharmaceutical formulation.[95, 153, 154] HEWL is used as the model protein in this study. HEWL consists of 129 amino acids, has a molecular weight about 14.4 kDa, and is with a relatively high isoelectric point (pI) of 11.1.[155-157]

Table 2.5 Summary of 5 crystal forms of hen egg white lysozyme crystals reported in protein data bank

Crystal Form	**Space Group**	**Crystallisation Experiment**	**Ref.**
monoclinic	P1 2_1 1	Sodium chloride, 1-propanol, pH 7.6, 40 °C, batch method	[158]
	P1 2_1 1	Sodium iodide, acetate buffer, pH 4.0/pH 8.0, microbatch method	[159]
	P1 2_1 1	Sodium nitrate, pH4.5	[160]
	P1 2_1 1	Potassium thiocyanate, acetate buffer, pH 4.5, hanging-drop vapour-diffusion method	[161]
tetragonal	P $4_3 2_1 2$	Sodium chloride, acetate buffer, 20 °C, counter-diffusion method/ batch method/ vapor-diffusion method	[162-164]
	P $4_3 2_1 2$	2-methyl-2,4-pentanediol, trishydroxymethylaminomethane, pH 8.0, 20 °C, hanging-drop vapor-diffusion method	[165]
triclinic	A 1	Sodium nitrate, acetate buffer, pH 4.5, microbatch method	[159]
	P 1	Sodium nitrate, acetate buffer, pH 4.5, batch method	[166]
orthorhombic	P 2_1 2_1 2_1	Sodium chloride, pH 9.6	[160]
	P 2_1 2_1 2_1	NaCl, sodium acetate buffer, pH 4.5, 40 °C	[167]
hexagonal	P 6_1 2 2	Sodium nitrate, acetone, pH 8.4, 20 °C, batch method	[168]

2.7.2. Thaumatin

Thaumatin, naturally originated from the fruit of *Thaumatococcus daniellii*, is a sweet protein 3000 times more sweet than sucrose on a weight basis.[169] It is considered as a potential alternative low-calorie sweetener. Apart from isolation from natural fruit, thaumatin can also be produced via bioproduction host such as bacteria, yeast, fungi, and transgenic plant.[169-173] Thaumatin consists of 207 amino acids, has a molecular weight about 22.2 kDa, and is with a high pI of 12.[174, 175] Thaumatin is also often used as a model protein in crystallisation studies since addition of tartrate ions can induce rapid crystallisation of thaumatin.[176]

Table 2.6 Summary of 4 crystal forms of thaumatin crystals reported in protein data bank

Crystal Form	**Space Group**	**Crystallisation Experiment**	**Ref.**
tetragonal	$P4_12_12$	sodium L-tartrate, sodium phosphate buffer, pH 7.1, 10 % v/v glycerol, 22 °C, microbatch	[177]
	$P4_12_12$	Na-ADA, agarose gel (0.15 % m/V), 20 °C, microdialysis method	[178]
	$P4_12_12$	sodium potassium tartrate, pH 6.8, 25 °C, hanging-drop vapour-diffusion method	[179]
orthorhombic	$P2_12_12_1$	sodium D-tartrate, sodium phosphate buffer, pH 7.1, 10 % v/v glycerol, 22 °C, microbatch	[177]
	$P2_12_12_1$	sodium meso-tartrate, sodium phosphate buffer, pH 7.3, 10 % v/v glycerol, 4 °C, microbatch	[177]
monoclinic	C2	PEG 3350, vapour-diffusion method	[180]
hexagonal	$P6_1$	Ammonium sulfate, glycerol, PEG 400, lithium sulfate, magnesium sulfate, sodium acetate, pH 4.5, 20 °C, hanging-drop vapour-diffusion method	[181]

3. Materials and Methods

3.1. Materials

Lysozyme from chicken egg white (L6876), thaumatin from *Thaumatococcus daniellii* (T7638), 1,4-Piperazinediethanesulfonic acid (PIPES) (≥ 99%), mesoporous SBA-15 (806803, <150 μm particle size, pore size 4 nm, hexagonal pore morphology), non-porous silica (904465, monodisperse, non-porous, 2.0 μm), mesoporous silica (806900, mesoporous, 2 μm particle size, pore size ~4 nm), potassium sodium tartrate tetrahydrate (99%), sodium chloride (≥ 99%), and sodium acetate anhydrous (≥ 99%) were purchased from Sigma-Aldrich (Dorset, UK). Sodium hydroxide (≥ 98.5%) and hydrochloric acid (37% w/w) were purchased from VWR (Lutterworth, UK). Deionised water was obtained using PURELAB Chorus 1 water purification system (ELGA LabWater). All chemicals were used as received without further purification.

3.2. Characterisation Methods

3.2.1. Characterisation of Protein Samples

UV-Vis Spectroscopy

Protein concentration in the solution was determined using Nanodrop One^{c} microvolume UV-Vis spectrophotometer (Thermo Scientific™) at the wavelength of 280 nm with mass extinction coefficient ($\varepsilon_{1\%}$) of 26.4 L/g-cm for lysozyme [182] and of 12.7 L/gm-cm for thaumatin [183]. An example of the spectrum of lysozyme and thaumatin solutions is shown in Figure 8.1. Protein solution with expected concentration higher than 50 mg/mL was diluted before measured by UV-Vis spectrophotometer. As shown in Figure 8.2, the relationship between absorbance and

protein concentration remained linear in the range of 0 - 50 mg/mL. 2 µL of solution was used each time and the measurement was repeated 3 times for each sample. For samples containing protein condensation or silica particles which might interfering with the UV light and thus affecting the results, 10 µL of aliquot was sampled and was centrifuged at 2000g (Thermo Scientific™ mySPIN™ 6) for 1 minute to settle any particles in the sample.

Optical Microscopy

Optical microscope (Olympus, CX41) was used for microscopy observation of the samples in this study. The magnification of the objective lens used was 5x, 10x, or 20x, and the magnification of the eyepieces was 10x. Microscopic images were captured by a mounted camera on the microscope (GT Vision, GXCAM HICHROME-MET). To identify the protein crystals from the salt crystals, 0.5 µL Izit Crystal Dye (Hampton Research, US) was added to the droplet. Protein crystals would be dyed to blue colour while the salt crystals would remain transparent.

Laser Diffraction

Crystal size distribution of the samples was determined by Mastersizer 2000 (Malvern Instruments, UK) with a small volume sample dispersion unit Hydro SM (Malvern Instruments, UK) at the speed of 1000 rpm. Ethanol was used as the dispersant. 0.5 – 1.0 mL of sample was used for the measurement.

Dynamic Light Scattering

The hydrodynamic diameters of lysozyme and thaumatin were determined using dynamic light scattering (DLS). DLS measurements were performed on aqueous

protein solutions in 0.1 M PIPES buffer pH 6.8 using Malvern Zetasizer μV (Malvern Instruments, UK) with disposable polystyrene cuvettes. Measurements were repeated at least 5 times and the averaged data are used.

Lysozyme Activity Test

The bioactivity of lysozyme was tested by using the lysozyme activity kit (LY0100, Sigma-Aldrich). Lysozyme can cleave the bonds between N-acetyl-D-glucosamine and N-acetylmuramic acid residues in mucopolysaccharides and the clycan skeletons of the peptidoglycans. The test was based on the ability of lysozyme in the cell disruption of *Micrococcus lysodeikticus*. The reaction of *Micrococcus lysodeikticus* cell suspension and lysozyme was monitored by Nanodrop One^{c} microvolume UV-Vis spectrophotometer (Thermo Scientific™) at the wavelength of 450 nm. Cuvette mode was used in lysozyme activity test.

3.2.2. Characterisation of Silica Particles

Nitrogen Adsorption

Pore size of the silica particles purchased from Sigma were further analyzed by nitrogen adsorption experiments. Silica particles were degassed at 120 °C for 24 hours before the nitrogen adsorption experiments. The nitrogen adsorption and desorption isotherms were then obtained by using TriStar3000 (Micromeritics Instrument Corporation, US). Calculated specific surface area based on Brunauer−Emmett−Teller (BET) model and calculated pore size distribution based on Barrett−Joyner−Halenda (BJH) model were given by the software (Micromeritics Instrument Corporation, US).

3.3. Protein Crystallisation Experiments

3.3.1. Hanging-Drop Vapour-Diffusion Crystallisation

Sodium chloride (NaCl) precipitant solution was prepared by dissolving NaCl in 0.1 M sodium acetate (NaAc) Buffer, pH 4.8. Potassium sodium tartrate tetrahydrate precipitant solution was prepared by dissolving potassium sodium tartrate tetrahydrate in 0.1 M PIPES buffer, pH 6.8. Precipitant solutions were filtered through 0.22 µm Millex-GS Syringe Filter Units (Merck Millipore, US). For experiments with silica particles, silica particles were suspended in the filtered precipitant solution. Protein solution was prepared by dissolving the protein powder into the buffer solution which was the same buffer as used for the precipitant solution preparation. Protein concentration in the solution was determined by Nanodrop One^{c} microvolume UV-Vis spectrophotometer (Thermo Scientific™) at 280 nm as described in section 3.2.1. Lysozyme-thaumatin mixtures were prepared by mixing lysozyme solution and thaumatin solution with known concentrations. Protein solutions were filtered through 0.22 µm syringe filter (VWR, UK). HDVD crystallisation experiments were conducted in 24-well VDX™ plate with sealant (Hampton Research, US). Each well was filled with 500 µL precipitant solution. A 4 µL droplet with equal volume of protein solution and precipitant solution was deposited on a borosilicate cover glass (VWR, UK). The cover glass with the droplet was inversed cautiously and then sealed onto the well filled with reservoir.

The crystallisation results were based on the observations of the droplets under the optical microscope. Lysozyme crystals and thaumatin crystals were distinguished by the shapes. Lysozyme crystals in this study were tetragonal lysozyme crystals with four hexagonal faces and eight rectangular faces while thaumatin crystals were in

bipyramidal shapes. All the droplets were categorised into (1) no crystal, (2) precipitation, (3) only lysozyme crystal(s), (4) only thaumatin crystal(s) and (5) both lysozyme crystal (s) and thaumatin crystal(s). Due to the limitation of the maximum amplification of the optical microscope, only crystals larger than about 5 μm can be observed and the shape of the crystal can be recognised, i.e., result was marked as '(5) both types of crystals' providing at least one lysozyme crystal larger than 5 μm and at least one thaumatin crystal larger than 5 μm were observed in the droplet at the same time. Conditions with protein concentration lower than 50 mg/mL were repeated 48 - 120 times. Conditions with higher protein concentration were repeated at least 12 times.

3.3.2. Batch Crystallisation

Crystallisation precipitant solution was prepared by dissolving potassium sodium tartrate tetrahydrate at 560 mg/mL in 0.1 M PIPES buffer, pH 6.8. Protein (lysozyme/thaumatin) solution was prepared by dissolving protein powder into the buffer solution. Lysozyme-thaumatin mixtures were prepared by mixing pre-prepared lysozyme solution and thaumatin solution with determined concentrations. All solutions were filtered through 0.22 μm Millex-GS Syringe Filter Units (Millipore) before crystallisation trials.

Batch crystallisation experiments were conducted at room temperature of 20 °C (± 1 °C) and each condition with at least 3 replicates if not specified. The experiments were implemented in 1.5 mL polypropylene centrifuge tubes with snap cap (Fisherbrand™) or 10 mL glass vial. Equal volume of protein solution and precipitant solution were added to the container and the solution was actively mixed manually by pipetting several times before sitting on the bench or on the shaker.

Samples for static batch crystallisation without agitation were placed on a bench without mechanical vibration. The samples were kept as static as possible. For sampling, only the snap cap was opened to avoid any additional agitation except the disturbance caused by pipetting.

Samples for agitated batch crystallisation were placed on the orbital shaker (SciQuip, SP2250-03, 20 mm orbital diameter) and were fixed by 2 bars (SciQuip, SP2250-SK180.1) immediately after mixing.

The protein crystallisation process was characterised by protein de-supersaturation process and optical imaging of the samples. To track the de-supersaturation process in a sample, the dissolved protein concentration was monitored off-line over time by Nanodrop One^{c} microvolume UV-Vis spectrophotometer at 280nm. Microscopy observation using optical microscope (Olympus, CX41) was conducted in addition to ensure the concentration change was from crystallisation rather than liquid-liquid phase separation, precipitation, or other amorphous condensations. Microscopic images were captured using a mounted camera on the microscope (GT Vision, GXCAM HICHROME-MET).

4. Protein Crystal Occurrence Domains in Crystallisation from Lysozyme-Thaumatin Mixture

4.1. Overview

In Chapter 4, suitable crystallisation conditions were determined by HDVD experiments for lysozyme, thaumatin, and lysozyme-thaumatin mixture. A precipitant was found to be able to crystallise out both lysozyme and thaumatin. A range of mixture composition was tested for two model proteins, and four occurrence domains of protein crystals were identified. These domains depended on the mixture composition though was time dependent. The crystallisation process as kinetically hindered in the presence of impurities. Here, we demonstrate that protein crystallisation is a feasible approach to separate proteins from a complex mixture. This study further provides the foundation knowledge for work on protein crystallisation for bioseparation, seeding/heterogeneous nucleation including process scale-up.

4.2. Experimental Methodology

In this Chapter, hanging-drop vapour-diffusion (HDVD) crystallisation method was used in all the experiments. HDVD crystallisation set-up was described in Chapter 3. And the experimental conditions listed in Table 4.1 were tested.

The crystallisation plates were observed under optical microscope regularly over time. The droplets were classified into 5 categories: (1) clear droplet, (2) precipitation, (3) only lysozyme crystal(s), (4) only thaumatin crystals, and (5) both lysozyme crystal(s) and thaumatin crystal(s). Only crystals larger than approximately 5 μm would be

recorded due to the limitation of resolution of the microscope. The shape of the crystals smaller than this value was not recognisable.

Protein crystallisation via vapour-diffusion method is considered as inherently poorly reproducible. And there were massive number of conditions tested at this stage. Therefore, it was not feasible to apply single crystal X-ray diffraction characterisation to each crystal due to the low-throughput, excessive time spam and difficulty in obtaining representative analysis for the whole sample population. The application of optical microscopic images of the droplet sample was a fast and robust way in screening the crystallisation conditions and the results were real-time and were relatively consistent and representative since all the droplets were examined rather than single crystals were sampled and tested off-line. To enhance the confidence level of the results, conditions with protein concentration lower than 50 mg/mL were repeated in 48 to 120 droplets. Conditions with protein concentration higher than 50 mg/mL were repeated at least 12 times to reassure the accuracy of the results.

Table 4.1 Experimental conditions tested in the experiments

Protein Type	**Temperature**	**Precipitant solution**	
		Sodium Chloride in 0.1 M Sodium Acetate Buffer, pH 4.8	Potassium Sodium Tartrate Tetrahydrate in 0.1 M PIPES Buffer, pH 6.8
Lysozyme	4 °C	5 - 50 mg/mL Lyso.	5 - 50 mg/mL Lyso.
	20 °C	10 - 100 mg/mL Lyso.	10 - 100 mg/mL Lyso.
Thaumatin	4 °C	5 - 50mg/mL Thau.	5 - 50 mg/mL Thau.
	20 °C	10 - 100 mg/mL Thau.	10 - 100 mg/mL Thau.
Lysozyme-Thaumatin Mixture	4 °C	/	/
	20 °C	/	10 - 100 mg/mL Lyso. and 10 - 100 mg/mL Thau.

4.3. Results and Discussion

4.3.1. Determination of Protein Crystallisation Condition in HDVD Crystallisation Experiments

The results in Table 4.2 show that lysozyme and thaumatin were able to be crystallised individually from their single-protein solutions against crystallisation condition in which potassium sodium tartrate tetrahydrate was used as precipitant. Yet, under the conditions investigated in this study, no thaumatin crystal was obtained by using sodium chloride as precipitant. The droplets remained clear or only precipitations were observed in the period of observation.

Figure 4.1 shows illustrative images of the crystallisation droplets crystallised using potassium sodium tartrate tetrahydrate as precipitant. The shapes of thaumatin crystals and lysozyme crystals grown using this precipitant were different. In the range of concentrations investigated in this study, tetragonal lysozyme crystals were obtained from lysozyme solution while bypiramidal thaumatin crystals were obtained from thaumatin solution. These two types of protein crystals can be distinguished under the optical microscope by their crystal shapes. Figure 4.1 reveals that both lysozyme crystals and thaumatin crystals can be crystallised out from a lysozyme-thaumatin mixture using the tartrate salt as the precipitant while still possessing distinct crystal shapes. Thaumatin crystals remained as bipyramidal shape in the mixture. Lysozyme crystals were tetragonal crystals though defects might be detected under certain conditions. Therefore, further experiments where preferential crystallisation from lysozyme-thaumatin binary protein mixture was attempted were conducted by using potassium sodium tartrate as precipitant rather than sodium chloride.

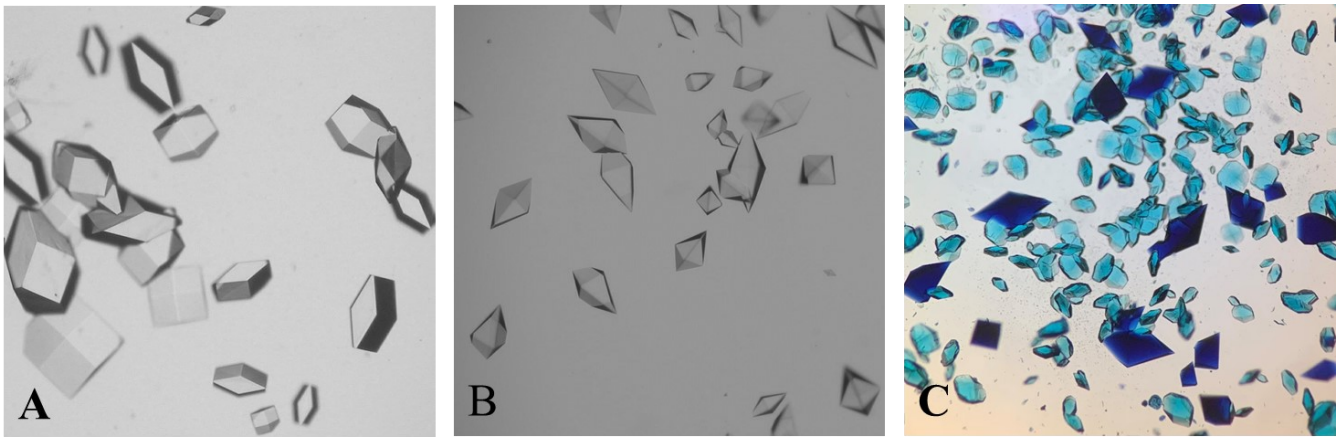

Figure 4.1 Representative images of lysozyme crystals and thaumatin crystals crystallised against 141 mg/mL potassium sodium tartrate tetrahydrate precipitant solution.
A: 50 mg/mL lysozyme. Only tetragonal lysozyme crystals in the droplet; B: 50 mg/mL thaumatin. Only bipyramidal thaumatin crystals in the droplet; C: 50 mg/mL thaumatin + 50 mg/mL lysozyme. Both lysozyme and thaumatin crystals in the droplet and this photo was captured after Izit Crystal Dye (Hampton Research, US) was added to the droplet. All the transparent crystals absorbed dye molecules and turned to be blue afterward. The bipyramidal thaumatin crystals were darker compared to lysozyme crystals.

Table 4.2 Summary of crystallisation experimental results from pure thaumatin solution and pure lysozyme solution under different crystallisation conditions used in this study

Protein Type	**Temperature**	**Precipitant solution**	
		Sodium Chloride in 0.1 M Sodium Acetate Buffer, pH 4.8	Potassium Sodium Tartrate Tetrahydrate in 0.1 M PIPES Buffer, pH 6.8
Lysozyme	4 °C	Tetragonal Crystal(s)	Tetragonal Crystal(s)
	20 °C	Tetragonal Crystal(s)	Tetragonal Crystal(s)
Thaumatin	4 °C	Clear/Precipitation	Bypiramidal Crystal(s)
	20 °C	Clear/Precipitation	Bypiramidal Crystal(s)

4.3.2. Protein Crystallisation from Binary-Protein Mixture

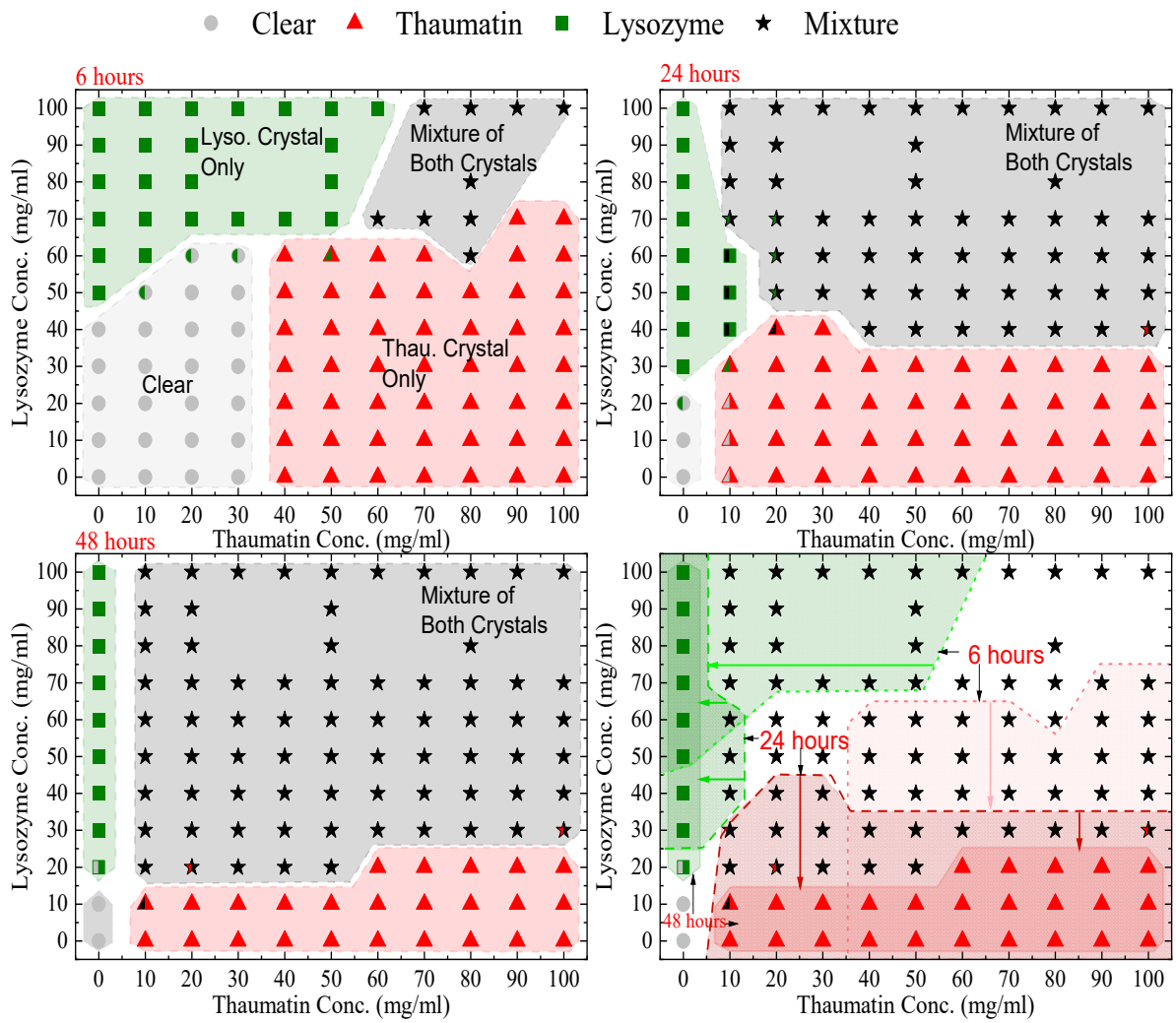

Figure 4.2 A schematic illustration of the protein crystal domains of crystallisation from lysozyme-thaumatin mixture in this study.

The time denotes the moment from the crystallisation plates were set up. Circle symbols (grey) represent experimental results where the droplets remained clear with no crystals observed; square symbols (green) represent experimental results where only lysozyme crystals were observed in the droplet; triangle symbols (red) represent results where only thaumatin crystals were observed in the droplet; star symbols (black) represent results where both lysozyme crystals and thaumatin crystals were observed in the same droplet. Each point in the figure 12 to 120 replicate droplets depending on the mixture composition. The symbols with only one colour represent 100% of the droplets in the study had the stated results. The symbols with two colours followed the results with the highest possibility. For instance, after 6 hours, 10 mg/mL thaumatin and 10 mg/mL lysozyme, most droplets only had thaumatin crystals, but a few droplets had both types of crystals. The shaded regions in the figure only serve as a visual guidance to highlight the domains where different situations were observed.

HDVD crystallisation method was used in this stage of crystallisation condition screening processes to investigate an operating window for crystallisation from the model mixture. An initial precipitant concentration of 141 mg/mL potassium sodium tartrate tetrahydrate in the buffered solution and temperature at 20 °C were kept the same for the whole set of experiments. The crystallisation plates were observed regularly and for simplicity of the diagram, results listed only included 6 hours, 24 hours, and 48 hours after the plates were set up. The crystallisation period was kept relatively short (days) because of the operation time in the future scaling-up experiment would not be run for weeks due to the stability of protein solution.

Four crystal occurrence domains were observed from the crystallisation droplets as shown in Figure 4.2: 1) clear domain with no crystal formation in which no crystal > 5 μm was detected (crystal smaller than 5 μm was not detectable using the optical microscope used in this study), 2 & 3) target domains with only one type of protein crystals (lysozyme crystals or thaumatin crystals only) and 4) mixture domain with a mixture of both types of protein crystals. Images in Figure 4.2 are not strict phase diagrams as discussed in section 2.2.3. The droplets were not at equilibrium at the given conditions. Figure 4.2 shows the evolution of crystallisation domains over time. The results also suggested that one type of protein was going to be crystallised out first from the mixture and followed by the other protein later. And the sequence was depending on the mixture composition. This suggests that within a certain period, harvesting a single type of protein crystals from the mixture for separation purpose is feasible. Comparing the crystallisation results of single protein solution and results of protein mixture, Figure 4.2 also reveals that the presence of another protein in the mixture would normally hinder the crystallisation process of the target protein. For instance, after 6 hours, crystals were observed in droplets containing 50 mg/mL

lysozyme, but it remained clear after the same amount of time when more than 20 mg/mL of thaumatin existing on top of the lysozyme in the droplet.

After 6 hours, a clear droplet domain existed in low protein concentration range with lysozyme concentration ≤ 40 mg/mL and thaumatin concentration ≤ 30 mg/mL. In this region, the degree of supersaturation was relatively low and thus crystallisation process was slow. However, after 2 weeks, crystals were observed in this region. Additionally, this clear region reached out to the range of lysozyme concentration of 50 - 60 mg/mL with a thaumatin concentration ≤ 30 mg/mL. In this extended part, though lysozyme crystals were observed from pure lysozyme solution with the same initial lysozyme concentration, no lysozyme crystallised out as the thaumatin was present in the mixture. Furthermore, when lysozyme concentration was 50 - 60 mg/mL with a thaumatin concentration > 30 mg/mL, there was still no lysozyme crystals observed. Lysozyme crystallisation was inhibited within 6 hours due to thaumatin in the mixture. A similar tendency was observed when the initial concentration of thaumatin was 40 – 60 mg/mL, when a higher amount of lysozyme presents in the mixture, no thaumatin crystals were observed after 6 hours while thaumatin crystals were observed in droplets with the same initial thaumatin concentrations. Thaumatin crystallisation was inhibited due to high amount of lysozyme in the solution. With a higher initial lysozyme concentration (> 70 mg/mL), lysozyme always crystallised out regardless of the thaumatin concentration in the mixture in the range studied in this work. In the mixture containing both high concentrations of lysozyme and thaumatin, a mixture of both types of protein crystals were observed.

After 24 hours, the mixture domain expanded, and protein crystals were observed in the regions with lower initial protein concentrations. Thaumatin crystal only domain still

existed for all mixture droplets with an initial lysozyme concentration no more than 30 mg/mL. However, the domain with only lysozyme crystals almost retreated to the region where no thaumatin was added from the beginning, i.e., pure lysozyme solution.

After 48 hours, the clear region shrank dramatically to the region where the initial lysozyme concentration was no greater than 10 mg/mL. So did the lysozyme crystal only domain and thaumatin crystal only domain. There was no domain with only lysozyme crystals in all the mixture compositions tested. Additionally, the domain with a mixture of both protein crystals expanded further. Apart from experiments 20 mg/mL lysozyme initially and thaumatin concentration higher than 50 mg/mL, in which only thaumatin crystals were observed after 48 hours, all mixture droplets with lysozyme concentration higher than 10 mg/mL had both types of protein crystals.

Figure 4.3 shows a set of representative microscopic photos of the crystallisation droplets 24 hours after the experiments started, both crystal size and crystal number of thaumatin crystals were reduced dramatically as lysozyme concentration increased. Nevertheless, when the initial lysozyme concentration was higher than 80 mg/mL, the number of thaumatin crystals increased. This increase may be due to that lysozyme crystallisation was faster resulting from the high degree of supersaturation. Consequently, free lysozyme in the solution decreased and thus thaumatin crystallisation was less affected by lysozyme in the mixture. Another assumption is based on the nature of protein crystal that protein crystal retains relatively high solvent content comparing to small molecule crystals[184]. Therefore, as more protein crystals formed from the mixture, less solvent was left in the mixture and thaumatin concentration might have increased accordingly.

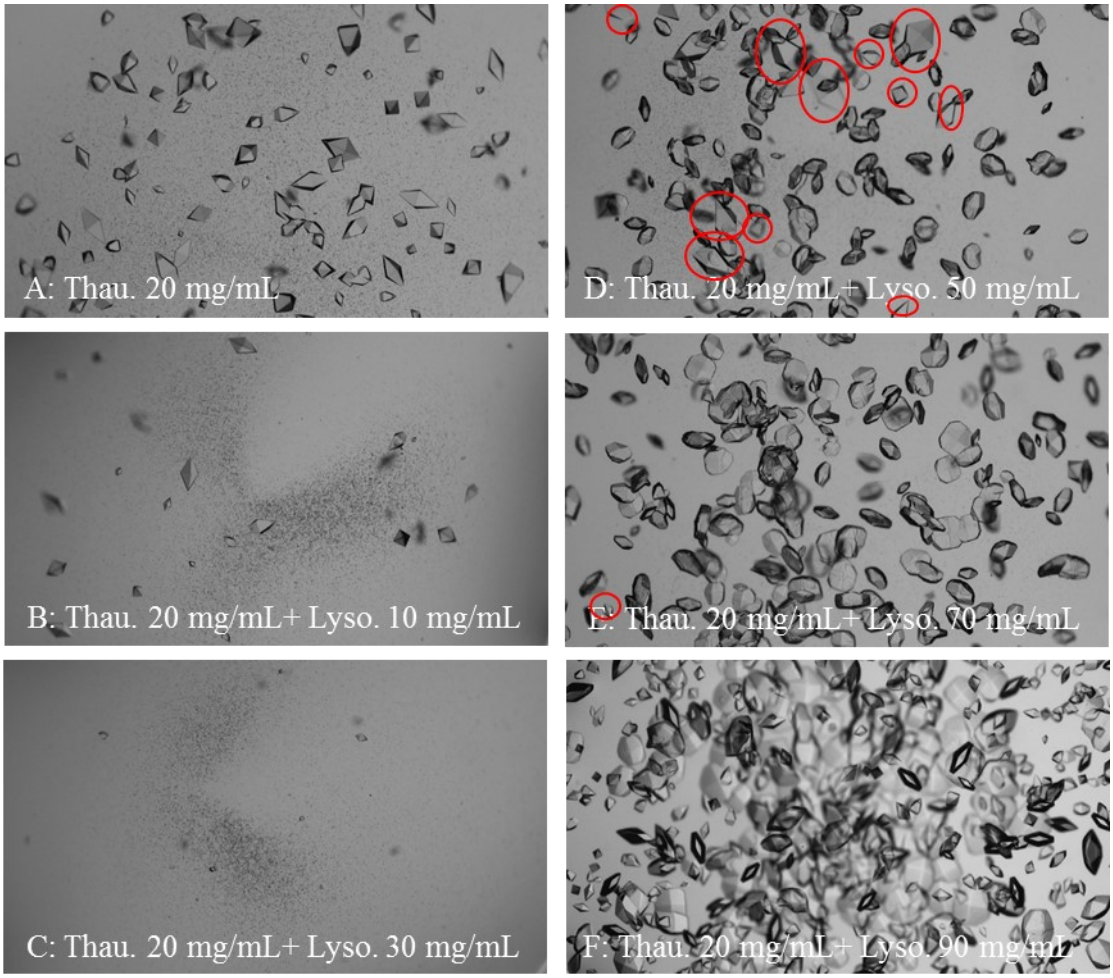

Figure 4.3 Representative images of lysozyme crystals and thaumatin crystals obtained from the crystallisation conditions after 24 hours starting with the same thaumatin concentration (20 mg/mL) but different lysozyme concentrations A: 0 mg/mL; B: 10 mg/mL; C: 30 mg/mL; D: 50 mg/mL; E: 70 mg/mL; F: 90 mg/mL). A, B, and C have only thaumatin crystals. D, E and F have a mixture of lysozyme crystals and thaumatin crystals. Thaumatin crystals were circled out in D and E.

Furthermore, as shown in Figure 4.2, when the initial thaumatin concentration was 10 – 20 mg/mL with a moderate lysozyme concentration of 30 – 70 mg/mL, the chance of successful crystallisation of each type of protein was not 100% and thus lead to an overlap of clear, target, and mixture domains. As shown in Figure 4.3 (D and E), in this composition region, due to the presence of lysozyme in the solution, both crystal

size and crystal number of thaumatin crystals were reduced significantly. Lysozyme crystallisation dominated in this region and there were chances that thaumatin did not crystallise when the initial thaumatin concentration was low.

In general, as shown in Figure 4.2, there was always one type of protein crystallised out from the solution first and then followed by the other protein crystals. And the sequence was decided by the composition of the mixture, i.e., degrees of supersaturation of the proteins. When enough time was provided, both lysozyme and thaumatin would crystallise out from the mixture. This suggests that when operation time was controlled properly, bio-separation can be achieved via preferential protein crystallisation even if protein impurity in the mixture was supersaturated and able to be crystallised out under the crystallisation condition.

We also suggest that the presence of another protein, acting as an impurity in the solution, will slow down the crystallisation process of both the target protein and the impurity protein itself. Still, the crystallisation process was not inhibited completely. Additionally, in the model system studied in this work, we did not find evidence that the existing lysozyme protein crystal could stimulate thaumatin crystallisation or vice versa. Hence protein crystals as seeding remains as an option to facilitate target protein crystallisation from the mixture without the risks of promoting the impurity crystallisation simultaneously.

4.4. Conclusions

In this study, we successfully demonstrated preferential protein crystallisation using lysozyme-thaumatin binary mixture as the model. Four domains were identified: 1)

clear domain, 2 & 3) target domains with only one type of protein crystals (lysozyme crystals or thaumatin crystals only) and 4) mixture domain with a mixture of both types of protein crystals. These domains depended on the mixture composition and shifted with time. There was no direct evidence in this study that protein solubility was changed due to the existence of protein impurity. In the model binary protein mixture, the presence of another protein impurity can slow down the crystallisation process of the target protein. This implies that crystallisation kinetics plays a key role for selective crystallisation from the mixture. Furthermore, as the kinetics of crystallisation can also be manipulated by the presence of the protein impurities, it highlights the importance of further investigation of the effect of protein impurities in more complex crystallisation system. This work demonstrates that protein crystallisation is not only applicable to high-purity protein solution but also a feasible approach to separate a target protein from a more complex mixture environment, even for protein mixtures with both proteins supersaturated. This work also provides a working model system with essential foundation knowledge for future work on protein crystallisation for bioseparation, such as scale-up crystallisation process, seeding, and crystallisation facilitated by heterogeneous nucleants.

5. Moving from Hanging-Drop Vapour-Diffusion Crystallisation to Batch Crystallisation

5.1. Overview

In Chapter 4, an experimental evidence of direct selective protein crystallization from lysozyme-thaumatin model binary mixture using HDVD crystallisation method was shown. Potassium sodium tartrate salt could induce crystallisation of both lysozyme and thaumatin. It was shown that protein impurity had adverse impact on target protein crystallisation. Due to the mechanism of HDVD method, the salt concentration and protein concentration kept changing in as the droplet vapourised and it was not feasible to evaluate the kinetics of protein crystallisation process due to the limited scale. To obtain quantitative data rather than qualitative results, the experiments moved from HDVD method to batch method.

In Chapter 5, both pure lysozyme solution and lysozyme-thaumatin mixture were used in batch mode crystallisation experiments. The experiments started with quiescent batch crystallisation. Different sampling strategies (sampling timing and frequency) were used and the variances between batches were significant regardless of the sampling strategies. Further experiments were conducted in agitated batch crystallisation set-up. Agitation was provided by orbital shaker in this study. In this chapter, the aim was to study whether agitation could improve the reproducibility in batch crystallisation. Furthermore, the effects of agitation on protein crystallisation process were studied.

5.2. Experimental Methodology

All batch crystallisation experiments in this study were conducted at room temperature of 20 °C (± 1 °C) with at least 3 replicates for each condition. The experiments were implemented in 1.5 mL polypropylene centrifuge tubes with snap cap (Fisherbrand™). 500 µL protein solution was added to the tube and then 500 µL precipitant solution was added to the same tube. The solution was actively mixed manually by several pipetting before sitting on the bench or the shaker. Samples for static batch crystallisation without agitation were placed on a 4-way interlocking tube rack (capacity of 32 for 1.5 mL tubes) on a bench without mechanical vibration. The samples were kept as static as achievable. For sampling, only the snap cap was opened to avoid any additional agitation except the disturbance caused by pipetting. Samples for agitated batch crystallisation were also placed on a 4-way interlocking tube rack (capacity of 32 for 1.5 mL tubes) and then the whole rack was positioned on the orbital shaker (SciQuip, SP2250-03, 20 mm orbital diameter) and was fixed by 2 bars (SciQuip, SP2250-SK180.1) immediately after mixing. The experimental conditions and sampling strategies are listed in Table 5.1.

The protein crystallisation process was characterised by protein de-supersaturation process and optical imaging of the samples. To track the de-supersaturation process in a sample, the dissolved protein concentration was monitored off-line over time by Nanodrop One^{c} microvolume UV-Vis spectrophotometer at 280nm. Microscopy observation using optical microscope (Olympus, CX41) was compiled to ensure the concentration change was from crystallisation rather than liquid-liquid phase separation, precipitation, or other amorphous condensations. Microscopic images were captured using a mounted camera on the microscope (GT Vision, GXCAM HICHROME-MET).

Table 5.1 Experimental conditions and sampling strategies.

	Condition 1 60 mg/mL Lyso.	Condition 2 60 mg/mL Lyso. + 6 mg/mL Thau.	Condition 3 60 mg/mL Lyso. + 12 mg/mL Thau.	Condition 4 6 mg/mL Thau.	Condition 5 12 mg/mL Thau.
Static	Case 1-6	Case 1-4	Case 1-4	Case 1, 4	Case 1, 4
50 rpm	Case 5, 6	-	-	-	-
100 rpm	Case 5, 6	-	-	-	-
150 rpm	Case 5, 6	Case 5	Case 5	-	-
200 rpm	Case 5, 6	-	-	-	-

Sampling Strategy	Symbol	Time (hour)																												
		0	0.5	1	1.5	2	2.5	3	4	5	6	7	8	9	10	11	12	13	14	15	16	17	18	19	20	21	22	23	24
Case 1	■	x	x	x	x	x	x	x	x	x	x	x																	x
Case 2	●	x		x		x		x	x	x	x	x	x	x	x	x	x													x
Case 3	★	x															x													x
Case 4	▲	x															x	x	x	x	x	x	x	x	x	x	x	x	x	x
Case 5	◆◆ ◆◆ ◆	x		x		x		x	x	x	x	x	x	x																
Case 6	◊◊◊◊ ◊	x												x																

5.3. Results and Discussions

5.3.1. Reproducibility issue with HDVD and batch crystallisation

Effect of Sampling Strategy on Static Batch Crystallisation. As mentioned above, due to its small scale (μL) and dynamic change of liquid composition, the reproducibility of HDVD crystallisation was relatively poor and it was merely feasible to evaluate the kinetics of the crystallisation process. Static batch crystallisation was studied first as a preliminary attempt to scale up the HDVD crystallisation experiment and to make the process of crystallisation quantifiable in terms of protein concentration profile in the solution over time. Since the measurement of protein concentration was offline and the personnel was not able to be in the lab to cover the time spam from nucleation to a relative high yield in the working hours, the initial attempt using different sampling strategies was to monitor the protein de-supersaturation process over a longer period (24 hours) to get a higher yield and to compare the effect of added protein impurity (thaumatin) on lysozyme crystallisation kinetics at different crystallisation stages.

Figure 5.2 showed that the sampling strategy, including timing and frequency of sampling, had strong impact on static batch crystallisation without agitation. For 3 different protein solutions, (a) 60 mg/mL lysozyme, (b) 60 mg/mL lysozyme + 6 mg/mL thaumatin, and (c) 60 mg/mL lysozyme + 12 mg/mL thaumatin, 4 different sampling strategies were applied as listed in Figure 5.1: case (1) every half hour from 0 to 3 hours and every hour from 4 to 6 hours, case (2) every hour from 0 to 12 hours, case (3) only 0, 12 and 24 hours, and case (4) 0 hour and every hour from 12 to 24 hours. And each case had 3 duplicates. Due to the high solvent content of protein crystal and its difficulty to obtain the final mass of lysozyme crystal out of the mother liquor, the

yield of lysozyme crystallization is simplified to the fraction of amount of lysozyme left the solution over the initial amount of lysozyme in the solution, with c_0 is initial lysozyme concentration and c_i is lysozyme concentration at time i.

$$\text{yield} = \frac{c_0 - c_i}{c_0} \times 100\% \quad (12)$$

Lysozyme concentrations were normalized with respect to the initial lysozyme concentration after mixing and the adjusted normalized lysozyme concentration calculation is shown in Figure 5.1. For comparison purpose, all concentration measured was calculated based on lysozyme extinction coefficient and then was normalised to initial lysozyme concentration after mixing, and thus for mixture the initial normalised protein concentration in the solution was higher than 100 % due to the added thaumatin. Thaumatin concentration was tracked and within 24 hours, the maximum decrease of thaumatin component was 0.639% and 2.224% (normalised to lysozyme concentration) for 6 mg/mL thaumatin and 12 mg/mL thaumatin, respectively. Considering the thaumatin crystallisation process could be inhibited by the presence of lysozyme in the mixture, and thus the drop of thaumatin concentration in the mixture could be lower compared to that in pure thaumatin solution. For simplification, we first assumed that no thaumatin left the mixture within 24 hours and thus we subtracted the part of normalised protein concentration associated with thaumatin. Considering that thaumatin did precipitate out, this was represented in Figure 5.1 by adding the maximum value of thaumatin condensation obtained from pure thaumatin case into

the error bar, 0.639% for 60 mg/mL lyso. + 6 mg/mL thau. And 2.224% for 60 mg/mL lyso. + 12 mg/mL thau..

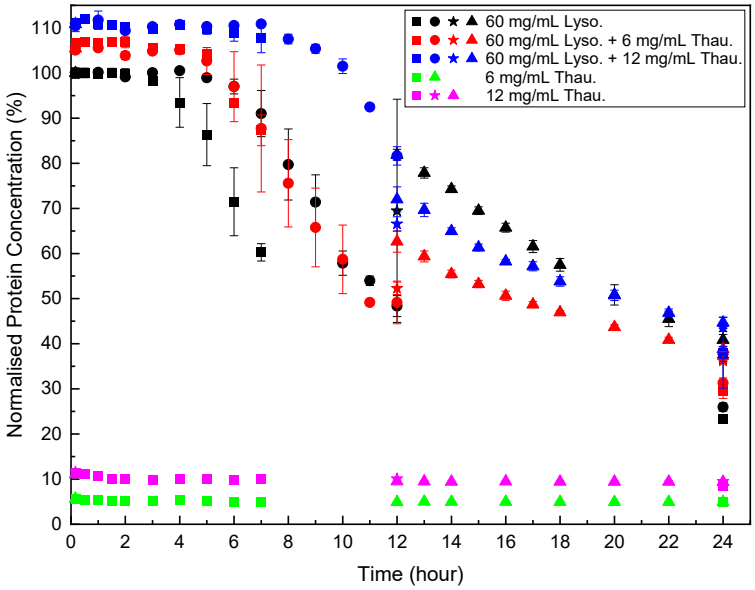

Figure 5.1 Protein concentration normalised to initial lysozyme concentration after mixed with precipitant solution.

As shown in Figure 5.1, due to the poor repeatability between different batches, a conclusion cannot be drawn to confirm whether the presence of thaumatin supress or promote lysozyme crystallisation due to the poor repeatability between different batches. De-supersaturation rate of pure lysozyme could be the fastest or slowest depended on the sampling strategy used. The yield after 12 hours was statistically different for all protein mixture when sampling strategies changed. After 24 hours, the system was approaching equilibrium and the de-supersaturation was relatively slow due to the low driving force caused by the decreased degree of supersaturation. And thus, the yield after 24 hours was more consistent than the yield after 12 hours.

Furthermore, the poor reproducibility was observed especially for pure lysozyme crystallisation without thaumatin. The yield after 12 hours varied from below 10% to above 50%. For pure lysozyme crystallisation, when the system was not disturbed at

early stage of crystallisation (case 3 and case 4), the system took a slower de-supersaturation process. Lysozyme concentration at 336 hours showed no significant difference regarding to the amount of added thaumatin in Figure 5.3. The slower protein concentration drop was very likely due to that lysozyme tended to crystallise heterogeneously on the wall of the container when the system was quiescent. And there was less crystals formed, and the crystals were larger as shown in Figure 5.1. However, when thaumatin was added as an impurity to the system, more fine lysozyme crystals were formed and less large lysozyme crystals on the wall were observed (no thaumatin crystals observed within the first 24 hours under microscope). This phenomenon might have occurred either because that thaumatin was more likely to be adsorbed on the wall causing less lysozyme heterogenous nucleation on the wall or that thaumatin formed light fine precipitation (detected under microscope) at the beginning and these particles suspended in the mixture and served as heterogenous nucleation sites. Though samples were actively mixed by repeated pipetting to assure homogenisation at the beginning of the crystallisation, as the nucleation and crystal growth proceeded, concentration depleted zone around growing crystals might appear. Diffusion limited mass transfer in static batch crystallisation and the chaotic nature of spontaneous nucleation led to poor reproducibility in static batch crystallisation which was more severe for pure lysozyme cases with fewer but larger protein crystals. In conclusion, quiescent batch crystallisation process was significantly influenced by sampling timing and frequency. Furthermore, even with the same sampling strategy, the results still could have poor reproducibility depending on crystallisation condition. Despite the expected stochastic nature of nucleation which could lead to fluctuations of the onset of nucleation events, the significant differences of the yield at the end of the experiments were the major concern for the quality control of the static batch

crystallisation process. And thus, static batch crystallisation is not a desirable crystallisation method for further scale-up study considering the poor reproducibility of the yield.

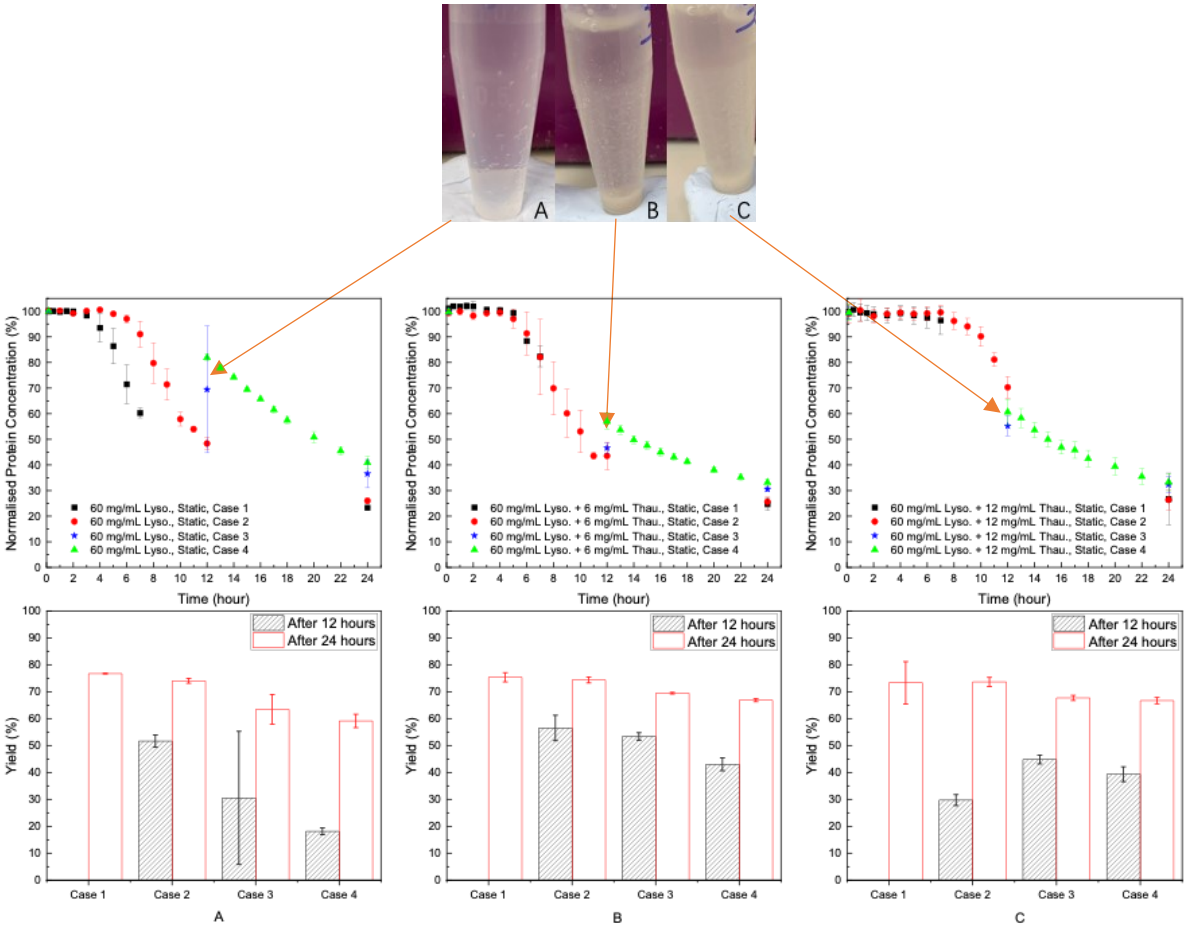

Figure 5.2 Representative image of the crystallisation tube after 12 hours, protein concentration profile of individual cases, and yield after 12 hours and after 24 hours. (A) 60 mg/mL lysozyme; (B) 60 mg/mL lysozyme + 6 mg/mL thaumatin; (C) 60 mg/mL lysozyme +12 mg/mL thaumatin. Square (■): case 1; circle(●): case 2; star(★): case 3; triangle(▲): case 4.

5.3.2. Effect of Shaking Speed in Agitated Batch Crystallisation

Previous section revealed poor reproducibility of yield in static batch crystallisation and the yield was also influenced by sampling strategy. As shown in Figure 5.1, the yield was much lower and less reproducible when samples were not taken for 12 hours compared to the yield where samples were taken every hour. In this section, two sampling strategies were employed in agitated batch crystallisation to test if agitation and eliminate the influence of sampling strategy, case (5) where samples were taken every hour and case (6) where samples were only taken at the start and the end of the experiments. Theoretically, the difference between batches were expected to be more obvious at earlier stage of crystallisation than when the system was approaching plateau as the driving force was reduced due to de-supersaturation of proteins in the solution. And thus, the experiments were shortened to 9 hours to be less time-consuming.

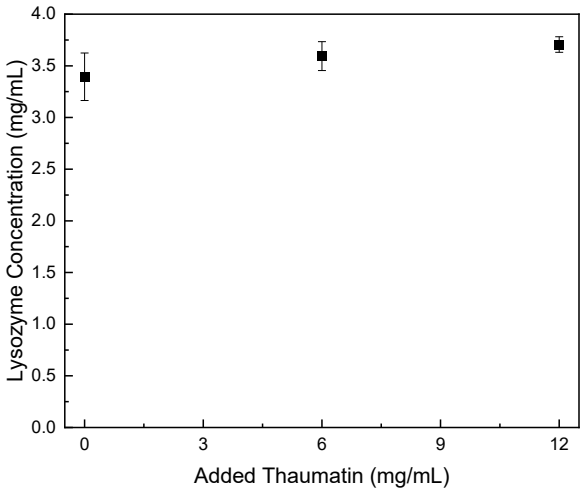

Figure 5.3 Average lysozyme concentration after 336 hours in static protein batch crystallisation

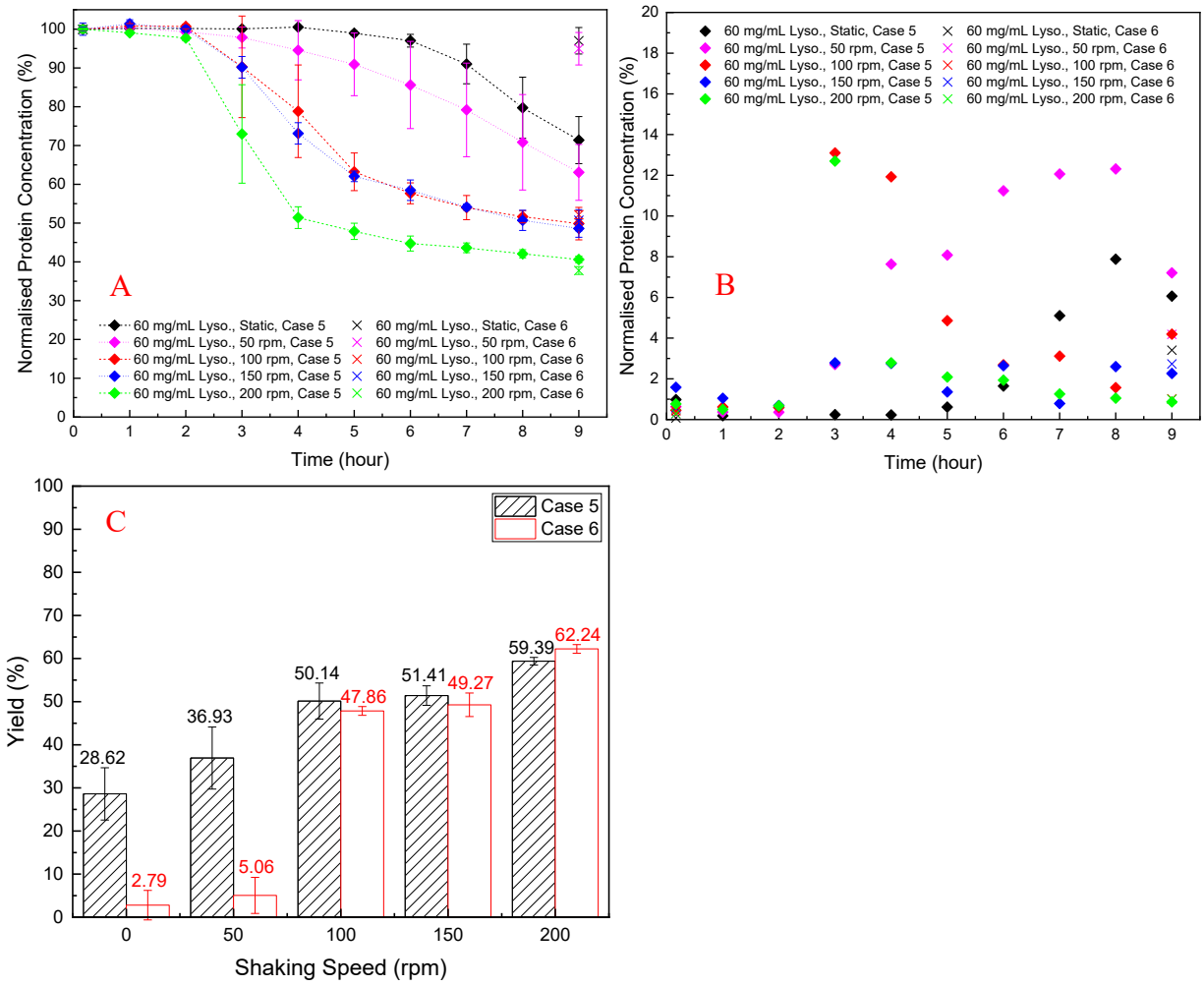

Figure 5.4 (A) Protein crystallisation concentration profile over time under different shaking speed; (B) Standard deviation between batches over time for different shaking speed; (C) yield after 9 hours for different sampling strategy under various shaking speed. Note: data for “60 mg/mL Lyso., Static, Case 5” was taken from “60 mg/mL Lyso., Static, Case 2” as the same sampling strategy in the first 9 hours was employed.

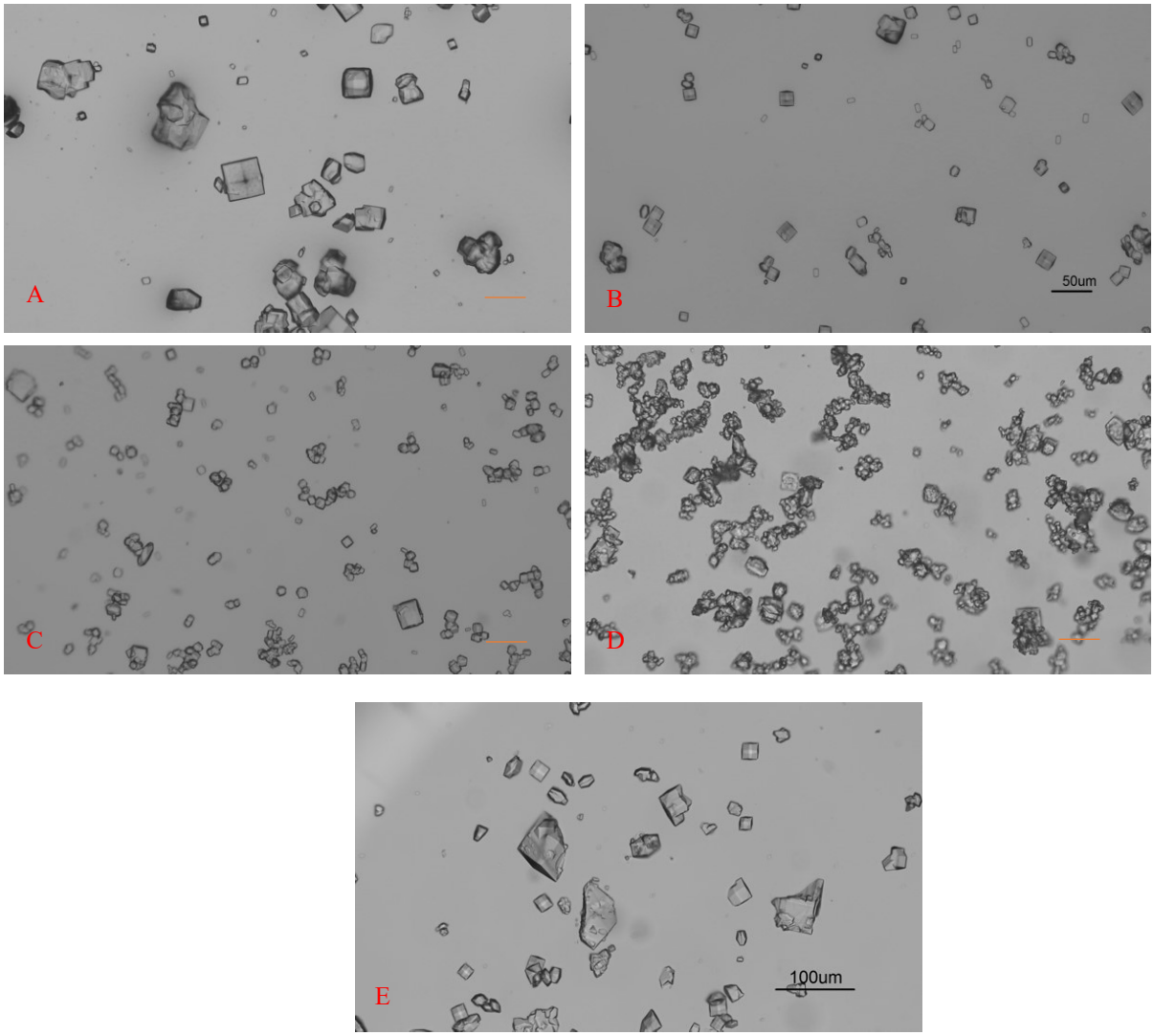

Figure 5.5 Representative images of crystals after 9 hours.

(A) 50 rpm; (B) 100 rpm; (C) 150 rpm; (D) 200 rpm; (E) static. A scale bar (in 'red' colour) of 50 µm applies to all the images. Note: Figure S4 (A), (B), (C), and (D) are the same images as Figure 3 (A), (B), (C), and (D) in the article main body. These images were used here to make the comparison to static protein crystals more directly.

As shown in Figure 5.4, lysozyme crystallisation was accelerated when shaking speed was increased. In the shaking speed range of 0 to 200 rpm, shorter induction time and higher yield were observed as shaking speed increased. In regard of reproducibility, one-way ANOVA test was performed for yields after 9 hours for case 5 and case 6 under various shaking speed (p-value = 0.00301, 0.00269, 0.41146, 0.35565, and 0.02021 for 0 rpm, 50 rpm, 100 rpm, 150 rpm, and 200 rpm, respectively). For 0 to 50 rpm, the yields after 9 hours were still significantly affected by the sampling strategy. For 100 to 150 rpm, the difference of yields after 9 hours between undisturbed system and frequently sampled system was not statistically significant. For 200 rpm, the difference between case 5 and case 6 were statistically different at level 0.05 but not as significant as at a lower shaking speed. Figure 5.4 also reveals that, though the final yield was relatively stable between batches for 100 to 200 rpm shaking speed, the standard deviation between batches were relatively high at 3 to 4 hours. The inconsistency at the early stage of crystallisation process might indicate that the crystallisation onset time was still varying between batches, especially for 100 rpm and 200 rpm. However, the difference was balanced later by the faster de-supersaturation rate caused at high shaking speed. This higher supersaturation exhaustion rate might be the result of promoted secondary nucleation through contact or shear and improved growth rate due to elimination of diffusion limited mass transport.

Reduction in protein crystal size was observed with increasing agitation. As shown in Figure 1, large well-defined tetragonal lysozyme protein crystals tended to nucleate and grow on the wall of the vessel in quiescent batch crystallisation. At 50 rpm, similar phenomenon was also observed but with a portion of crystals accumulated at the bottom of the vial. As shown in Figure 5.5, when there is no agitation or only gently

stirred, the crystal size ranged from less than 10 μm to around 100 μm and there were larger crystals broken while sampling by pipette. As shaking speed further increased, less well-defined single lysozyme crystals were observed. However, Figure 5.5 shows that at 200 rpm, agglomeration where fine lysozyme crystals attached together was observed, and fewer well-defined crystals were found. Wang et al. also found that agitation could lead to wider crystal size distribution and, unlike small molecule crystallisation, the distribution did not get narrower over time.[185] Additionally, bubble entrainment might be more serious at higher shaking speed.[186] Shaking and stirring could promote renewing air-liquid interface of protein solution which was the driving force of protein aggregation and precipitation.[186] Though lysozyme is a relatively robust protein and not very sensitive to shear as its enzymatic activity were well preserved after shearing,[187, 188] in order to obtain better defined lysozyme crystals with less agglomeration and to avoid bubble entrainment, vigorous agitation is not desirable for lysozyme crystallisation.

In general, in the shaking speed range investigated, increased agitation accelerated supersaturation exhaustion rate of protein crystallisation, improved yield and its reproducibility and reduced protein crystal size. Nevertheless, increased agitation could have advert effect on final products in respect of crystal aggregation.

5.3.3. Effect of Protein Impurity in Agitated Batch Crystallisation

Figure 5.6 shows that lysozyme crystallisation slowed down due to the addition of thaumatin. The more thaumatin, the longer the induction time of lysozyme

crystallisation. However, at later stage of crystallisation, the influence of thaumatin was less noticeable.

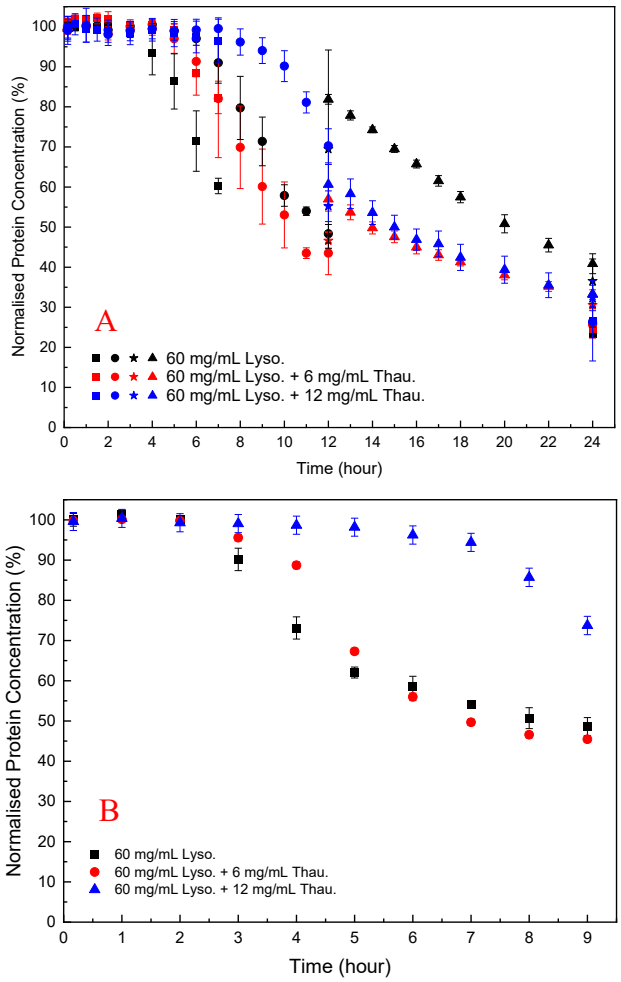

Figure 5.6 Normalised protein concentration profile over time. (A) static batch crystallisation; (B) agitated batch crystallisation on shaker at 150 rpm. Note: Figure 4A was a summary of all the protein concentration data presented in Figure 1.

As shown in Figure 5.4B, the lysozyme concentrations without thaumatin and with 6 mg/mL thaumatin almost converged after 6 hours. The effect of impurity was more obvious at earlier stage of crystallisation. Thaumatin sometimes caused faster crystallisation of lysozyme in quiescent batch crystallisation as mentioned above. We suspected that this phenomenon could result from either that thaumatin is more likely

to be adsorbed on the wall and thus less lysozyme nucleation on the wall or thaumatin formed light fine precipitation at the beginning and these particles suspended in the mixture and served as heterogenous nucleation sites. With agitation, we see a clearer trend of delaying of crystallisation of lysozyme caused by the addition of thaumatin. Hence the hypothesis of precipitated/denatured thaumatin enhanced lysozyme nucleation seems not valid in this case. Kovalchuk et al. showed that oligomer including dimer and octamer of lysozyme might be the essential building block for tetragonal lysozyme crystallisation.[189] The presence of thaumatin could lower the probability of formation of such oligomer and thus delayed nucleation. Once nuclei were formed, the effect of added thaumatin were less significant when agitation was involved to promote mass transport of lysozyme molecules. In conclusion, agitated batch crystallisation results revealed that the presence of protein impurity could slow down target protein crystallisation process, mainly by delaying the induction time.

5.4. Conclusions

The study showed that agitation is essential to obtain consistent protein crystallisation results when moving from preliminary screenings to scaled-up batch crystallisation experiments. In the absence of agitation, poor reproducibility between batches were observed albeit the same sampling timing and frequency applied. When different sampling strategies (timing and frequency) were employed, inconsistent results for different protein solution conditions would be obtained. The dependency of protein crystallisation results may mislead to confusing results such as whether the protein impurity accelerates or suppresses the target protein crystallisation. When agitation was employed in batch crystallisation, 0-200 rpm in the current study, reproducibility

of lysozyme crystallisation was improved. Additionally, increased agitation accelerated supersaturation exhaustion rate of protein crystallisation, improved yield, and, potentially, reduced protein crystal size. Furthermore, in agitated batch crystallisation experiments, it was found that target protein crystallisation process was decelerated in the presence of protein impurity, mainly by delaying the induction time.

6. Protein crystallisation facilitated by silica particles

6.1. Overview

In this Chapter, silica particles were used to improve target protein batch crystallisation from a binary protein mixture at 5 mL scale. Lysozyme (40 mg/mL) was used as the target protein and thaumatin (0.1 – 8 mg/mL) was regarded as a protein impurity. It was demonstrated that even an impurity at the concentration as low as 0.1 mg/mL (0.25 w/w% of target protein) would delay target protein crystallisation, predominantly by extending the induction time. When silica particles were employed in the system to facilitate crystallisation, target protein crystallisation was significantly improved with much shorter induction time and higher yield at the end of the experiment. It was also shown that the effectiveness of silica on target protein crystallisation depended on impurity concentration and silica loading amount.

6.2. Experimental Methodology

Silica particles purchased from Sigma were further investigated by using TriStar3000 (Micromeretics Instrument Corporation) to confirm their pore sizes. The nitrogen adsorption and desorption isotherms were then obtained as shown in Figure 8.5, Figure 8.6, and Figure 8.7. The hydrodynamic diameters of lysozyme and thaumatin were determined using dynamic light scattering (DLS).

Hanging-drop vapour-diffusion (HDVD) crystallisation method was first used to test the efficiency of different types of silica particles. Lysozyme solution was prepared by dissolving the protein powder into the buffer solution which was the same buffer as used for precipitant preparation. The crystallisation plates were then placed into the

incubator (20 °C ± 0.5 °C). The plates were observed using CX41 optical microscope (Olympus) regularly after they were set-up. Microscopic images were captured using a GXCAM HICHROME-MET camera (GT Vision).

Batch crystallisation experiments were later used to investigate the optimum loading of silica particles. All batch crystallisation experiments in this study were conducted at room temperature of 21 °C (± 1 °C) with at least 2 replicates for each condition. The experiments were implemented in 10 mL glass vial. Silica particles were added to the glass vial carefully avoiding attachment to the container wall. 2500 µL protein solution was added to the tube and then 2500 µL precipitant solution was added to the same tube. The solution was actively mixed manually by several pipetting before sitting on the bench or the shaker. Samples were placed on orbital shaker (SciQuip, SP2250-03, 20 mm orbital diameter) immediately after mixing. To track the crystallisation process in a sample, the dissolved protein concentration was monitored off-line over time as discussed in section 3.3.2.

6.3. Results and Discussion

6.3.1. Adverse impact of thaumatin in lysozyme crystallisation in HDVD experiments

Effect of thaumatin as protein impurity on lysozyme crystallisation kinetics

As shown in Figure 6.1, protein impurity had negative impact on target protein crystallisation in the model system studied. Thaumatin had adverse impact on lysozyme concentration even for a low impurity concentration of 0.1 mg/mL (0.25 w/w %

of target protein concentration). The more thaumatin added, the slower the desupersaturation process and the lower the yield was achieved after 9 hours. This agrees with our previous results from HDVD experiments in which lysozyme crystals appeared later in droplet with thaumatin compared to droplet with only lysozyme.[190] Considering the maximum error bar from pure lysozyme crystallisation experiments with more repeats, for low impurity concentration, once target protein crystallisation started, the yields at 9th hour were not significantly different comparing to the yield from pure lysozyme crystallisation. In our previous study, we shown that lysozyme concentrations after 2 weeks were not dependent on thaumatin concentration in the system.[191] And thus we hypothesised that lysozyme solubility, in the impurity concentration range investigated in this study, was not influenced by thaumatin impurity. Thaumatin impurity tended to delay lysozyme nucleation rather than later stage of crystallisation dominated by crystal growth in batch crystallisation. Kovalchuk et al. showed that oligomer including dimer and octamer of lysozyme might be the essential building block for tetragonal lysozyme crystallisation.[189] The presence of thaumatin could lower the probability of formation of such oligomer and thus delayed nucleation. Once nuclei were formed, the effect of added thaumatin were less significant, especially in a non-diffusion-limited system when shaking was involved to promote mass transport of lysozyme molecules.

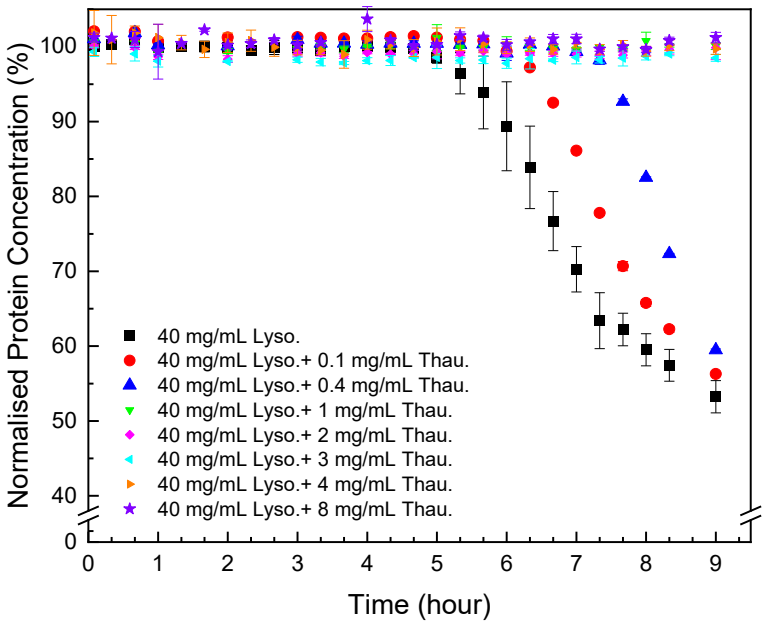

Figure 6.1 Normalised lysozyme concentration over time with different amount of thaumatin in the solution.

6.3.2. Effect of Silica Particles in Pure Lysozyme Batch Crystallisation

As shown in Figure 6.2A, in HDVD experiments, the success rate of lysozyme crystallisation was increased by addition of silica particles and SBA-15 had the most noticeable impact while mesoporous silica had the least when the same amount of silica particles was used. For more qualitative and scalable study of the impact of silica particles, batch crystallisation at 5 mL with agitation was conducted.

In Figure 6.2B, all cases with silica particles showed accelerated lysozyme crystallisation compared to experiments without silica employed. Agreeing with HDVD experimental results, SBA-15 had the most noticeable impact even at a lower amount

and non-porous silica worked more effectively than mesoporous silica when the same silica loading was used. Figure 8.8 in the appendix shows a schematic illustration of determination of induction time in this study. The black line represents 100% normalised protein concentration. The red line represents initial linear range of the desupersaturation curve. The blue denotes the vertical intercept of the red and black lines and its intercept with the time-axis gives the estimated induction time. The induction time was estimated by desupersaturation rate. Concentration drop caused by nucleation in protein crystallisation in this experimental scale usually is not detectable by UV-Vis spectrophotometer and thus induction time mentioned in this study was not the onset of nucleation process. The concentration drop in the desupersaturation curve mainly attributes to crystal growth of the protein crystals. The initial crystal growth rate can be deduced using a linear line fitted to the concentration profile data. The slope of this line should correspond to the initial crystal growth rate. The vertical intercept of this approximated linear line with the 100% normalised concentration line (initial concentration) corresponds to the induction time. As shown in Figure 6.3, the yield was improved by addition of SBA-15 and the induction time was dramatically reduced compared to non-seeded experiments. Addition of 1 mg SBA-15 was able to reduce induction time by about 3 hours while further addition of SBA-15 had no significant further improvement on induction time reduction. With a similar induction time, 10 mg of SBA-15 gave a better yield, especially in the first 6 hours. The induction time would be significantly reduced by silica particles. The difference of the yields at the end of the experiments with and without silica particles ranged from less than 1 % to around 15%. Silica particles were discovered to have more impact on accelerate crystallisation on the early stage of crystallisation. Our previous study has demonstrated non-porous silica can mitigate the negative impact

from protein impurity via adsorption of protein on particle surfaces while no effect of silica particles on protein solubility was observed.[91] Researchers also showed that porous silica have positive impact as heterogenous nucleants.[89, 90, 92] As shown in Table 1, mesoporous silica had the highest surface area while non-porous silica had the lowest. Contradicting our hypothesis, non-porous silica worked better on improving lysozyme crystallisation comparing to mesoporous silica. The hydrodynamic diameter measured by DLS was 4.48 ± 0.74 nm for lysozyme and was 6.57 ± 1.61 nm for thaumatin. Considering the size of lysozyme molecules and pore size of the silica, the pores seemed not accessible for thaumatin in all cases and only accessible for lysozyme when SBA-15 silica was used. Though mesoporous silica had the highest surface area, most of them would not be beneficial for lysozyme adsorption and further facilitating lysozyme nucleation.

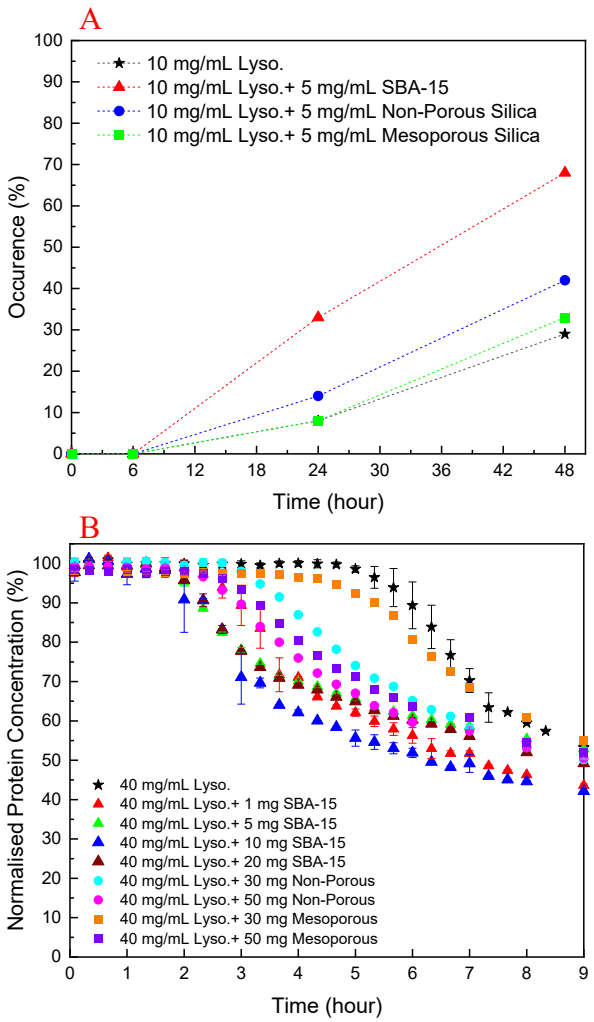

Figure 6.2 (A) Occurrence of lysozyme crystal(s) in HDVD experiments with different silica particles; (B) Normalised lysozyme concentration over time in batch lysozyme crystallisation (5 mL) with different amount of silica particles.

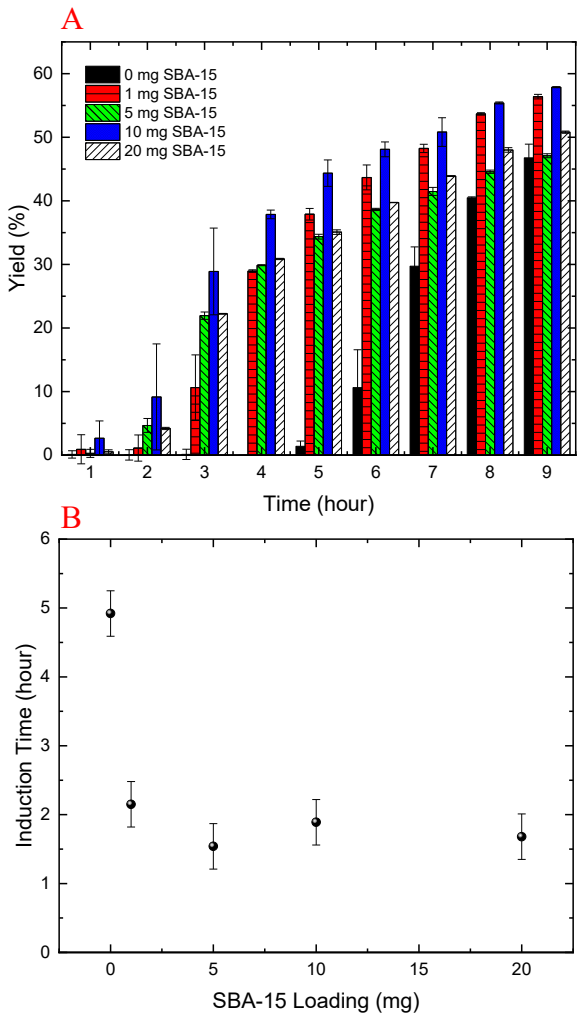

Figure 6.3 (A) Yield of protein crystallisation (lysozyme at 40 mg/mL starting concentration) with different amount of SBA-15; (B) Induction time of lysozyme crystallisation (40 mg/mL) with different amount of silica loading.

Table 6.1 Silica particle properties determined by nitrogen adsorption and desorption experiments

	BET Surface Area (m^2/g)	BJH Adsorption Average Pore Diameter (nm)	BJH Desorption Average Pore Diameter (nm)
SBA-15 Silica	470.75	5.20	5.06
Mesoporous Silica	502.02	4.10	4.40
Non-Porous Silica	2.67	-	-

6.3.3. Using Silica Particles to Compensate Adverse Impact from Protein Impurity

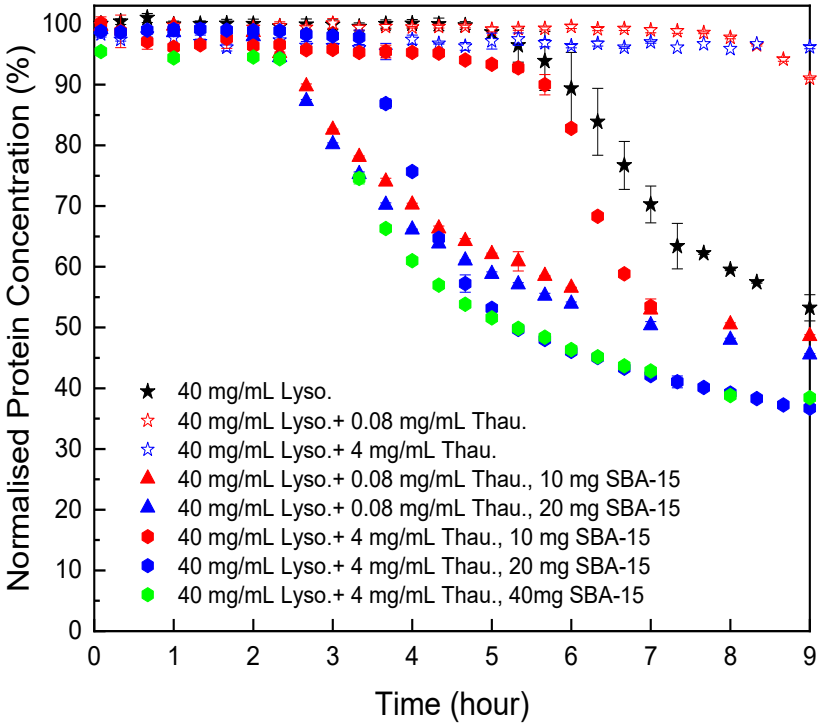

Figure 6.4 Normalised lysozyme concentration profiles with different amount of thaumatin impurity and silica particle.

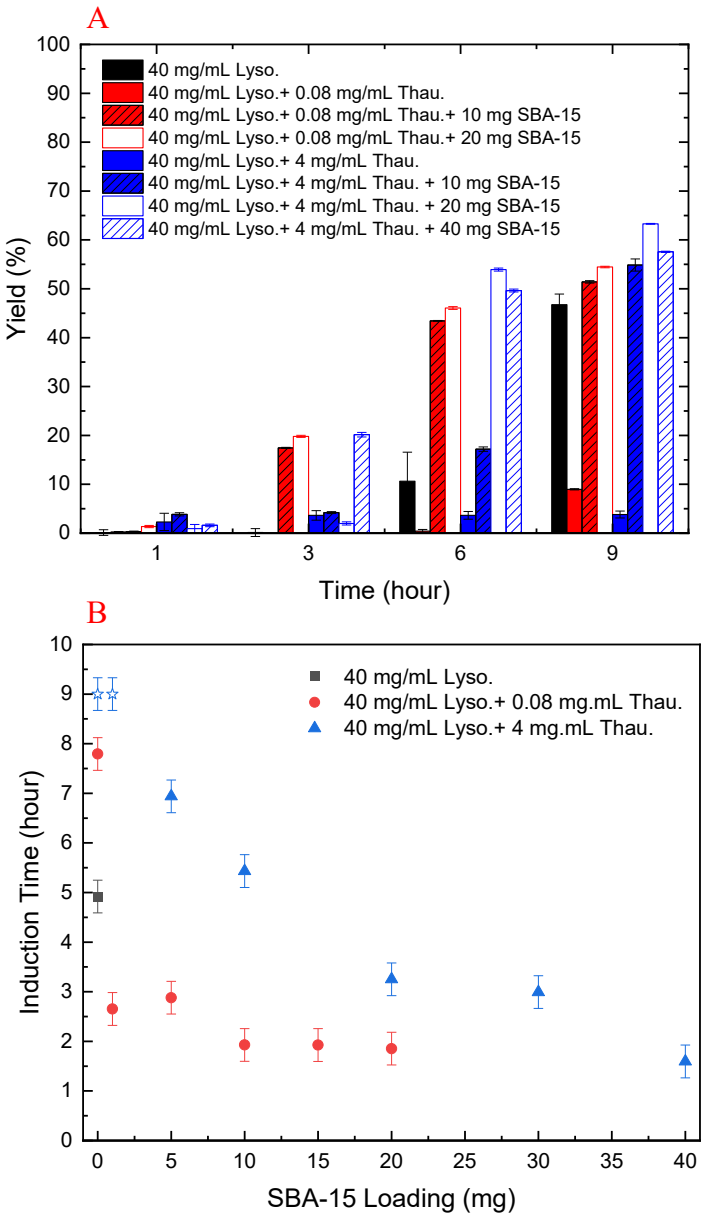

Figure 6.5(A) Yield of batch protein crystallisation with different amount of thaumatin and amount of SBA-15; (B) Induction time of batch lysozyme crystallisation with different amount thaumatin and silica loading. Note: blue stars represent experiments which did not crystallise within 9 hours and thus the real induction time was higher than 9 hours in these cases.

As shown in Figure 6.4, SBA-15 silica particle could also accelerate lysozyme crystallisation in the protein mixture system by shortening the induction time of

crystallisation. As shown in Figure 6.5, a minimum induction time could be achieved by addition of silica particles further addition of silica nucleants would not reduce the induction time. With increasing amount of thaumatin, the amount of silica nucleants would be higher to reach a similar induction time as the lower impurity level experiments as the adsorption of protein on silica surface was non-specific. In addition, as shown in Table 6.1, the pore size of SBA-15 was not larger than the hydrodynamic diameters of the proteins, and thus the possibility that the mixture was purified by the addition of silica particles is rejected in this study. Both types of protein molecules would be driven to the surface and the existence of thaumatin would reduce the chance of target protein to form nuclei on the silica surface when not enough surface area was provided. Induction time was dramatically reduced by addition of 1 mg SBA-15 to experiments with 0.08 mg/mL thaumatin and the induction time remained similar for SBA-15 loading amount above 10 mg. For experiments with higher amount of thaumatin, 4 mg/mL, 30 mg more SBA-15 was required to shorten the induction time to a similar level. The amount of silica required to mitigate the adverse impact of protein impurity increased with increasing protein impurity content. Similar to crystallisation from pure lysozyme, even when thaumatin presented as impurity in the system, silica mainly facilitated target protein crystallisation in early stage of crystallisation. As mentioned above, the induction time defined in this study did not only involve the time of nucleation but also include a period of crystal growth, and thus the shorter induction time may not mean a shorter nucleation time. A reduced induction time may also be caused by a faster growth rate or enhanced secondary nucleation. Further investigation is required to decouple the impact of silica particles on nucleation and crystal growth. Additionally, the induction time was shortened rather than the final yield at the end of the experiments. And thus, we assumed that the final equilibrium

state was not manipulated by addition of silica. The improvement of crystallisation was at the early stage of crystallisation rather than changing the protein solubility.

6.4. Conclusions

This study demonstrated the negative impact of protein impurity on target protein crystallisation. In our model system, even trace amount of thaumatin impurity would delay lysozyme crystallisation by hours. Silica particles, porous or non-porous could accelerate lysozyme crystallisation in pure protein crystallisation experiments or in crystallisation from protein mixture. Optimal silica loading amount depended on lysozyme concentration and thaumatin impurity concentration. The more the impurity, the more silica was required to compensate the negative impacts on target protein crystallisation. The study indicated that the accessible surface provided by the silica particles played a role in accelerating the protein crystallisation process via heterogenous nucleation. In future study, for the design of silica nucleants to optimise protein crystallisation process, the roles of silica particle size and the correlation between protein size and pore size of silica would need to be further investigated.

7. Conclusions and Future Outlook

7.1. Conclusions

The aim of this project was to investigate the role of protein impurity in selective crystallisation of the target protein and to demonstrate the efficiency of silica nanonucleants on promoting protein crystallisation.

In this study, we successfully demonstrated preferential protein crystallisation using lysozyme-thaumatin binary mixture as the model. This work demonstrates that protein crystallisation is not only applicable to high-purity protein solution but also a feasible approach to separate a target protein from a more complex mixture environment, even for protein mixtures with both proteins supersaturated. The effect of protein impurity was studied using a model protein system, lysozyme-thaumatin binary protein mixture. The experiments were moved from μL-scale hanging-drop vapour-diffusion (HDVD) to mL-scale batch crystallisation. Additionally, the critical role of agitation was verified in scaling-up process moving from HDVD experiments to batch experiments. To test the efficiency of heterogenous nucleants in protein crystallisation, engineered silica particles with different porosities and particle sizes were used, including SBA-15, mesoporous silica, and non-porous silica. The effectiveness of these nanonucleants at different loading amount were examined in crystallisation from both pure protein solution and protein mixture.

In terms of the effect of protein impurity on target protein crystallisation, it was demonstrated that, in the model system, the presence of another protein impurity can slow down the crystallisation process of the target protein in both HDVD experiments and batch experiments. In our model system, even trace amount of thaumatin impurity

as low as 0.1 mg/mL (0.25 % w/w of target protein) would delay lysozyme crystallisation by hours.

In terms of the effect of silica nanonucleants, silica particles, porous or non-porous could increase the success rate of lysozyme crystallisation in HDVD experiments and accelerate lysozyme crystallisation in pure protein crystallisation experiments or in crystallisation from protein mixture in 5 mL batch experiments. Induction time was reduced by 3 hours with addition of 1 mg SBA-15 particles for pure lysozyme solution. Optimal silica loading amount depended on lysozyme concentration and thaumatin impurity concentration. The more the impurity, the more silica was required to compensate the negative impacts on target protein crystallisation. Induction time was dramatically reduced by addition of 1 mg SBA-15 to experiments with 0.08 mg/mL thaumatin and the induction time remained similar for SBA-15 loading amount above 10 mg. For experiments with higher amount of thaumatin, 4 mg/mL, 30 mg more SBA-15 was required to shorten the induction time to a similar level. The study indicated that the accessible surface provided by the silica particles played a role in accelerating in the early stage of protein crystallisation process, most possibly via heterogenous nucleation.

In terms of scaling-up, the study showed that agitation is essential to obtain consistent protein crystallisation results when moving from preliminary screenings to scaled-up batch crystallisation experiments. In the absence of agitation, poor reproducibility between batches were observed albeit the same sampling timing and frequency applied. When different sampling strategies (timing and frequency) were employed, inconsistent results for different protein solution conditions would be obtained. The dependency of protein crystallisation results may mislead to confusing results such as

whether the protein impurity accelerates or suppresses the target protein crystallisation. When agitation was employed in batch crystallisation, 0-200 rpm in the current study, reproducibility of lysozyme crystallisation was improved. Additionally, increased agitation accelerated supersaturation exhaustion rate of protein crystallisation, improved yield, and, potentially, reduced protein crystal size. Furthermore, in agitated batch crystallisation experiments, it was found that target protein crystallisation process was decelerated in the presence of protein impurity, mainly by delaying the induction time.

This work provides a working model system with essential foundation knowledge for future work on protein crystallisation for bioseparation, such as scale-up crystallisation process, seeding, and crystallisation facilitated by heterogeneous nucleants.

7.2. Outlook

As the kinetics of crystallisation can be manipulated by the presence of the protein impurities, it highlights the importance of further investigation of the effect of protein impurities in more complex crystallisation system. The adverse effect of protein impurities should be examined in other protein mixture system, for example, with structurally similar protein impurities.

In batch experiments, the impacts of crystalliser were noticed. The nucleation time was different when glass vessel was used compared to that in the polypropylene tubes. The surface chemistry of the crystalliser vessel and geometry of the crystalliser would be critical to the crystallisation process, especially in scaling-up process.

Agitation was achieved by shaking for a higher throughput purpose in this study. More practical and scalable agitation method should be considered in future studies to achieve industrial crystallisation. Agitation could be realised by using either overhead stirrer in conventional batch or continuous MSMPR crystalliser. It could also be achieved in continuous baffled tubular crystalliser. Additionally, relevant parameter to quantify the effect of agitation is indeed, for example, dimensionless parameter such as Reynolds number.

In future study, the mechanisms of heterogenous nucleation in protein crystallisation facilitated by engineered silica nanonucleants require further studies. It needs to be examined whether the improvement of nucleation process is via reducing the energy barrier thermodynamically or via accelerating the process kinetically. For the design of silica nucleants to optimise protein crystallisation process, the roles of silica particle size and the correlation between protein size and pore size of silica would need to be further investigated. Additionally, the surface chemistry of silica should be studied. Furthermore, sedimentation of silica nucleants and crystals was noticed in this study. The effect of distribution of silica particles in the crystalliser should be examined in the future study.

8. Appendix

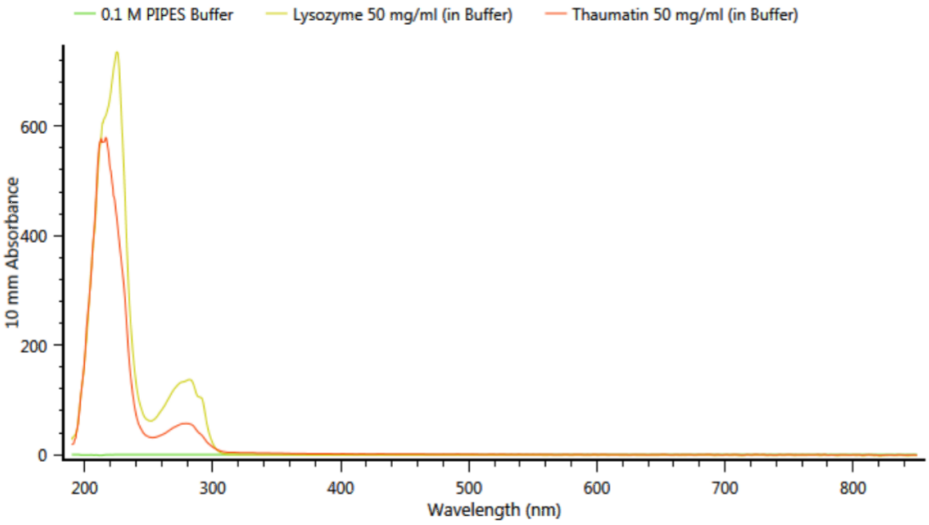

Figure 8.1 UV-Vis spectrum of thaumatin and lysozyme in 0.1 M PIPES buffer

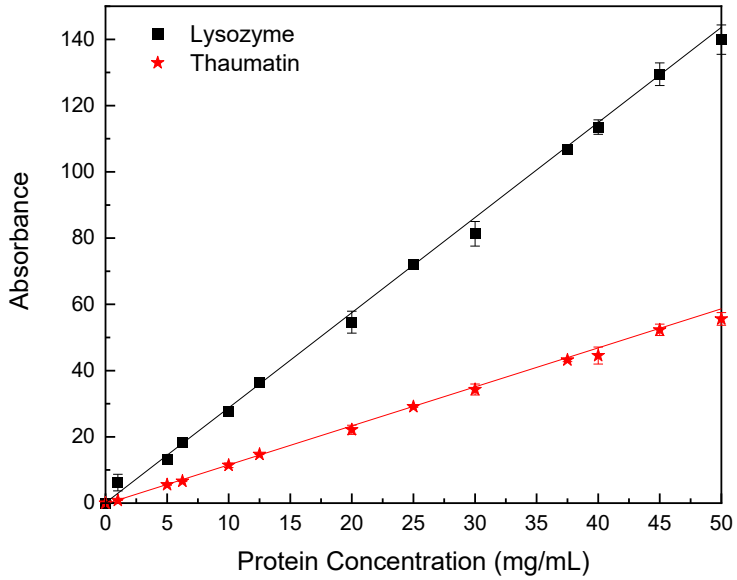

Figure 8.2 Lysozyme and thaumatin absrobance at 280 nm wavelength

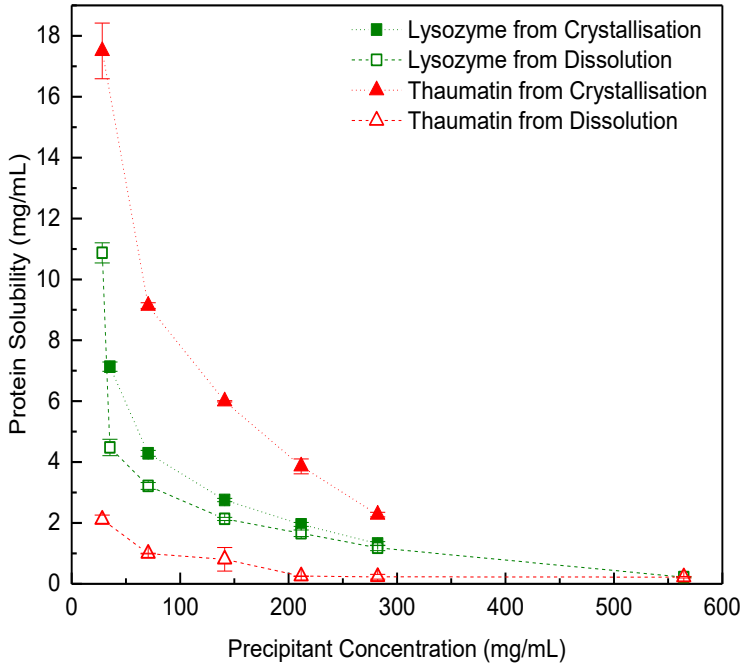

Figure 8.3 Lysozyme solubility and thaumatin solubility measured from crystallisation and dissolution methods

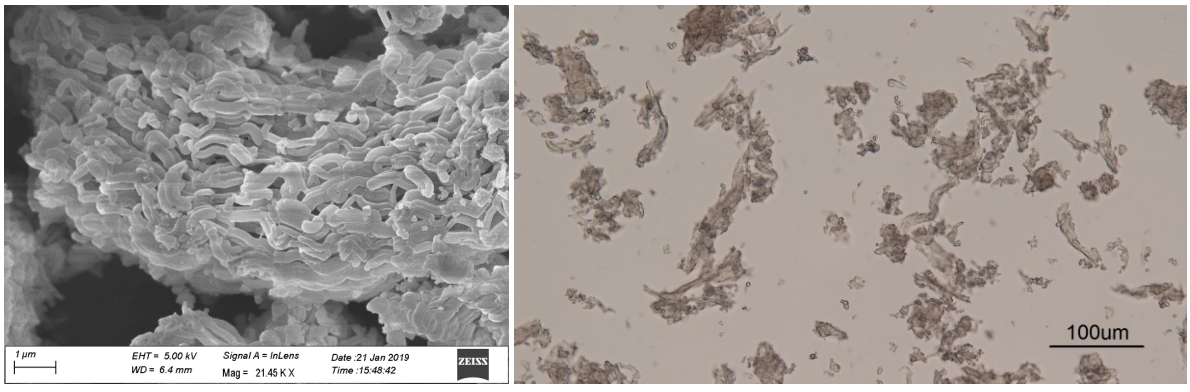

Figure 8.4 SEM image and optical microscope image of SBA-15

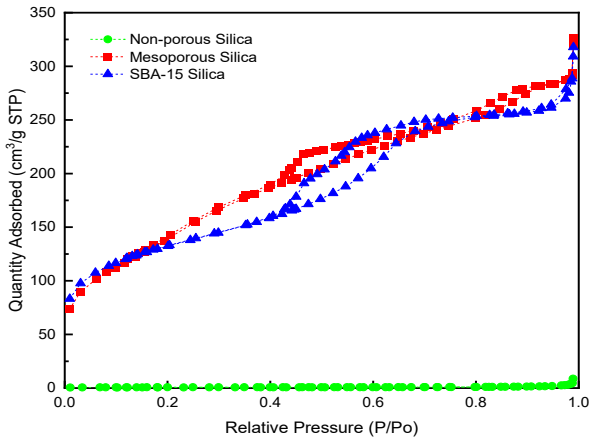

Figure 8.5 Nitrogen adsorption and desorption isotherms for the silica particles

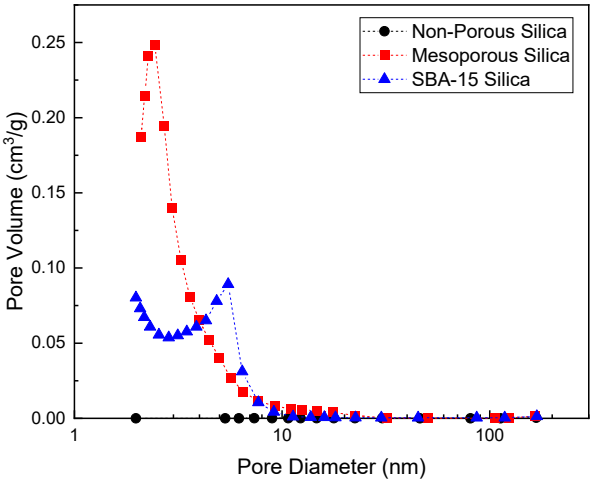

Figure 8.6 Pore size distribution calculated based on BJH adsorption

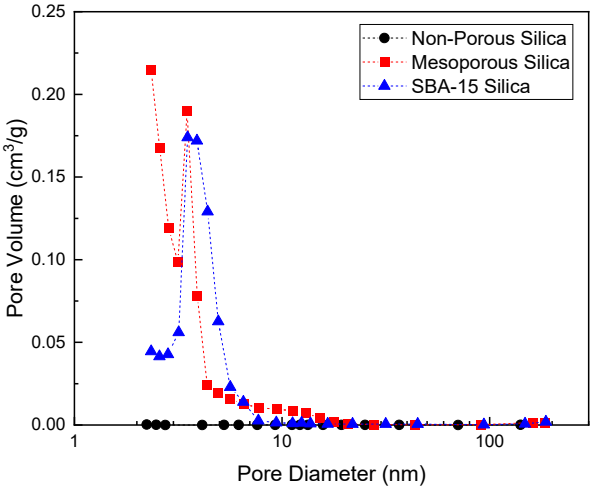

Figure 8.7 Pore size distribution calculated based on BJH desorption

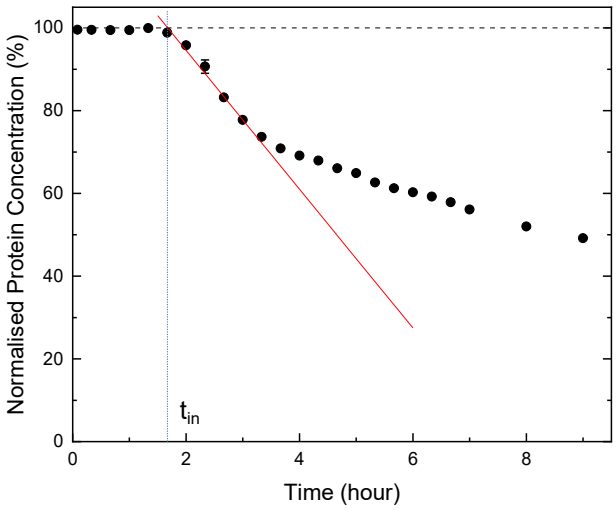

Figure 8.8 A schematic illustration of protein concentration desupersaturation curve determined by UV-Vis spectrophotometer in protein crystallisation process. induction time determination.

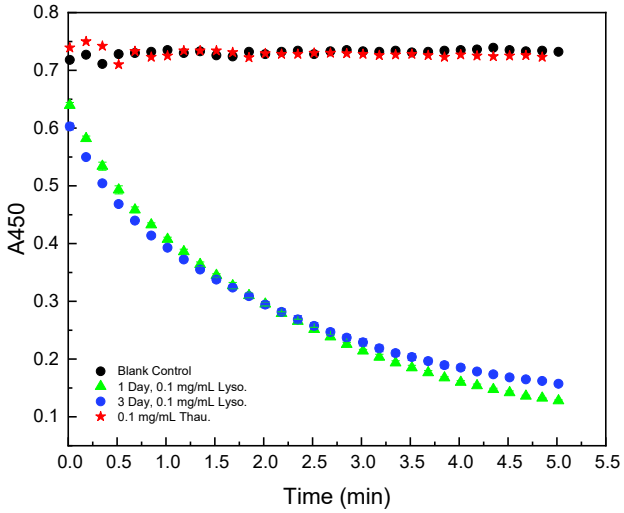

Figure 8.9 Lysozyme activity test of crystals re-disolved after days.

9. References

1. Mullin, J. W., 5. Nucleation. In *Crystallization (4th Edition)*, Elsevier.

2. Asherie, N., Protein crystallization and phase diagrams. *Methods* **2004,** *34* (3), 266-272.

3. Agrawal, S. G.; Paterson, A. H. J., Secondary Nucleation: Mechanisms and Models. *Chemical Engineering Communications* **2015,** *202* (5), 698-706.

4. Vekilov, P. G., Dense Liquid Precursor for the Nucleation of Ordered Solid Phases from Solution. *Crystal Growth & Design* **2004,** *4* (4), 671-685.

5. Vekilov, P. G., The two-step mechanism of nucleation of crystals in solution. *Nanoscale* **2010,** *2* (11), 2346-2357.

6. Vekilov, P. G., Nucleation. *Crystal Growth & Design* **2010,** *10* (12), 5007-5019.

7. McPherson, A., Introduction to protein crystallization. *Methods* **2004,** *34* (3), 254-265.

8. Sauter, C.; Lorber, B.; McPherson, A.; Giegé, R., General methods. In *International Tables for Crystallography*, pp 99-121.

9. Ruyters, G.; Betzel, C., Protein Crystallization in Space: Early Successes and Drawbacks in the German Space Life Sciences Program. In *Biotechnology in Space*, Ruyters, G.; Betzel, C.; Grimm, D., Eds. Springer International Publishing: Cham, 2017; pp 11-26.

10. Chayen, N. E., Turning protein crystallisation from an art into a science. *Current Opinion in Structural Biology* **2004,** *14* (5), 577-583.

11. Mullin, J. W., 6. Crystal Growth. In *Crystallization (4th Edition)*, Elsevier.

12. Ducruix, A. F.; Ries-Kautt, M. M., Solubility diagram analysis and the relative effectiveness of different ions on protein crystal growth. *Methods* **1990,** *1* (1), 25-30.

13. Erdemir, D.; Lee, A. Y.; Myerson, A. S., Nucleation of Crystals from Solution: Classical and Two-Step Models. *Accounts of Chemical Research* **2009,** *42* (5), 621-629.

14. De Yoreo, J. J.; Vekilov, P. G., Principles of crystal nucleation and growth. *Reviews in mineralogy and geochemistry* **2003,** *54* (1), 57-93.

15. Rader, R. A., (Re)defining biopharmaceutical. *Nature Biotechnology* **2008,** *26* (7), 743-751.

16. Craik, D. J.; Fairlie, D. P.; Liras, S.; Price, D., The Future of Peptide-based Drugs. *Chemical Biology & Drug Design* **2013,** *81* (1), 136-147.

17. Mitragotri, S.; Burke, P. A.; Langer, R., Overcoming the challenges in administering biopharmaceuticals: formulation and delivery strategies. *Nature Reviews Drug Discovery* **2014,** *13* (9), 655-672.

18. Kesik-Brodacka, M., Progress in biopharmaceutical development. *Biotechnology and Applied Biochemistry* **2018,** *65* (3), 306-322.

19. Walsh, G., Biopharmaceutical benchmarks 2018. *Nature Biotechnology* **2018,** *36* (12), 1136-1145.

20. Ecker, D. M.; Jones, S. D.; Levine, H. L., The therapeutic monoclonal antibody market. *Mabs* **2015,** *7* (1), 9-14.

21. Elgundi, Z.; Reslan, M.; Cruz, E.; Sifniotis, V.; Kayser, V., The state-of-play and future of antibody therapeutics. *Advanced Drug Delivery Reviews* **2017,** *122*, 2-19.

22. Shukla, A. A.; Thommes, J., Recent advances in large-scale production of monoclonal antibodies and related proteins. *Trends in Biotechnology* **2010,** *28* (5), 253-261.

23. Natarajan, V.; Zydney, A. L., Protein A Chromatography at High Titers. *Biotechnology and Bioengineering* **2013,** *110* (9), 2445-2451.

24. Roque, A. C. A.; Pina, A. S.; Azevedo, A. M.; Aires-Barros, R.; Jungbauer, A.; Di Profio, G.; Heng, J. Y. Y.; Haigh, J.; Ottens, M., Anything but Conventional Chromatography Approaches in Bioseparation. *Biotechnology Journal* **2020,** *15* (8).

25. Thommes, J.; Etzel, M., Alternatives to chromatographic separations. *Biotechnology Progress* **2007,** *23* (1), 42-45.

26. Hekmat, D., Large-scale crystallization of proteins for purification and formulation. *Bioprocess and Biosystems Engineering* **2015,** *38* (7), 1209-1231.

27. dos Santos, R.; Carvalho, A. L.; Roque, A. C. A., Renaissance of protein crystallization and precipitation in biopharmaceuticals purification. *Biotechnology Advances* **2017,** *35* (1), 41-50.

28. Hilbrig, F.; Freitag, R., Protein purification by affinity precipitation. *Journal of Chromatography B-Analytical Technologies in the Biomedical and Life Sciences* **2003,** *790* (1-2), 79-90.

29. Wong, F. W. F.; Ariff, A. B.; Stuckey, D. C., Downstream protein separation by surfactant precipitation: a review. *Critical Reviews in Biotechnology* **2018,** *38* (1), 31-46.

30. Rosa, P. A. J.; Ferreira, I. F.; Azevedo, A. M.; Aires-Barros, M. R., Aqueous two-phase systems: A viable platform in the manufacturing of biopharmaceuticals. *Journal of Chromatography A* **2010,** *1217* (16), 2296-2305.

31. Lee, S. Y.; Khoiroh, I.; Ooi, C. W.; Ling, T. C.; Show, P. L., Recent Advances in Protein Extraction Using Ionic Liquid-based Aqueous Two-phase Systems. *Separation and Purification Reviews* **2017,** *46* (4), 291-304.

32. Orr, V.; Zhong, L. Y.; Moo-Young, M.; Chou, C. P., Recent advances in bioprocessing application of membrane chromatography. *Biotechnology Advances* **2013,** *31* (4), 450-465.

33. Saxena, A.; Tripathi, B. P.; Kumar, M.; Shahi, V. K., Membrane-based techniques for the separation and purification of proteins: An overview. *Advances in Colloid and Interface Science* **2009,** *145* (1-2), 1-22.

34. Stolnik, S.; Shakesheff, K., Formulations for delivery of therapeutic proteins. *Biotechnology Letters* **2009,** *31* (1), 1-11.

35. Basu, S. K.; Govardhan, C. P.; Jung, C. W.; Margolin, A. L., Protein crystals for the delivery of biopharmaceuticals. *Expert Opinion on Biological Therapy* **2004,** *4* (3), 301-317.

36. Yang, M. X.; Shenoy, B.; Disttler, M.; Patel, R.; McGrath, M.; Pechenov, S.; Margolin, A. L., Crystalline monoclonal antibodies for subcutaneous delivery. *Proceedings of the National Academy of Sciences of the United States of America* **2003,** *100* (12), 6934-6939.

37. Judge, R. A.; Johns, M. R.; White, E. T., PROTEIN-PURIFICATION BY BULK CRYSTALLIZATION - THE RECOVERY OF OVALBUMIN. *Biotechnology and Bioengineering* **1995,** *48* (4), 316-323.

38. Jacobsen, C.; Garside, J.; Hoare, M., Nucleation and growth of microbial lipase crystals from clarified concentrated fermentation broths. *Biotechnology and Bioengineering* **1998,** *57* (6), 666-675.

39. Hebel, D.; Huber, S.; Stanislawski, B.; Hekmat, D., Stirred batch crystallization of a therapeutic antibody fragment. *Journal of Biotechnology* **2013,** *166* (4), 206-211.

40. Mullin, J. W., 1. The Crystalline State. In *Crystallization (4th Edition)*, Elsevier.

41. Hunefeld, F., Die Chemismus in der thierischen Organization. *Brockhaus: Leipzig* **1840**, 158-163.

42. McPherson, A., A BRIEF-HISTORY OF PROTEIN CRYSTAL-GROWTH. *Journal of Crystal Growth* **1991,** *110* (1-2), 1-10.

43. Durbin, S. D.; Feher, G., Protein crystallization. *Annual Review of Physical Chemistry* **1996,** *47*, 171-204.

44. Bernal, J. D.; Crowfoot, D., X-Ray Photographs of Crystalline Pepsin. *Nature* **1934,** *133* (3369), 794-795.

45. Strandberg, B., Chapter 1: Building the Ground for the First Two Protein Structures: Myoglobin and Haemoglobin. *Journal of Molecular Biology* **2009,** *392* (1), 2-10.

46. Green, D. W.; Ingram, V. M.; Perutz, M. F.; Bragg, W. L., The structure of haemoglobin - IV. Sign determination by the isomorphous replacement method. *Proceedings of the Royal Society of London. Series A. Mathematical and Physical Sciences* **1954,** *225* (1162), 287-307.

47. Kendrew, J. C.; Bodo, G.; Dintzis, H. M.; Parrish, R. G.; Wyckoff, H.; Phillips, D. C., A Three-Dimensional Model of the Myoglobin Molecule Obtained by X-Ray Analysis. *Nature* **1958,** *181* (4610), 662-666.

48. Callaway, E., The revolution will not be crystallized: a new method sweeps through structural biology. *Nature* **2015,** *525* (7568), 172-174.

49. Wei, G. W., Protein structure prediction beyond AlphaFold. *Nature Machine Intelligence* **2019,** *1* (8), 336-337.

50. Loll, P. J., Membrane proteins, detergents and crystals: what is the state of the art? *Acta Crystallogr F Struct Biol Commun* **2014,** *70* (Pt 12), 1576-1583.

51. Wiencek, J., 12 - Crystallization of proteins. In *Handbook of Industrial Crystallization (Second Edition)*, Myerson, A. S., Ed. Butterworth-Heinemann: Woburn, 2002; pp 267-285.

52. Russo Krauss, I.; Merlino, A.; Vergara, A.; Sica, F., An Overview of Biological Macromolecule Crystallization. *International Journal of Molecular Sciences* **2013,** *14* (6), 11643-11691.

53. Mullin, J. W., 3. Solutions and Solubility. In *Crystallization (4th Edition)*, Elsevier.

54. Mittal, B., Chapter 2 - Pharmacokinetics and Preformulation. In *How to Develop Robust Solid Oral Dosage Forms from Conception to Post-Approval*, Mittal, B., Ed. Academic Press: 2017; pp 17-37.

55. Retailleau, P.; Riès-Kautt, M.; Ducruix, A., No salting-in of lysozyme chloride observed at low ionic strength over a large range of pH. *Biophys. J.* **1997,** *73* (4), 2156-2163.

56. Boistelle, R.; Astier, J. P.; Marchis-Mouren, G.; Desseaux, V.; Haser, R., Solubility, phase transition, kinetic ripening and growth rates of porcine pancreatic α-amylase isoenzymes. *Journal of Crystal Growth* **1992,** *123* (1), 109-120.

57. Feeling-Taylor, A. R.; Banish, R. M.; Hirsch, R. E.; Vekilov, P. G., Miniaturized scintillation technique for protein solubility determinations. *Review of Scientific Instruments* **1999,** *70* (6), 2845-2849.

58. Haire, L. F.; Blow, D. M., A novel spin filter method for the measurement of solubility. *Journal of Crystal Growth* **2001,** *232* (1), 17-20.

59. Gray, R. J.; Hou, W. B.; Kudryavtsev, A. B.; DeLucas, L. J., A new approach to the measurement of protein solubility by Michaelson interferometry. *Journal of Crystal Growth* **2001,** *232* (1-4), 10-16.

60. Nakazato, K.; Homma, T.; Tomo, T., Rapid solubility measurement of protein crystals as a function of precipitant concentration with micro-dialysis cell and two-beam interferometer. *Journal of Synchrotron Radiation* **2004,** *11*, 34-37.

61. Wiendahl, M.; Volker, C.; Husemann, I.; Krarup, J.; Staby, A.; Scholl, S.; Hubbuch, J., A novel method to evaluate protein solubility using a high throughput screening approach. *Chemical Engineering Science* **2009,** *64* (17), 3778-3788.

62. Berg, A.; Schuetz, M.; Dismer, F.; Hubbuch, J., Automated measurement of apparent protein solubility to rapidly assess complex parameter interactions. *Food and Bioproducts Processing* **2014,** *92* (C2), 133-142.

63. Gu, Q.; Li, Z.; Coffman, J. L.; Przybycien, T. M.; Zydney, A. L., High throughput solubility and redissolution screening for antibody purification via combinedPEGand zinc chloride precipitation. *Biotechnology Progress* **2020,** *36* (6).

64. McPherson, A., *Crystallization of biological macromolecules*. Cold Spring Harbor Laboratory Press: Cold Spring Harbor, NY, 1999.

65. Chayen, N. E.; Saridakis, E.; Sear, R. P., Experiment and theory for heterogeneous nucleation of protein crystals in a porous medium. *Proceedings of the National Academy of Sciences of the United States of America* **2006,** *103* (3), 597.

66. Chen, W. Q.; Li, X. Y.; Guo, M. X.; Link, F. J.; Ramli, S. S.; Ouyang, J. B.; Rosbottom, I.; Heng, J. Y. Y., Biopurification of monoclonal antibody (mAb) through crystallisation. *Separation and Purification Technology* **2021,** *263*.

67. Hekmat, D.; Hebel, D.; Schmid, H.; Weuster-Botz, D., Crystallization of lysozyme: From vapor diffusion experiments to batch crystallization in agitated ml-scale vessels. *Process Biochemistry* **2007,** *42* (12), 1649-1654.

68. Bergfors, T. M., *Protein Crystallization*. 2 ed.; International University Line: La Jolla, California, 2009.

69. Chayen, N. E.; Shaw Stewart, P. D.; Blow, D. M., Microbatch crystallization under oil — a new technique allowing many small-volume crystallization trials. *Journal of Crystal Growth* **1992,** *122* (1), 176-180.

70. Chen, J.; Sarma, B.; Evans, J. M. B.; Myerson, A. S., Pharmaceutical Crystallization. *Crystal Growth & Design* **2011,** *11* (4), 887-895.

71. Espinosa, J. R.; Vega, C.; Valeriani, C.; Frenkel, D.; Sanz, E., Heterogeneous versus homogeneous crystal nucleation of hard spheres. *Soft Matter* **2019,** *15* (47), 9625-9631.

72. Bolanos-Garcia, V. M.; Chayen, N. E., New directions in conventional methods of protein crystallization. *Progress in Biophysics and Molecular Biology* **2009,** *101* (1), 3-12.

73. Doran, P. M., Chapter 11 - Unit Operations. In *Bioprocess Engineering Principles (Second Edition)*, Doran, P. M., Ed. Academic Press: London, 2013; pp 445-595.

74. Xu, S.; Hou, Z.; Chuai, X.; Wang, Y., Overview of Secondary Nucleation: From Fundamentals to Application. *Industrial & Engineering Chemistry Research* **2020,** *59* (41), 18335-18356.

75. Nakamuro, T.; Sakakibara, M.; Nada, H.; Harano, K.; Nakamura, E., Capturing the Moment of Emergence of Crystal Nucleus from Disorder. *Journal of the American Chemical Society* **2021,** *143* (4), 1763-1767.

76. Becker, R.; Döring, W., Kinetische Behandlung der Keimbildung in übersättigten Dämpfen. *Annalen der Physik* **1935,** *416* (8), 719-752.

77. Volmer, M., *Kinetik der Phasenbildung*. Steinkopff: Leipzig, 1939.

78. Gibbs, J. W., *The collected works of J. Willard Gibbs. Volume 1: Thermodynamics*. Longmans, Green and Co.: New York, 2013.

79. Wolde, P. R. t.; Frenkel, D., Enhancement of Protein Crystal Nucleation by Critical Density Fluctuations. *Science* **1997,** *277* (5334), 1975-1978.

80. Shah, U. V.; Amberg, C.; Diao, Y.; Yang, Z.; Heng, J. Y. Y., Heterogeneous nucleants for crystallogenesis and bioseparation. *Current Opinion in Chemical Engineering* **2015,** *8*, 69-75.

81. Zhou, R.-B.; Cao, H.-L.; Zhang, C.-Y.; Yin, D.-C., A review on recent advances for nucleants and nucleation in protein crystallization. *CrystEngComm* **2017,** *19* (8), 1143-1155.

82. Chayen, N. E.; Saridakis, E.; El-Bahar, R.; Nemirovsky, Y., Porous silicon: an effective nucleation-inducing material for protein

crystallization11Edited by R. Huber. *Journal of Molecular Biology* **2001,** *312* (4), 591-595.

83. Ghatak, A.; Rawal, G.; Ghatak, A., Precipitant-Free Crystallization of Protein Molecules Induced by Incision on Substrate. *Crystals* **2017,** *7* (8), 245.

84. Sengupta Ghatak, A.; Ghatak, A., Precipitantless Crystallization of Protein Molecules Induced by High Surface Potential. *Cryst. Growth Des.* **2016,** *16* (9), 5323-5329.

85. Leite, J. P.; Rodrigues, D.; Ferreira, S.; Figueira, F.; Almeida Paz, F. A.; Gales, L., Mesoporous Metal–Organic Frameworks as Effective Nucleating Agents in Protein Crystallography. *Cryst. Growth Des.* **2019,** *19* (3), 1610-1615.

86. dos Santos, R.; Romão, M. J.; Roque, A. C. A.; Carvalho, A. L., Magnetic particles used in a new approach for designed protein crystallization. *CrystEngComm* **2021,** *23* (5), 1083-1090.

87. Zhang, B.; Mei, A. R.; Isbell, M. A.; Wang, D.; Wang, Y.; Tan, S. F.; Teo, X. L.; Xu, L.; Yang, Z.; Heng, J. Y. Y., DNA Origami as Seeds for Promoting Protein Crystallization. *ACS Applied Materials & Interfaces* **2018,** *10* (51), 44240-44246.

88. Link, F. J.; Heng, J. Y. Y., Enhancing the crystallisation of insulin using amino acids as soft-templates to control nucleation. *CrystEngComm* **2021,** *23* (22), 3951-3960.

89. Shah, U. V.; Williams, D. R.; Heng, J. Y. Y., Selective Crystallization of Proteins Using Engineered Nanonucleants. *Cryst. Growth Des.* **2012,** *12* (3), 1362-1369.

90. Shah, U. V.; Jahn, N. H.; Huang, S.; Yang, Z.; Williams, D. R.; Heng, J. Y. Y., Crystallisation via novel 3D nanotemplates as a tool for

protein purification and bio-separation. *Journal of Crystal Growth* **2017,** *469*, 42-47.

91. Chen, W.; Cheng, T. N. H.; Khaw, L. F.; Li, X.; Yang, H.; Ouyang, J.; Heng, J. Y. Y., Protein purification with nanoparticle-enhanced crystallisation. *Separation and Purification Technology* **2021,** *255*, 117384.

92. Chen, W.; Park, S. J.; Kong, F.; Li, X.; Yang, H.; Heng, J. Y. Y., High Protein-Loading Silica Template for Heterogeneous Protein Crystallization. *Cryst. Growth Des.* **2020,** *20* (2), 866-873.

93. Tang, L.; Cheng, J. J., Nonporous silica nanoparticles for nanomedicine application. *Nano Today* **2013,** *8* (3), 290-312.

94. Slowing, I. I.; Vivero-Escoto, J. L.; Wu, C.-W.; Lin, V. S. Y., Mesoporous silica nanoparticles as controlled release drug delivery and gene transfection carriers. *Advanced Drug Delivery Reviews* **2008,** *60* (11), 1278-1288.

95. Chrzanowska, A.; Derylo-Marczewska, A.; Borowski, P., Comprehensive characterization of biocomposite surface based on the mesoporous silica and lysozyme molecules: Chemistry, morphology, topography, texture and micro-nanostructure. *Applied Surface Science* **2020,** *525*.

96. Giegé, R.; Dock, A. C.; Kern, D.; Lorber, B.; Thierry, J. C.; Moras, D., The role of purification in the crystallization of proteins and nucleic acids. *Journal of Crystal Growth* **1986,** *76* (3), 554-561.

97. Thomas, B. R.; Vekilov, P. G.; Rosenberger, F., Heterogeneity determination and purification of commercial hen egg-white lysozyme. *Acta Crystallogr. Sect. D-Biol. Crystallogr.* **1996,** *52*, 776-784.

98. Judge, R. A.; Forsythe, E. L.; Pusey, M. L., The effect of protein impurities on lysozyme crystal growth. *Biotechnology and Bioengineering* **1998,** *59* (6), 776-785.

99. Kors, C. A.; Wallace, E.; Davies, D. R.; Li, L.; Laible, P. D.; Nollert, P., Effects of impurities on membrane-protein crystallization in different systems. *Acta Crystallogr. Sect. D-Struct. Biol.* **2009,** *65*, 1062-1073.

100. Hekmat, D.; Breitschwerdt, P.; Weuster-Botz, D., Purification of proteins from solutions containing residual host cell proteins via preparative crystallization. *Biotechnology Letters* **2015,** *37* (9), 1791-1801.

101. Ewing, F. L.; Forsythe, E. L.; vanderWoerd, M.; Pusey, M. L., Effects of purification on the crystallization of lysozyme. *Journal of Crystal Growth* **1996,** *160* (3-4), 389-397.

102. Vekilov, P. G.; Monaco, L. A.; Thomas, B. R.; Stojanoff, V.; Rosenberger, F., Repartitioning of NaCl and protein impurities in lysozyme crystallization. *Acta Crystallogr. Sect. D-Struct. Biol.* **1996,** *52*, 785-798.

103. Skouri, M.; Lorber, B.; Giege, R.; Munch, J. P.; Candau, J. S., EFFECT OF MACROMOLECULAR IMPURITIES ON LYSOZYME SOLUBILITY AND CRYSTALLIZABILITY - DYNAMIC LIGHT-SCATTERING, PHASE-DIAGRAM, AND CRYSTAL-GROWTH STUDIES. *Journal of Crystal Growth* **1995,** *152* (3), 209-220.

104. Li, X.; Heng, J. Y. Y., The critical role of agitation in moving from preliminary screening results to reproducible batch protein crystallisation. *Chemical Engineering Research and Design* **2021,** *173*, 81-88.

105. Lorber, B.; Skouri, M.; Munch, J. P.; Giege, R., THE INFLUENCE OF IMPURITIES ON PROTEIN CRYSTALLIZATION - THE CASE OF LYSOZYME. *Journal of Crystal Growth* **1993,** *128* (1-4), 1203-1211.

106. Bhamidi, V.; Hanson, B. L.; Edmundson, A.; Skrzypczak-Jankun, E.; Schall, C., The influence of a homologous protein impurity on lysozyme crystal growth. *Journal of Crystal Growth* **1999,** *204* (4), 542-552.

107. Chen, W. Q.; Cheng, T. N. H.; Khaw, L. F.; Li, X. Y.; Yang, H. Y.; Ouyang, J. B.; Heng, J. Y. Y., Protein purification with nanoparticle-enhanced crystallisation. *Separation and Purification Technology* **2021,** *255*.

108. Hirschler, J.; FontecillaCamps, J. C., Contaminant effects on protein crystal morphology in different growth environments. *Acta Crystallogr. Sect. D-Biol. Crystallogr.* **1996,** *52*, 806-812.

109. Carter, D. C.; Lim, K.; Ho, J. X.; Wright, B. S.; Twigg, P. D.; Miller, T. Y.; Chapman, J.; Keeling, K.; Ruble, J.; Vekilov, P. G.; Thomas, B. R.; Rosenberger, F.; Chernov, A. A., Lower dimer impurity incorporation may result in higher perfection of HEWL crystals grown in microgravity: A case study. *Journal of Crystal Growth* **1999,** *196* (2), 623-637.

110. Kurihara, K.; Miyashita, S.; Sazaki, G.; Nakada, T.; Durbin, S. D.; Komatsu, H.; Ohba, T.; Ohki, K., Incorporation of impurity to a tetragonal lysozyme crystal. *Journal of Crystal Growth* **1999,** *196* (2), 285-290.

111. Gavira, J. A.; Otalora, F.; Gonzalez-Ramirez, L. A.; Melero, E.; van Driessche, A. E. S.; Garcia-Ruiz, J. M., On the Quality of Protein Crystals Grown under Diffusion Mass-transport Controlled Regime (I). *Crystals* **2020,** *10* (2).

112. Yu, Y.; Li, K.; Lin, H.; Li, J. C., The Study of the Mechanism of Protein Crystallization in Space by Using Microchannel to Simulate Microgravity Environment. *Crystals* **2018,** *8* (11).

113. Snell, E. H.; Judge, R. A.; Crawford, L.; Forsythe, E. L.; Pusey, M. L.; Sportiello, M.; Todd, P.; Bellamy, H.; Lovelace, J.; Cassanto, J. M.; Borgstahl, G. E. O., Investigating the Effect of Impurities on Macromolecule Crystal Growth in Microgravity. *Crystal Growth & Design* **2001,** *1* (2), 151-158.

114. Otalora, F.; Gavira, J. A.; Ng, J. D.; Garcia-Ruiz, J. M., Counterdiffusion methods applied to protein crystallization. *Progress in Biophysics & Molecular Biology* **2009,** *101* (1-3), 26-37.

115. Van Driessche, A. E. S.; Otálora, F.; Gavira, J. A.; Sazaki, G., Is Agarose an Impurity or an Impurity Filter? In Situ Observation of the Joint Gel/Impurity Effect on Protein Crystal Growth Kinetics. *Crystal Growth & Design* **2008,** *8* (10), 3623-3629.

116. Vekilov, P. G.; Rosenberger, F., Protein crystal growth under forced solution flow: experimental setup and general response of lysozyme. *Journal of Crystal Growth* **1998,** *186* (1), 251-261.

117. Vekilov, P. G.; Rosenberger, F.; Lin, H.; Thomas, B. R., Nonlinear dynamics of layer growth and consequences for protein crystal perfection. *Journal of Crystal Growth* **1999,** *196* (2), 261-275.

118. Chen, W.; Yang, H.; Yew Heng, J. Y., CHAPTER 10 Continuous Protein Crystallization. In *The Handbook of Continuous Crystallization*, The Royal Society of Chemistry: 2020; pp 372-392.

119. Smejkal, B.; Helk, B.; Rondeau, J. M.; Anton, S.; Wilke, A.; Scheyerer, P.; Fries, J.; Hekmat, D.; Weuster-Botz, D., Protein

crystallization in stirred systemsscale-up via the maximum local energy dissipation. *Biotechnology and Bioengineering* **2013,** *110* (7), 1956-1963.

120. Yang, H. Y.; Chen, W. Q.; Peczulis, P.; Heng, J. Y. Y., Development and Workflow of a Continuous Protein Crystallization Process: A Case of Lysozyme. *Crystal Growth & Design* **2019,** *19* (2), 983-991.

121. Konstantinov, K. B.; Cooney, C. L., White Paper on Continuous Bioprocessing May 20-21, 2014 Continuous Manufacturing Symposium. *Journal of Pharmaceutical Sciences* **2015,** *104* (3), 813-820.

122. Hummel, J.; Pagkaliwangan, M.; Gjoka, X.; Davidovits, T.; Stock, R.; Ransohoff, T.; Gantier, R.; Schofield, M., Modeling the Downstream Processing of Monoclonal Antibodies Reveals Cost Advantages for Continuous Methods for a Broad Range of Manufacturing Scales. *Biotechnology Journal* **2019,** *14* (2).

123. Cataldo, A. L.; Burgstaller, D.; Hribar, G.; Jungbauer, A.; Satzer, P., Economics and ecology: Modelling of continuous primary recovery and capture scenarios for recombinant antibody production. *Journal of Biotechnology* **2020,** *308*, 87-95.

124. Gerstweiler, L.; Bi, J. X.; Middelberg, A. P. J., Continuous downstream bioprocessing for intensified manufacture of biopharmaceuticals and antibodies. *Chemical Engineering Science* **2021,** *231*.

125. Sao Pedro, M. N.; Silva, T. C.; Patil, R.; Ottens, M., White paper on high-throughput process development for integrated continuous biomanufacturing. *Biotechnology and Bioengineering* **2021**.

126. Gjoka, X.; Gantier, R.; Schofield, M., Transfer of a three step mAb chromatography process from batch to continuous: Optimizing

productivity to minimize consumable requirements. *Journal of Biotechnology* **2017,** *242*, 11-18.

127. Kamga, M. H.; Cattaneo, M.; Yoon, S., Integrated continuous biomanufacturing platform with ATF perfusion and one column chromatography operation for optimum resin utilization and productivity. *Preparative Biochemistry & Biotechnology* **2018,** *48* (5), 383-390.

128. Lofgren, A.; Gomis-Fons, J.; Andersson, N.; Nilsson, B.; Berghard, L.; Hagglund, C. L., An integrated continuous downstream process with real-time control: A case study with periodic countercurrent chromatography and continuous virus inactivation. *Biotechnology and Bioengineering* **2021,** *118* (4), 1664-1676.

129. Vazquez-Villegas, P.; Aguilar, O.; Rito-Palomares, M., Study of biomolecules partition coefficients on a novel continuous separator using polymer-salt aqueous two-phase systems. *Separation and Purification Technology* **2011,** *78* (1), 69-75.

130. Rosa, P. A. J.; Azevedo, A. M.; Sommerfeld, S.; Mutter, M.; Backer, W.; Aires-Barros, M. R., Continuous purification of antibodies from cell culture supernatant with aqueous two-phase systems: From concept to process. *Biotechnology Journal* **2013,** *8* (3), 352-362.

131. Turpeinen, D. G.; Joshi, P. U.; Kriz, S. A.; Kaur, S.; Nold, N. M.; O'Hagan, D.; Nikam, S.; Masoud, H.; Heldt, C. L., Continuous purification of an enveloped and non-enveloped viral particle using an aqueous two-phase system. *Separation and Purification Technology* **2021,** *269*.

132. Burgstaller, D.; Jungbauer, A.; Satzer, P., Continuous integrated antibody precipitation with two-stage tangential flow microfiltration enables constant mass flow. *Biotechnology and Bioengineering* **2019,** *116* (5), 1053-1065.

133. Li, Z.; Gu, Q.; Coffman, J. L.; Przybycien, T.; Zydney, A. L., Continuous precipitation for monoclonal antibody capture using countercurrent washing by microfiltration. *Biotechnology Progress* **2019,** *35* (6).

134. Neugebauer, P.; Khinast, J. G., Continuous Crystallization of Proteins in a Tubular Plug-Flow Crystallizer. *Crystal Growth & Design* **2015,** *15* (3), 1089-1095.

135. Thomas, K. M.; Kwon, S.; Lakerveld, R., Continuous Protein Crystallization in Mixed-Suspension Mixed-Product-Removal Crystallizers. *Crystal Growth & Design* **2021,** *21* (2), 757-769.

136. Peters, J.; Minuth, T.; Schroder, W., Implementation of a crystallization step into the purification process of a recombinant protein. *Protein Expression and Purification* **2005,** *39* (1), 43-53.

137. Smejkal, B.; Agrawal, N. J.; Helk, B.; Schulz, H.; Giffard, M.; Mechelke, M.; Ortner, F.; Heckmeier, P.; Trout, B. L.; Hekmat, D., Fast and scalable purification of a therapeutic full-length antibody based on process crystallization. *Biotechnology and Bioengineering* **2013,** *110* (9), 2452-2461.

138. Huettmann, H.; Berkemeyer, M.; Buchinger, W.; Jungbauer, A., Preparative Crystallization of a Single Chain Antibody Using an Aqueous Two-Phase System. *Biotechnology and Bioengineering* **2014,** *111* (11), 2192-2199.

139. Mathew Thomas, K.; Lakerveld, R., An Airlift Crystallizer for Protein Crystallization. *Industrial & Engineering Chemistry Research* **2019,** *58* (44), 20381-20391.

140. Fernández-Penas, R.; Verdugo-Escamilla, C.; Martínez-Rodríguez, S.; Gavira, J. A., Production of Cross-Linked Lipase Crystals at a Preparative Scale. *Crystal Growth & Design* **2021,** *21* (3), 1698-1707.

141. Roberts, M. M.; Heng, J. Y. Y.; Williams, D. R., Protein Crystallization by Forced Flow through Glass Capillaries: Enhanced Lysozyme Crystal Growth. *Crystal Growth & Design* **2010,** *10* (3), 1074-1083.

142. Hekmat, D.; Huber, M.; Lohse, C.; von den Eichen, N.; Weuster-Botz, D., Continuous Crystallization of Proteins in a Stirred Classified Product Removal Tank with a Tubular Reactor in Bypass. *Crystal Growth & Design* **2017,** *17* (8), 4162-4169.

143. Yang, H.; Peczulis, P.; Inguva, P.; Li, X.; Heng, J. Y. Y., Continuous protein crystallisation platform and process: Case of lysozyme. *Chemical Engineering Research and Design* **2018,** *136*, 529-535.

144. Li, F.; Lakerveld, R., Electric-Field-Assisted Protein Crystallization in Continuous Flow. *Crystal Growth & Design* **2018,** *18* (5), 2964-2971.

145. Oliva, J. A.; Wu, W. L.; Greene, M. R.; Pal, K.; Nagy, Z. K., Continuous Spherical Crystallization of Lysozyme in an Oscillatory Baffled Crystallizer Using Emulsion Solvent Diffusion in Droplets. *Crystal Growth & Design* **2020,** *20* (2), 934-947.

146. Chen, R.; Weng, J.; Chow, S. F.; Lakerveld, R., Integrated Continuous Crystallization and Spray Drying of Insulin for Pulmonary Drug Delivery. *Crystal Growth & Design* **2021,** *21* (1), 501-511.

147. Pu, S. Y.; Hadinoto, K., Improving the reproducibility of size distribution of protein crystals produced in continuous slug flow

crystallizer operated at short residence time. *Chemical Engineering Science* **2021,** *230*.

148. Pu, S. Y.; Hadinoto, K., Comparative evaluations of bulk seeded protein crystallization in batch versus continuous slug flow crystallizers. *Chemical Engineering Research & Design* **2021,** *171*, 139-149.

149. Fleming, A.; Wright, A. E., On a remarkable bacteriolytic element found in tissues and secretions. *Proceedings of the Royal Society of London. Series B, Containing Papers of a Biological Character* **1922,** *93* (653), 306-317.

150. Blake, C. C. F.; Koenig, D. F.; Mair, G. A.; North, A. C. T.; Phillips, D. C.; Sarma, V. R., Structure of Hen Egg-White Lysozyme: A Three-dimensional Fourier Synthesis at 2 Å Resolution. *Nature* **1965,** *206* (4986), 757-761.

151. Jolles, P.; Jolles, J., WHATS NEW IN LYSOZYME RESEARCH - ALWAYS A MODEL SYSTEM, TODAY AS YESTERDAY. *Molecular and Cellular Biochemistry* **1984,** *63* (2), 165-189.

152. Phillips, D. C., The Three-dimensional Structure of an Enzyme Molecule. *Scientific American* **1966,** *215* (5), 78-93.

153. Proctor, V. A.; Cunningham, F. E., THE CHEMISTRY OF LYSOZYME AND ITS USE AS A FOOD PRESERVATIVE AND A PHARMACEUTICAL. *Crc Critical Reviews in Food Science and Nutrition* **1988,** *26* (4), 359-395.

154. Vachier, M. C.; Piot, M.; Awadé, A. C., Isolation of hen egg white lysozyme, ovotransferrin and ovalbumin, using a quaternary ammonium bound to a highly crosslinked agarose matrix. *Journal of Chromatography B: Biomedical Sciences and Applications* **1995,** *664* (1), 201-210.

155. Mine, S.; Ueda, T.; Hashimoto, Y.; Imoto, T., Analysis of the internal motion of free and ligand-bound human lysozyme by use of N-15

NMR relaxation measurement: A comparison with those of hen lysozyme. *Protein Science* **2000,** *9* (9), 1669-1684.

156. Elagamy, E. I.; Ruppanner, R.; Ismail, A.; Champagne, C. P.; Assaf, R., Purification and characterization of lactoferrin, lactoperoxidase, lysozyme and immunoglobulins from camel's milk. *International Dairy Journal* **1996,** *6* (2), 129-145.

157. Shiomori, K.; Honbu, T.; Kawano, Y.; Kuboi, R.; Komasawa, I., Formation and Structure Control of Reverse Micelles by the Addition of Alkyl Amines and their Applications for Extraction Processes of Proteins. In *Studies in Surface Science and Catalysis*, Iwasawa, Y.; Oyama, N.; Kunieda, H., Eds. Elsevier: 2001; Vol. 132, pp 141-144.

158. Harata, K.; Akiba, T., Structural phase transition of monoclinic crystals of hen egg-white lysozyme. *Acta Crystallogr D Biol Crystallogr* **2006,** *62* (Pt 4), 375-82.

159. Steinrauf, L. K., Structures of monoclinic lysozyme iodide at 1.6 angstrom and of triclinic lysozyme nitrate at 1.1 angstrom. *Acta Crystallogr. Sect. D-Struct. Biol.* **1998,** *54*, 767-779.

160. Artymiuk, P. J.; Blake, C. C. F.; Rice, D. W.; Wilson, K. S., The structures of the monoclinic and orthorhombic forms of hen egg-white lysozyme at 6 Å resolution. *Acta Crystallographica Section B* **1982,** *38* (3), 778-783.

161. Vaney, M. C.; Broutin, I.; Retailleau, P.; Douangamath, A.; Lafont, S.; Hamiaux, C.; Prange, T.; Ducruix, A.; Ries-Kautt, M., Structural effects of monovalent anions on polymorphic lysozyme crystals. *Acta Crystallogr. Sect. D-Struct. Biol.* **2001,** *57*, 929-940.

162. Sauter, C.; Otalora, F.; Gavira, J. A.; Vidal, O.; Giege, R.; Garcia-Ruiz, J. M., Structure of tetragonal hen egg-white lysozyme at

0.94 angstrom from crystals grown by the counter-diffusion method. *Acta Crystallogr. Sect. D-Struct. Biol.* **2001,** *57*, 1119-1126.

163. Yamada, H.; Nagae, T.; Watanabe, N., High-pressure protein crystallography of hen egg-white lysozyme. *Acta Crystallogr. Sect. D-Struct. Biol.* **2015,** *71*, 742-753.

164. Kurinov, I. V.; Harrison, R. W., THE INFLUENCE OF TEMPERATURE ON LYSOZYME CRYSTALS - STRUCTURE AND DYNAMICS OF PROTEIN AND WATER. *Acta Crystallogr. Sect. D-Biol. Crystallogr.* **1995,** *51*, 98-109.

165. Weiss, M. S.; Palm, G. J.; Hilgenfeld, R., Crystallization, structure solution and refinement of hen egg-white lysozyme at pH 8.0 in the presence of MPD. *Acta Crystallogr. Sect. D-Struct. Biol.* **2000,** *56*, 952-958.

166. Ramos, J.; Laux, V.; Haertlein, M.; Erba, E. B.; McAuley, K. E.; Forsyth, V. T.; Mossou, E.; Larsen, S.; Langkilde, A. E., Structural insights into protein folding, stability and activity using in vivo perdeuteration of hen egg-white lysozyme. *Iucrj* **2021,** *8*, 372-386.

167. Saijo, S.; Yamada, Y.; Sato, T.; Tanaka, N.; Matsui, T.; Sazaki, G.; Nakajima, K.; Matsuura, Y., Structural consequences of hen egg-white lysozyme orthorhombic crystal growth in a high magnetic field: validation of X-ray diffraction intensity, conformational energy searching and quantitative analysis of B factors and mosaicity. *Acta Crystallogr. Sect. D-Struct. Biol.* **2005,** *61*, 207-217.

168. Brinkmann, C.; Weiss, M. S.; Weckert, E., The structure of the hexagonal crystal form of hen egg-white lysozyme. *Acta Crystallogr. Sect. D-Struct. Biol.* **2006,** *62*, 349-355.

169. Joseph, J. A.; Akkermans, S.; Nimmegeers, P.; Van Impe, J. F. M., Bioproduction of the Recombinant Sweet Protein Thaumatin: Current State of the Art and Perspectives. *Frontiers in Microbiology* **2019,** *10*.

170. Faus, I.; Patino, C.; delRio, J. L.; delMoral, C.; Barroso, H. S.; Rubio, V., Expression of a synthetic gene encoding the sweet-tasting protein thaumatin in Escherichia coli. *Biochemical and Biophysical Research Communications* **1996,** *229* (1), 121-127.

171. Edens, L.; Vanderwel, H., MICROBIAL SYNTHESIS OF THE SWEET-TASTING PLANT PROTEIN THAUMATIN. *Trends in Biotechnology* **1985,** *3* (3), 61-64.

172. Faus, I.; del Moral, C.; Adroer, N.; del Rio, J. L.; Patino, C.; Sisniega, H.; Casas, C.; Blade, J.; Rubio, V., Secretion of the sweet-tasting protein thaumatin by recombinant strains of Aspergillus niger var. awamori. *Applied Microbiology and Biotechnology* **1998,** *49* (4), 393-398.

173. Bartoszewski, G.; Niedziela, A.; Szwacka, M.; Niemirowicz-Szczytt, K., Modification of tomato taste in transgenic plants carrying a thaumatin gene from Thaumatococcus daniellii Benth. *Plant Breeding* **2003,** *122* (4), 347-351.

174. Pechkova, E.; Bragazzi, N. L.; Nicolini, C., Chapter Five - Advances in Nanocrystallography as a Proteomic Tool. In *Advances in Protein Chemistry and Structural Biology*, Donev, R., Ed. Academic Press: 2014; Vol. 95, pp 163-191.

175. Izawa, K.; Amino, Y.; Kohmura, M.; Ueda, Y.; Kuroda, M., 4.16 - Human–Environment Interactions – Taste. In *Comprehensive Natural Products II*, Liu, H.-W.; Mander, L., Eds. Elsevier: Oxford, 2010; pp 631-671.

176. Asherie, N.; Ginsberg, C.; Blass, S.; Greenbaum, A.; Knafo, S., Solubility of thaumatin. *Crystal Growth & Design* **2008,** *8* (6), 1815-1817.

177. Asherie, N.; Jakoncic, J.; Ginsberg, C.; Greenbaum, A.; Stojanoff, V.; Hrnjez, B. J.; Blass, S.; Berger, J., Tartrate Chirality Determines Thaumatin Crystal Habit. *Crystal Growth & Design* **2009,** *9* (9), 4189-4198.

178. Sauter, C.; Lorber, B.; Giegé, R., Towards atomic resolution with crystals grown in gel: the case of thaumatin seen at room temperature. *Proteins* **2002,** *48* (2), 146-50.

179. Warkentin, M.; Badeau, R.; Hopkins, J. B.; Thorne, R. E., Spatial distribution of radiation damage to crystalline proteins at 25-300 K. *Acta Crystallogr D Biol Crystallogr* **2012,** *68* (Pt 9), 1108-17.

180. Ko, T. P.; Day, J.; Greenwood, A.; McPherson, A., STRUCTURES OF 3 CRYSTAL FORMS OF THE SWEET PROTEIN THAUMATIN. *Acta Crystallogr. Sect. D-Struct. Biol.* **1994,** *50*, 813-825.

181. Charron, C.; Giegé, R.; Lorber, B., Structure of thaumatin in a hexagonal space group: comparison of packing contacts in four crystal lattices. *Acta Crystallogr D Biol Crystallogr* **2004,** *60* (Pt 1), 83-9.

182. Aune, K. C.; Tanford, C., Thermodynamics of the denaturation of lysozyme by guanidine hydrochloride. I. Dependence on pH at 25°. *Biochemistry* **1969,** *8* (11), 4579-4585.

183. Asherie, N.; Ginsberg, C.; Greenbaum, A.; Blass, S.; Knafo, S., Effects of Protein Purity and Precipitant Stereochemistry on the Crystallization of Thaumatin. *Crystal Growth & Design* **2008,** *8* (12), 4200-4207.

184. Matthews, B. W., Solvent content of protein crystals. *Journal of Molecular Biology* **1968,** *33* (2), 491-497.

185. Tang, X. H.; Liu, J. J.; Zhang, Y.; Wang, X. Z., Study on the influence of lysozyme crystallization conditions on crystal properties in crystallizers of varied sizes when temperature is the manipulated variable. *J. Cryst. Growth* **2018,** *498*, 186-196.

186. Wiesbauer, J.; Cardinale, M.; Nidetzky, B., Shaking and stirring: Comparison of controlled laboratory stress conditions applied to the human growth hormone. *Process Biochemistry* **2013,** *48* (1), 33-40.

187. Byington, M. C.; Safari, M. S.; Conrad, J. C.; Vekilov, P. G., Shear flow suppresses the volume of the nucleation precursor clusters in lysozyme solutions. *Journal of Crystal Growth* **2017,** *468*, 493-501.

188. Yang, H.; Chen, W.; Peczulis, P.; Heng, J. Y. Y., Development and Workflow of a Continuous Protein Crystallization Process: A Case of Lysozyme. *Cryst. Growth Des.* **2019,** *19* (2), 983-991.

189. Kovalchuk, M. V.; Blagov, A. E.; Dyakova, Y. A.; Gruzinov, A. Y.; Marchenkova, M. A.; Peters, G. S.; Pisarevsky, Y. V.; Timofeev, V. I.; Volkov, V. V., Investigation of the Initial Crystallization Stage in Lysozyme Solutions by Small-Angle X-ray Scattering. *Cryst. Growth Des.* **2016,** *16* (4), 1792-1797.

190. Li, X.; Chen, W.; Yang, H.; Yang, Z.; Heng, J. Y. Y., Protein crystal occurrence domains in selective protein crystallisation for bio-separation. *CrystEngComm* **2020,** *22* (27), 4566-4572.

191. Li, X.; Heng, J. Y. Y., The critical role of agitation in moving from preliminary screening results to reproducible batch protein crystallisation. *Chemical Engineering Research and Design* **2021**.